

# Transmit Diversity and Its Application to Cooperative Networking

Submitted in fulfilment of the requirements for the degree of

MASTER OF ENGINEERING BY RESEARCH  
(ELECTRICAL ENGINEERING)

by

Venatkumar Venkatasubramanian

School of Electrical Engineering

Victoria University

February 2006

©Venatkumar Venkatasubramanian

Produced in L<sup>A</sup>T<sub>E</sub>X 2<sub>ε</sub>

# Abstract

Wireless communications has been so far largely based on centralized control, which in effect has limited its deployment, coverage and application scenarios. The paradigm of peer-to-peer wireless communications is fundamentally to remove this bottleneck and to further expand wireless communications into new applications. The technical and design challenges in implementing these networks are however plenty and exist in all the layers of the OSI protocol stack.

In this thesis, we only consider the physical layer model of these networks. We identify multiple antenna systems as a vital component of physical layer solutions. We first investigate the case of multiple antenna space-time coding techniques to achieve spatial diversity. We observe that when correlation between the antennas in a local antenna array becomes high due to space constraints in a terminal, current performance achieving strategies do not actually deliver good results. Moreover, most mobile terminals are currently equipped with only one antenna. In view of this limitation, we study the recently proposed user cooperation techniques for exploiting spatial diversity with user power constraints for a simple three terminal network. We find that these systems are beneficial even with relatively simple protocols such as selection relaying. Finally, with simulation results, we demonstrate that the system performance can be improved significantly via near-to optimal selection relaying.

# Declaration

"I, Venkatakumar Venkatasubramanian, declare that the Master by Research thesis entitled "Transmit Diversity and Its Application to Cooperative Networking" is no more than 60,000 words in length, exclusive of tables, figures, appendices, references and footnotes. This thesis contains no material that has been submitted previously, in whole or in part, for the award of any other academic degree or diploma. Except where otherwise indicated, this thesis is my own work".

Signature

Date

# Contents

<b>Abstract</b>	<b>i</b>
<b>Declaration</b>	<b>ii</b>
<b>Contents</b>	<b>iii</b>
<b>List of figures</b>	<b>v</b>
<b>List of acronyms</b>	<b>vii</b>
<b>List of symbols</b>	<b>x</b>
<b>Acknowledgement</b>	<b>xi</b>
<b>Publications</b>	<b>xii</b>
<b>1 Introduction</b>	<b>1</b>
1.1 Overview of Ad hoc networks . . . . .	1
1.2 Literature survey . . . . .	3
1.2.1 Multiple antenna systems . . . . .	3
1.2.2 Cooperative networking . . . . .	4
1.3 Summary of contributions . . . . .	6
1.4 Structure of the thesis . . . . .	7
<b>2 Space-Time Block coding</b>	<b>8</b>
2.1 Introduction . . . . .	8

2.2	Space-time block encoder . . . . .	9
2.3	Orthogonal designs . . . . .	11
2.3.1	Example codes . . . . .	12
2.3.2	Maximum likelihood decoding . . . . .	15
2.3.3	Equivalent channel representation . . . . .	15
2.3.4	Capacity and Performance . . . . .	17
2.4	Non-orthogonal designs . . . . .	17
2.4.1	Maximum likelihood decoding . . . . .	18
2.5	Constellation rotation . . . . .	21
2.6	Multimodulation scheme . . . . .	24
2.7	Conclusion . . . . .	25
<b>3</b>	<b>Space-Time block Coding in correlated channels</b>	<b>26</b>
3.1	Introduction . . . . .	26
3.2	Channel correlation model . . . . .	27
3.3	Constellation rotation scheme over correlated channels . . . . .	29
3.3.1	Effect on the PEP . . . . .	29
3.3.2	Analysis . . . . .	31
3.4	Numerical examples . . . . .	33
3.5	Conclusion . . . . .	36
<b>4</b>	<b>User Cooperation</b>	<b>37</b>
4.1	Introduction . . . . .	37
4.2	Multihop network . . . . .	39
4.3	Three terminal model . . . . .	40
4.3.1	Relay diversity . . . . .	41
4.3.2	Multiple relay network . . . . .	44
4.4	Relay node functionality . . . . .	47
4.5	Cooperation schemes . . . . .	49
4.5.1	Virtual antenna array . . . . .	49

4.5.2	User cooperation in MAC . . . . .	51
4.6	Distributed space-time coding . . . . .	54
4.6.1	Distributed Alamouti coding . . . . .	56
4.7	Detection techniques . . . . .	57
4.7.1	Maximum likelihood detection . . . . .	58
4.7.2	Weighted combiner . . . . .	60
4.8	Simulation example . . . . .	63
4.9	Conclusion . . . . .	65
<b>5</b>	<b>Selection Relaying</b>	<b>66</b>
5.1	Introduction . . . . .	66
5.2	Optimal threshold for orthogonal relaying . . . . .	67
5.2.1	Thresholding . . . . .	69
5.2.2	Additional diversity . . . . .	71
5.3	Optimal threshold for Alamouti relaying . . . . .	72
5.3.1	Detection at the destination node . . . . .	73
5.3.2	Thresholding . . . . .	75
5.3.3	Additional diversity . . . . .	77
5.4	Channel estimation errors . . . . .	79
5.5	Numerical examples . . . . .	81
5.6	Conclusion . . . . .	85
<b>6</b>	<b>Conclusions and Perspectives</b>	<b>87</b>
6.1	Conclusions . . . . .	87
6.2	Perspectives . . . . .	88
	<b>References</b>	<b>89</b>

# List of Figures

2.1	Space-time block code encoder. . . . .	9
2.2	Minima of $\xi$ against angle of rotation. . . . .	23
3.1	Loss function against correlation coefficient. . . . .	31
3.2	Uncoded bit error rate for QPSK modulation for uncorrelated antennas ( $\alpha = 0$ ). . .	35
3.3	Uncoded bit error rate for QPSK modulation for uncorrelated antennas ( $\alpha = 0.9$ ). .	35
3.4	Uncoded bit error rate for QPSK modulation for uncorrelated antennas ( $\alpha = 1$ ). . .	36
4.1	Multihop network with 3 hops. . . . .	39
4.2	Multihop model with $n$ hops. . . . .	40
4.3	Three terminal model. . . . .	41
4.4	Three terminal relay diversity. . . . .	42
4.5	Destination receiver. . . . .	43
4.6	Multiple relay model. . . . .	44
4.7	Parallel relay model. . . . .	46
4.8	Transmitter cooperation: Broadcast channel. . . . .	50
4.9	Receiver cooperation: MAC. . . . .	50
4.10	Cooperative MIMO. . . . .	51
4.11	Cluster cooperation. . . . .	51
4.12	User cooperation in MAC. . . . .	52
4.13	Coded cooperation. . . . .	54
4.14	Parallel relay case with superpositioning. . . . .	55
4.15	Distributed space-time coding. . . . .	56

4.16 Receiver schematic. . . . .	57
4.17 Distributed Alamouti scheme with channel estimation errors at the relay. . . . .	64
5.1 Distributed Alamouti scheme. . . . .	84
5.2 Distributed Alamouti scheme with channel estimation errors at the relay. . . . .	84
5.3 Distributed Alamouti scheme after MRC combining with information in frame index $i$ . . . . .	85
5.4 Distributed Alamouti scheme when MRC combined but with channel estimation errors at the relay. . . . .	85

# List of acronyms

<b>4G</b>	fourth generation
<b>AF</b>	amplify and forward
<b>AWGN</b>	additive white gaussian noise
<b>BC</b>	broadcast channel
<b>BER</b>	bit error rate
<b>CDMA</b>	code division multiple access
<b>CrNO-STBC</b>	constellation rotated non orthogonal space-time block code
<b>DARPA</b>	defense advanced projects agency
<b>DF</b>	decode and forward
<b>MAC</b>	multiple access channel
<b>MANET</b>	mobile ad hoc network
<b>MIMO</b>	multiple input multiple output
<b>ML</b>	maximum likelihood
<b>MPRN</b>	multihop packet radio network
<b>MRC</b>	maximum ratio combining
<b>MSD</b>	maximal symbolwise diversity
<b>NO-STBC</b>	non orthogonal space-time block code
<b>O-STBC</b>	orthogonal space -time block code
<b>PEP</b>	pairwise error probability
<b>PSK</b>	phase shift keying
<b>QPSK</b>	quadrature phase shift keying
<b>QAM</b>	quadrature amplitude modulation

<b>STTC</b>	space-time trellis code
<b>SNR</b>	signal to noise ratio
<b>TDMA</b>	time division multiple access
<b>VAA</b>	virtual antenna array
<b>V-BLAST</b>	vertical bell laboratories layered space-time architecture

# List of symbols

$E[X]$	expectation of a random variable $X$
$var[X]$	variance of a random variable $X$
$\mathbf{a}$	vector notation
$\mathbf{A}$	matrix notation
$\mathbf{A}^H$	Hermitian of a matrix $\mathbf{A}$
$\mathbf{A}^T$	Transpose of a matrix $\mathbf{A}$
$P(X)$	probability of an event $X$
$diag(x_1, x_2, \dots, x_n)$	diagonal matrix with entries $x_1, x_2, \dots, x_n$
$\ \mathbf{A}\ _F$	Frobenius norm of a matrix $\mathbf{A}$
$\ \mathbf{a}\ $	norm of a vector $\mathbf{a}$
$\lambda_i(\mathbf{A})$	$i^{th}$ eigen value of a matrix $\mathbf{A}$
$\Re(a + jb)$	$a$
$\Im(a + jb)$	$b$
$tr(\mathbf{A})$	sum of all diagonal elements of a matrix $\mathbf{A}$
$\prod_{i=1}^n a_i$	$a_1 a_2 a_3 \dots a_n$
$\sum_{i=1}^n a_i$	$a_1 + a_2 + a_3 \dots + a_n$
$ a + jb $	$\sqrt{a^2 + b^2}$

# Acknowledgements

First of all, I would sincerely like to express my gratitude to my supervisor, Assoc. Prof Fu-Chun Zheng for his academic guidance and financial support throughout my research.

I would also like to acknowledge Prof. Michael Faulkner for his encouragement. Thanks to Dr. Scott Leyonhjelm for helpful suggestions in research. I also wish to give my special thanks to my colleagues Dr. Aaron Reid, Kevin Tom, Matthew Williamson and Mukul Mahajan for their support and friendship. Sincere acknowledgments to my colleague, Melvyn Pereira, for his genuine help. Thanks to all other staff and students of Center of Telecommunications and Micro-Electronics, Victoria University.

Most of all, I am especially grateful to my parents for their sacrifices and tremendous love to help me complete this thesis. Without them this thesis would have been nigh impossible.

# Related Publications

- V.VenkatKumar and F.-C.Zheng, “ On the Performance of Constellation Rotated NO-STBC over Correlated Fading Channels”, *AUSCTW'05*, 2- 5 Feb 2005, Brisbane , Australia.
- V.VenkatKumar and F.-C.Zheng, “ On the Performance of Constellation Rotated NO-STBC over Correlated Fading Channels”, *Proc. of IEEE VTC'05-F*, pp. 1074 - 1078 , 2- 5 Sept. 2005, Dallas , Texas, USA.

# Chapter 1

## Introduction

4G wireless communication systems are projected to provide a wide variety of new services, from high quality voice and high-speed data to high-resolution video. The overall vision for this evolving technology can be summarized in one word: *convergence* [69]. 4G systems are about seamlessly integrating terminals, wired, wireless, cellular networks and applications to form a network of networks. As of now two characteristics have emerged as all but certain components of 4G: end-end IP protocol and peer-peer networking [70]. For the wireless world, peer-peer networking is completely a new paradigm which makes *wireless ad hoc peer-peer networking* the definitive feature of future wireless systems.

### 1.1 Overview of Ad hoc networks

Ad hoc networks are typically a collection of wireless mobile nodes dynamically forming temporary networks without the aid of any established infrastructure or centralized administration[68]. In principle, distinctive features of these networks include their rapid deployment as well as resulting robustness. In these networks, network tasks are conceived to be distributed rather than centralized, topology is dynamic and routing is adaptive. Much of the ground breaking research in ad hoc wireless networks was supported by Defense Advanced projects agency (DARPA), the same organization that developed the Internet. The layered architecture of ad hoc networks is therefore largely based upon the prevalent wired Internet model.

Another important characteristic of these networks is mobility of the nodes in the network. Due to this, these networks are also popularly referred to as Mobile ad hoc networks (MANETS)[71], packet radio networks [73] or distributed packet radio networks. A large wireless network can ideally comprise many such ad hoc networks, i.e, it is a network of networks. In ad hoc network community, these localized networks are commonly categorized as clusters and information flow in a large wireless network is achieved by communication between clusters or *cluster communication* [23].

For the reasons pointed out above, ad hoc networks are highly appealing for future telecommunications. However, there exist numerous design challenges for implementing these networks. The design challenges exist at each layer in the protocol stack and can be solved either locally at each layer or in *unison*. However, amongst other reasons, layer interdependencies arise in a wireless ad hoc network primarily due to link connectivity problems and radio interference issues, both unique to the wireless media. As a result, a wireless ad hoc network design is typically considered to be a cross-layer problem [74].

The upper bound of the aggregate capacity region by multi hopping using intermediate nodes in arbitrary ad hoc networks with  $n$  nodes per unit area has been shown to follow  $O(\sqrt{n})$  bit-meters per second behavior [22], i.e., a transmission rate of  $O(\frac{1}{\sqrt{n}})$  bits per second for a source/destination pair. From this expression we can understand that inspite of being power efficient, multiple hop routing with too many hops is not desirable for throughput performance. Delay constraints, impact of bottle neck links, error propagation are few of the other issues in multi hopping which cannot be neglected. In other words, there exists a engineering trade-off between the number of hops and range in a wireless network.

Multiple antenna systems, as part of link layer solutions can help achieve this vital trade off in multi-hop networks. These systems have been shown to improve the spectral efficiency and power efficiency of point-point wireless links, thus basically facilitating efficient multi-hopping with limited number of hops. Also, communication in wireless channel happens via electro magnetic waves which evolve in three dimensions. This means that any user who is willing and is also capable of

receiving the signal can tune in to “hear” it. Therefore, with peer-peer links enabled in the wireless domain, *both cascaded and parallel* communication processes could be orchestrated amongst the intermediate nodes. Cascaded topology is popularly referred to as multi hop routing in the literature while the parallel topology has recently emerged as “cooperative networking”. Ideally, both topologies need to work in tandem by complementing one’s shortcoming with the other’s advantages in wireless ad hoc networks. In a large scale, cooperation rather than competition between radio nodes is conceived to be optimal for network performance.

## 1.2 Literature survey

This chapter summarizes important references from the vast literature that relate to the problems discussed in this thesis.

### 1.2.1 Multiple antenna systems

Recently, there has been great interest in the use of physical antenna arrays at the transmitters and/or receivers in a wireless system. The fundamental observation in [52],[64] is that when the number of transmit antennas ( $N_T$ ) and receive antennas ( $N_R$ ) increase, the link capacity grows in theory as  $\min(N_T, N_R)$ . Multiple transmit and receiver antennas can also be used for achieving diversity to combat fading in wireless communication. In the beginning, multiple receiver antennas were the primary focus of antenna diversity systems. However, because it is normally infeasible to provide large inter-antenna spacing in mobile terminals due to space limitations in handset designs, transmitter diversity by using multiple transmit antennas at the base station has attracted attention recently. The transmit and receiver diversity techniques can be combined in MIMO systems to achieve reliability in communications rather by sacrificing the capacity gain. This classical problem of spatial multiplexing-diversity trade off for multiple antenna channels has been addressed in [53]. Space-Time coding [47] is a technique to achieve spatial and temporal diversity using multiple transmit and receiver antennas. A simple form of space-time coding for achieving spatial diversity when the channel is quasi-static over the block length of the code is space-time block coding. Orthogonal space-time block codes (O-STBC) employ orthogonal signal transmissions from the transmit antennas over the block length in order to minimize interference between the transmit antennas [48].

However, full rate O-STBCs do not exist for complex constellations [48]. For full rate, codes called non-orthogonal (NO-STBC) or quasi orthogonal space time block codes [49],[67] were proposed by sacrificing the achievable diversity degree of O-STBCs. More recently, full rate constellation rotated non orthogonal codes (Cr-NOSTBC) [54],[58] have been shown to achieve diversity asymptotically and outperform non-orthogonal codes in Rayleigh fading channels. However, multiplexing and diversity benefits of multiple antenna systems can be realised only when the inter-antenna spacing is sufficient to provide low spatial correlations. In scenarios where sufficient inter-antenna spacing cannot be provided, for example, in uplink of a cellular network, cooperation by antenna sharing between users can be used to achieve better end-end link performance. Such relay cooperations are promising in both single hop and multi-hop networking scenarios as compared to multiple antenna systems which have been studied in single hop network scenarios.

### 1.2.2 Cooperative networking

The classical three terminal relay network which is central for cooperative networking was originally developed by Van der Muelen in [45]. Cover and El Gamal made further progress by developing upper and lower bounds on capacity [20]. They broadly categorized forwarding strategies of a relay as cooperation, facilitation and estimation [20]. Gastpar *et al* show that wireless network of  $n$  nodes in an unit area with  $n - 2$  nodes acting as relays follows a  $O(\log n)$  bits per second per node behavior [30]. Schein introduced a parallel relay architecture and also studied the lower and upper bounds on capacity in [17]. The classical relay architectures considered above are based on one node acting as a source with other nodes assisting the source without their own information to transmit. A cooperative architecture with more than one source is referred to as user cooperation. Carleial has examined multiple-access channel with generalized feedback from the final destination [21]. Laneman *et al* analyzed the diversity gains achievable by simple protocols in user cooperation diversity and find them to be promising at high SNR's [3]. Cooperation architectures for point-point MIMO and multi-user MIMO have also gained attention recently. The idea of relays mimicking a local antenna array at a user has been termed Virtual Antenna Array (VAA). Space-Time coding technique extended to these VAAs is termed distributed space-time coding [4]. As an alternative to these rate reducing techniques, distributed turbo coding or coded cooperation

has been proposed in [14]. Sendonaris *et al* considered cooperative diversity for a multiple-access channel with relaying and fading [4],[5]. They note that the performance criterion is the throughput, i.e, received bits/second rather than the transmitted bits/second and observe that at high SNR, cooperation enlarges the achievable rate region for the network.

### 1.3 Summary of contributions

The first contribution of this work is to analyze the effect of antenna correlation on full rate full diversity space-time block codes. To this end, we investigate the performance of a constellation rotated space-time block code in correlated rayleigh fading channels. We statistically model the correlation using first order Markov process. Under this model, the loss function on the pair-wise error probability against correlation coefficient is characterized. We also study the matched filter output at the receiver to further understand the performance. In the results, we compare the performance degradation of the NO-STBC and Cr-NOSTBC schemes. It is observed that the performance benefit of constellation rotations reduces as correlation increases. The key observation is that performance of both robust NO-STBC and Cr-NOSTBC begin to resemble the matched filter bound as correlation increases.

In highly spatially correlated channel conditions, it has been shown that multiple antenna diversity benefits are not significant. In scenarios where multiple antenna systems are not always feasible or when the gains are limited, relay diversity systems are a good alternative way of realising diversity gains. In addition, the fundamentals of transmit diversity techniques can be extended to the relay case if the users engage in a simple physical layer antenna sharing strategy. Therefore, we now move on relay diversity schemes to analyse the gains that can be achieved using such schemes. In particular, we investigate low complexity relaying for the simple three terminal network. We first observe that a blind symbol-wise decode and forward scheme does not achieve any diversity benefit in Rayleigh fading channels. To overcome this problem, we make use of selection relaying as a technique to improve relay reliability. For selection relaying, we derive optimal thresholds at the relay for the three terminal network using channel estimation at the receiver. We observe that relaying via this means significantly improves the BER performance over the blind decode and forward scheme and thereby demonstrate the sensitivity of threshold levels for achieving performance benefits. The BER improvement using these thresholds only gets better if the target diversity is 3 in the network. Finally, we analyze the impact of channel estimation errors at the relay on the performance of selection relaying. It is observed that near-optimality of the threshold cushions the impact of channel estimation errors on the uncoded BER performance at the destination receiver.

## 1.4 Structure of the thesis

The thesis is organized as follows.

In chapter 2, a literature survey on space-time block coding techniques is carried out. The fundamentals of the theory of space-time block coding is discussed for various techniques. Based on the literature survey, full-diversity orthogonal schemes, full-rate non-orthogonal schemes are explained in detail in this chapter. Diversity achieving constellation rotation schemes for full rate-non orthogonal schemes are also explained in some detail in this chapter.

Chapter 3 concerns the performance of space-time block coding under spatial correlation. Specifically, we characterize the performance loss of a full diversity, full rate robust constellation rotated code in this chapter by using a statistical channel model. We explain the performance loss of the scheme based on an analytic approach on the PEP.

In chapter 4 we conduct a literature survey on the principles of user cooperation. The system model of the classical three terminal network is introduced in this chapter. Relay node functionalities and relaying strategies are briefly discussed. Architectures under which user cooperation becomes feasible and at the same time useful are also outlined. Following this, system models of relay diversity systems such as  $n$ -terminal orthogonal parallel relay network and distributed space-time coding are addressed. Finally, some useful detection strategies are briefed.

Chapter 5 is dedicated to the derivation of an optimal threshold for a selection relay-three terminal network. Thresholds which minimize the BER under various scenarios in a three terminal network are presented.

## Chapter 2

# Space-Time Block coding

### 2.1 Introduction

A reliable and power-efficient operation in wireless channels can be achieved when the same data appears in multiple time instants, frequencies or antennas at the receiver. This is popularly known as “diversity” and it is the most significant contributor to reliable wireless communications. In most wireless communication systems, a number of diversity methods are used in order to obtain the required performance. In the recently developed concepts, multiple transmit antennas are used to provide diversity at the receiver and is popularly known as ‘transmit diversity’. Transmit diversity is particularly appealing because of its relative simplicity of implementation and the feasibility of multiple antennas at the base station. By using multiple transmit antennas, the transmitted signal can now be arranged in both space (antennas) and time dimensions. This concept is known as “Space-Time Coding”.

The Alamouti scheme [46] was historically the first scheme to achieve full diversity with two transmit antennas with a simple maximum-likelihood decoding algorithm. This scheme was generalized to an arbitrary number of transmit antennas and formally termed “Space-Time Block codes” (STBC) in [48]. In this chapter, the concept of Space-Time Block coding for achieving diversity is reviewed. First, the orthogonal designs which were originally introduced in [48] are described. Then, non-orthogonal designs which provide higher data rate are discussed, and finally, the concept of

constellation rotation for achieving full diversity in non-orthogonal designs is explained in detail.

## 2.2 Space-time block encoder

Figure 1. shows an encoder structure for space-time block codes. A space-time block code employing  $N_T$  transmit antennas and  $T$  symbol periods is described by a  $T \times N_T$  matrix  $\mathbf{X}$ . In a linear space-time coded scheme, the space-time transmission matrix  $\mathbf{X}$  is a linear function of the  $Q$  symbols to be transmitted. A characteristic property of the Space-Time Block codes is that they are defined as matrices and are typically linear codes over the field of complex numbers without an underlying trellis structure. In contrast with this, space-time codes used in Space-Time trellis codes (STTC) and in basic MIMO systems are typically vectors. Also, STTC's are not linear codes over the field of complex numbers because they are functions of encoded bits (with memory). A linear space-time transmission matrix can be expressed as

$$\mathbf{X} = \sum_{k=1}^Q \mathbf{X}_{\mathbf{k}}(x_k; x_k^*) \quad (2.1)$$

where  $\mathbf{X}_{\mathbf{k}}$  is a  $T \times N_T$  matrix with complex entries which are linear functions of symbol  $x_k$  or  $x_k^*$ . Thus the symbol rate, the number of complex symbols transmitted in time period  $T$  is  $R = \frac{Q}{T}$ .

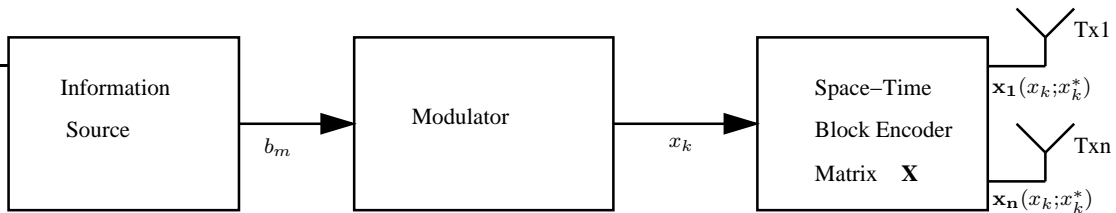


Figure 2.1: Space-time block code encoder.

Fig 2.1 shows a Space-Time Block code encoder. Information bits  $b_m$  from a source are mapped to symbols  $x_k$  at the modulator.  $Q$  symbols are then fed to the space-time block code encoder.  $N_T$  transmit antennas transmit according to their transmission vectors  $\mathbf{x}_i(x_k; x_k^*) \quad i = 1..N_T$  (of dimension  $T$ ) defined as per the  $T \times N_T$  space-time code matrix  $\mathbf{X} = \begin{bmatrix} \mathbf{x}_1 & \mathbf{x}_2 & \dots & \mathbf{x}_{N_T} \end{bmatrix}$ .

The system model for  $N_R$  receive antennas for a flat fading channel model then reads

$$\mathbf{Y} = \sqrt{E_s} \mathbf{X} \mathbf{H} + \sqrt{N_o} \mathbf{N}, \quad (2.2)$$

where  $\mathbf{H}$  is a  $N_T \times N_R$  channel matrix with entries  $h_{ik}$  as the complex channel gain from the  $i^{\text{th}}$  transmit antenna to the  $k^{\text{th}}$  receiver antenna.  $\mathbf{N}$  is the  $T \times N_R$  noise matrix and  $\mathbf{Y}$  is the  $T \times N_R$  matrix of received signals. The  $n^{\text{th}}$  transmit antenna therefore transmits a column vector  $\mathbf{x}_n$  for  $T$  symbol periods such that  $\mathbf{x}_n$  is a linear combination of symbols  $x_k, x_k^*$ . The average symbol power is normalized to one, i.e,  $E[|x_i|^2] = 1$ . The total radiated power from the terminal is constrained to  $P$  regardless of the number of transmitter antennas, i.e,  $E_s = \frac{P}{N_T}$  such that  $\frac{P}{N_o}$  is the received  $SNR$  at each receiver antenna at a time slot. For reliable detection it is assumed that the channel coherence time is greater than  $T$  symbol periods.

In quasi-static Rayleigh fading channels, minimizing the pairwise error probability of deciding in favor of an erroneous matrix  $\tilde{\mathbf{X}}$  when transmitting  $\mathbf{X}$  leads to the well known rank and determinant criterion. The code difference matrix can be expressed as  $\mathbf{A} = \tilde{\mathbf{X}} - \mathbf{X}$ . As a consequence of linearity in the space-time code design, the codeword difference matrix can be expressed in terms of the space-time code as  $\mathbf{A} = \mathbf{X}(\Delta)$ . Therefore, the pairwise error probability conditioned on  $\mathbf{H}$  can be written as

$$P(\mathbf{X}, \tilde{\mathbf{X}} | \mathbf{H}) = Q\left(\frac{E_s}{2N_o} d^2(\mathbf{X}, \tilde{\mathbf{X}})\right), \quad (2.3)$$

where  $E_s$  is the energy per symbol at each transmit antenna and  $Q(x)$  is the complimentary error function defined by  $Q(x) = \frac{1}{\sqrt{2\pi}} \int_x^\infty e^{-\frac{t^2}{2}} dt$  and  $d^2(\mathbf{X}, \tilde{\mathbf{X}}) = \|\mathbf{H} \cdot \mathbf{A}\|_F^2$ . The conditional pair wise error probability can be upper bounded by [47],

$$P(\mathbf{X}, \tilde{\mathbf{X}} | \mathbf{H}) \leq \exp\left(-d^2(\mathbf{X}, \tilde{\mathbf{X}}) \frac{E_s}{4N_o}\right). \quad (2.4)$$

The pair wise error probability has been derived for quasi-static Rayleigh fading channels as [47]

$$P(\mathbf{X}, \tilde{\mathbf{X}}) \leq \prod_{i=1}^{N_T} \left(1 + \lambda_i(\mathbf{A}^H \mathbf{A}) \frac{E_s}{4N_o}\right)^{-N_R}, \quad (2.5)$$

where  $\lambda_i(\mathbf{X})$  denotes the  $i^{th}$  eigen value of a matrix  $\mathbf{X}$ , or equivalently,

$$P(\mathbf{X}, \tilde{\mathbf{X}}) \leq \det(\mathbf{I}_{N_T} + \frac{E_s}{4N_o} \mathbf{A}^H \mathbf{A})^{-N_R}. \quad (2.6)$$

At high SNR's , this takes the form

$$P(\mathbf{X}, \tilde{\mathbf{X}}) \leq \prod_{i=1}^s (\lambda_i(\mathbf{A}^H \mathbf{A}))^{-N_R} \left(\frac{E_s}{4N_o}\right)^{-sN_R} \quad (2.7)$$

where  $s$  is the minimum rank of matrix  $\mathbf{A}$  over all codeword pairs.

From the above equation we have the well-known rank and determinant criteria [47].

**Rank criteria:** The transmit diversity of a space-time code is  $\min_{\Delta \neq 0} Rank(\mathbf{A})$ . To achieve maximal diversity, the code difference matrix should have full rank for all code word pairs.

**Determinant criteria:** To optimize performance, the space-Time code should be designed to maximize  $\min_{\Delta \neq 0} \prod_{i=1}^r \lambda_i$  of matrix  $\mathbf{A}$ . Note that  $\prod_{i=1}^r \lambda_i$  is the absolute value of the sum of determinants of all the principal co-factors of code distance matrix  $\mathbf{A}^H \mathbf{A}$ .

## 2.3 Orthogonal designs

The Alamouti scheme [46] transmits two orthogonal sequences with the two transmit antennas to achieve transmit diversity. This scheme was a starting point for similar schemes using more than two transmit antennas. For more than two transmit antennas, the Alamouti scheme was generalized using the theory of orthogonal designs and was termed ‘‘Space-Time Block codes’’. Therefore, the term ‘‘Space-Time Block code’’ was originally introduced only for orthogonal designs in [48].

The defining characteristics of orthogonal designs are linearity and unitarity such that

$$\mathbf{X}^H \mathbf{X} = \text{diag}(\|\mathbf{x}_1\|^2, \|\mathbf{x}_2\|^2, \dots, \|\mathbf{x}_{N_T}\|^2), \quad (2.8)$$

where  $\mathbf{x}_i$  is the transmission sequence from the  $i^{th}$  transmit antenna, or simplistically [48]

$$\mathbf{X}^H \mathbf{X} = c \sum_{k=1}^Q |x_k|^2 \mathbf{I}_{N_T}. \quad (2.9)$$

where  $c \geq 1$  is any integer. A linear space-time transmission matrix can also be expressed as [17]

$$\mathbf{X} = \sum_{k=1}^{2Q} c_k \mathbf{G}^k, \quad (2.10)$$

using a set of matrices  $\mathbf{G}^k$ , where  $c_{2k-1}, c_{2k}$  are the real and imaginary parts of the symbol  $x_k$ . The signals sequences from any two transmit antennas are orthogonal such that

$$\sum_{i=1}^T \mathbf{x}_i \cdot \mathbf{x}_j = 0. \quad (2.11)$$

The transmitted signals form an orthonormal basis for the signal space. Therefore for specific constellation symbols  $S$ ,  $N_T$  transmission vectors  $\mathbf{x}_1, \mathbf{x}_2 \dots \mathbf{x}_n$  create a basis for a  $T$ -dimensional space. This means that interference between any two basis matrices is null [62].

$$\mathbf{S}^{ik} = \mathbf{G}^{iH} \mathbf{G}^k + \mathbf{G}^{kH} \mathbf{G}^i = \mathbf{0} \quad \forall \quad i \neq k. \quad (2.12)$$

and also,

$$\mathbf{G}^{iH} \mathbf{G}^i = \mathbf{I}_{N_T} \quad \forall \quad i. \quad (2.13)$$

Code constructions which satisfy Eq(2.13) achieve maximal symbolwise diversity (MSD) [49],[50],[61]. For example, the codes in [3] for real and complex constellations satisfy the maximal symbolwise diversity criterion.

### 2.3.1 Example codes

#### 2.3.1.1 Real signal constellations

For any arbitrary real signal constellation, it has been shown that space-time block codes with  $N_T \times N_T$  square transmission matrix exist if and only if the number of transmit antennas  $N_T = 2, 4, 8$  [48]. These codes are full rate  $R = 1$  and offer full transmit diversity of  $N_T$ .

The transmission matrices are given by [48] for  $N_T = 2$

$$\mathbf{X} = \begin{bmatrix} x_1 & -x_2 \\ x_2 & x_1 \end{bmatrix}, \quad (2.14)$$

and for  $N_T = 4$

$$\mathbf{X} = \begin{bmatrix} x_1 & -x_2 & -x_3 & -x_3 \\ x_2 & x_1 & x_4 & -x_3 \\ x_3 & -x_4 & x_1 & x_2 \\ x_4 & x_3 & -x_2 & x_1 \end{bmatrix}. \quad (2.15)$$

It has also been shown that that the minimum number of transmission periods  $T$  for a full rate rectangular design is [48]

$$\min(2^{4c+d}) \quad (2.16)$$

where the minimization is taken over the set

$$c, d \quad | \quad 0 \leq c, \quad 0 \leq d \leq 4 \quad 8c + 2^d \geq N_T \quad (2.17)$$

### 2.3.1.2 Complex signal constellations

Allowing complex signal constellations severely restricts the number of transmit antennas for which  $R = 1$  codes exist. Indeed,  $R = 1$  complex space-time block codes exist only for two transmit antennas [48] and is the well-known Alamouti design given by

$$\mathbf{X} = \begin{bmatrix} x_1 & -x_2^* \\ x_2 & x_1^* \end{bmatrix}. \quad (2.18)$$

For  $N_T = 4$  transmit antennas a half rate scheme was presented in [48] as

$$\mathbf{X} = \begin{bmatrix} x_1 & x_2 & x_3 & x_4 \\ -x_2 & x_1 & -x_4 & x_3 \\ -x_3 & x_4 & x_1 & -x_2 \\ -x_4 & -x_3 & x_2 & x_1 \\ x_1^* & x_2^* & x_3^* & x_4^* \\ -x_2^* & x_1^* & -x_4^* & x_3^* \\ -x_3^* & x_4^* & x_1^* & -x_2^* \\ -x_4^* & -x_3^* & x_2^* & x_1^* \end{bmatrix}. \quad (2.19)$$

Apart from the above rate-halving scheme, a  $R = \frac{3}{4}$  scheme for four transmit antennas was presented in [48] as

$$\mathbf{X} = \begin{bmatrix} x_1 & x_2 & \frac{1}{\sqrt{2}}x_3 & \frac{1}{\sqrt{2}}x_3 \\ -x_2^* & x_1^* & \frac{1}{\sqrt{2}}x_3 & -\frac{1}{\sqrt{2}}x_3 \\ \frac{1}{\sqrt{2}}x_3^* & \frac{1}{\sqrt{2}}x_3^* & -\Re[x_1] + j\Im[x_2] & j\Im[x_1] - \Re[x_2] \\ \frac{1}{\sqrt{2}}x_3^* & -\frac{1}{\sqrt{2}}x_3^* & j\Im[x_1] + \Re[x_2] & -\Re[x_1] - j\Im[x_2] \end{bmatrix}. \quad (2.20)$$

The above design has also been simplified in [51] as

$$\mathbf{X} = \begin{bmatrix} x_1 & x_2 & x_3 & 0 \\ -x_2^* & x_1^* & 0 & -x_3 \\ -x_3^* & 0 & x_1^* & x_2 \\ 0 & x_3^* & -x_2^* & x_1 \end{bmatrix}. \quad (2.21)$$

### 2.3.2 Maximum likelihood decoding

Maximum likelihood detector chooses matrix  $\tilde{\mathbf{X}}$  which maximizes the likelihood function

$$\Omega = \exp[-tr((\mathbf{Y} - \tilde{\mathbf{X}}\mathbf{H})^H(\mathbf{Y} - \tilde{\mathbf{X}}\mathbf{H}))]. \quad (2.22)$$

From this we obtain the maximum likelihood distance metric

$$d = tr((\mathbf{Y} - \tilde{\mathbf{X}}\mathbf{H})^H(\mathbf{Y} - \tilde{\mathbf{X}}\mathbf{H})). \quad (2.23)$$

This is equivalent to maximizing the metric

$$\acute{d} = tr(2\Re(\mathbf{H}^H \tilde{\mathbf{X}}^H \mathbf{Y}) - \mathbf{H}^H \tilde{\mathbf{X}}^H \tilde{\mathbf{X}} \mathbf{H}). \quad (2.24)$$

For orthogonal designs, this can be rewritten as

$$\acute{d} = tr(2\Re(\mathbf{H}^H \tilde{\mathbf{X}}^H \mathbf{Y})) - \|\mathbf{H}\|_F^2 \sum_{k=1}^Q |\tilde{x}_k|^2 \mathbf{I}_{N_T}. \quad (2.25)$$

Because  $tr(2\Re(\mathbf{H}^H \tilde{\mathbf{X}}^H \mathbf{Y}))$  is a linear function in symbols  $\tilde{x}_k$ , we can observe that in Eq(2.24),  $\acute{d}$  is linear in symbols  $x_k$  and therefore maximum likelihood detection becomes possible with linear complexity. Infact, because the signals get naturally decoupled in maximum likelihood detection, orthogonal designs represent the matched filter bound or the MRC bound for transmit diversity (without any interference).

### 2.3.3 Equivalent channel representation

Due to linearity of the scheme in real symbols  $\mathbf{c}$ , the system can be expressed in the form

$$\hat{\mathbf{y}} = \hat{\mathbf{H}}\mathbf{c} + \mathbf{n}, \quad (2.26)$$

where  $\hat{\mathbf{y}}$  is  $(TN_R) \times 1$  vector obtained by re-arranging the received signal matrix  $\mathbf{Y}$ , the matrix  $\hat{\mathbf{H}}$  is termed the equivalent channel matrix with dimensions  $TN_R \times 2Q$  and  $\mathbf{c}$  is a vector of real

symbols of dimension  $2Q$ . If during one symbol period, only symbols or complex conjugates are transmitted, then the signal model can be written in terms of complex symbols as

$$\hat{\mathbf{y}} = \hat{\mathbf{H}}\mathbf{x} + \mathbf{n}, \quad (2.27)$$

where  $\hat{\mathbf{H}}$  is a  $TN_R \times Q$  matrix and  $\hat{\mathbf{y}}$  is  $(TN_R) \times 1$  obtained by re-arranging matrix  $\mathbf{Y}$ . Maximum likelihood detection can also be alternatively carried out using the signals models in Eq(2.26) or Eq(2.27). From Eq(2.27), it is straightforward to express the likelihood function for decoding complex symbols as

$$\Omega = \exp[-\|(\hat{\mathbf{y}} - \hat{\mathbf{H}}\tilde{\mathbf{x}})\|^2]. \quad (2.28)$$

This is equivalent to maximizing

$$2\Re(\tilde{\mathbf{x}}^H \hat{\mathbf{H}}^H \hat{\mathbf{y}}) - \tilde{\mathbf{x}}^H \hat{\mathbf{H}}^H \hat{\mathbf{H}} \tilde{\mathbf{x}}. \quad (2.29)$$

In Eq(2.29), the term  $\mathbf{z} = \hat{\mathbf{H}}^H \hat{\mathbf{y}}$  represents the sufficient statistics for detection which is the matched filter outputs of the received signal at the receiver. It can be seen that, if the matched filter outputs are decoupled, then the maximum likelihood detection is linear in complexity. This is the basic premise of space-time block coding.

For example, consider the Alamouti scheme in Eq(2.18) for  $N_R = 1$ . From the maximum likelihood detection metric in Eq(2.23) we have

$$d = |y_1 - h_1\tilde{x}_1 - h_2\tilde{x}_2|^2 + |y_2 + h_1\tilde{x}_2^* - h_2\tilde{x}_1^*|^2. \quad (2.30)$$

Expanding the above metric, it is easy to see that it is equivalent to maximizing

$$\hat{d} = 2\Re(\tilde{x}_1 z_1^*) + 2\Re(\tilde{x}_2 z_2^*) - (|h_1|^2 + |h_2|^2)(|\tilde{x}_1|^2 + |\tilde{x}_2|^2) \quad (2.31)$$

where, comparing with Eq(2.29),  $z_1 = h_1^* y_1 + h_2 y_2^*$ ,  $z_2 = h_2^* y_1 - h_1 y_2^*$  form the sufficient statistics from the matched filter output. Therefore we can deduce that if Grammmian matrix of  $\mathbf{X}$ ,  $\mathbf{X}^H \mathbf{X} =$

$c \sum_{i=1}^Q |x_i|^2 \mathbf{I}_{N_T}$  or equivalently, if  $\hat{\mathbf{H}}^H \hat{\mathbf{H}} = \|\mathbf{H}\|_F^2 \mathbf{I}_Q$ , then maximum likelihood decoding in linear complexity with maximal diversity becomes possible.

### 2.3.4 Capacity and Performance

It has been shown in [52] that MIMO capacity grows linearly with  $\min(N_T, N_R)$ . This gain is also popularly known as the spatial multiplexing gain. It is also very clear that multiple transmit and receiver antennas can be used to provide diversity gain at the receiver. The trade off between multiplexing gain and diversity gain has been characterized as Diversity-Multiplexing trade off in [53]. It has also been shown in [53] that the Alamouti scheme achieves this trade off if  $N_R = 1$ . This naturally lends itself to that, if a linear full rate complex orthogonal design exists, it will achieve the trade off for arbitrary number of transmit antennas and for one receiver antenna. In other words, a complex orthogonal design is capacity optimal if  $N_R = 1$ . This is in contrast to the results established in [7] which show that when the transmission scheme is a full rate vector it reaches capacity for arbitrary number of  $N_T \times N_R$  antennas. In addition to this, it turns out that a full rate linear complex orthogonal design does not exist for  $N_T > 2$  [48]. This makes existing linear complex orthogonal schemes capacity sub-optimal even for  $N_R = 1$  if  $N_T > 2$ .

## 2.4 Non-orthogonal designs

Space-Time transmission matrices as discussed in the previous section follow three constructions criteria of linearity, orthogonality and diversity. From the performance viewpoint the above options translate to a rate-diversity tradeoff in constructing the code.

The Space-Time Block codes [48] achieve full diversity with simultaneous orthogonality and linearity. The most attractive feature of this scheme is that maximum likelihood decoding with linear complexity becomes possible as the signals get decoupled at the receiver. However, they are not full rate codes for  $N_T > 2$  and therefore make inefficient use of multiple antennas. To increase the symbol rate, either the diversity gain may be sacrificed retaining orthogonality and linearity, or orthogonality may be compromised retaining linearity or otherwise linearity could be sacrificed to achieve diversity gain. Either choice has its own advantages and disadvantages. However com-

promising on orthogonality or linearity typically results in an increase in decoding complexity. Linear non-orthogonal designs compromise on orthogonality and retain the linearity in space-time transmission matrices. Therefore, for a non-orthogonal scheme we have that the Grammian matrix,

$$\mathbf{X}^H \mathbf{X} \neq \text{diag}(\|\mathbf{x}_1\|^2, \|\mathbf{x}_2\|^2, \dots, \|\mathbf{x}_{N_T}\|^2) \quad (2.32)$$

where  $\mathbf{x}_1, \mathbf{x}_2, \dots, \mathbf{x}_{N_T}$  are the transmission sequences from the transmit antennas. The Grammian matrix of  $\mathbf{X}$  can therefore be generalized as

$$\mathbf{X}^H \mathbf{X} = \mathbf{D} + \mathbf{X}_I, \quad (2.33)$$

where  $\mathbf{X}_I$  trivially characterizes interference caused by the non-orthogonality of signal sequences between transmit antennas and  $\mathbf{D} = \text{diag}(\|\mathbf{x}_1\|^2, \|\mathbf{x}_2\|^2, \dots, \|\mathbf{x}_{N_T}\|^2)$ .

In addition to this, if

$$\mathbf{D} = \sum_{k=1}^Q |x_k|^2 \mathbf{I}_{N_T} \quad (2.34)$$

or equivalently if

$$\mathbf{G}^{iH} \mathbf{G}^i = \mathbf{I}_{N_T} \quad \forall i \quad (2.35)$$

then the non-orthogonal scheme provides maximal symbolwise diversity [49],[50]. From Eq(2.10) and Eq(2.33), it is easy to see that interference between any two basis matrices of the symbols is non vanishing for these designs such that

$$\mathbf{S}^{ik} = \mathbf{G}^{iH} \mathbf{G}^k + \mathbf{G}^{kH} \mathbf{G}^i \neq \mathbf{0} \quad \forall \quad i \neq k. \quad (2.36)$$

#### 2.4.1 Maximum likelihood decoding

The maximum likelihood detector metric is similar to Eq(2.24)

$$\hat{d} = \text{tr}(2\Re(\mathbf{H}^H \tilde{\mathbf{X}}^H \mathbf{Y}) - \mathbf{H}^H \tilde{\mathbf{X}}^H \tilde{\mathbf{X}} \mathbf{H}). \quad (2.37)$$

However, due to non-orthogonality between the transmission sequences, the Grammian matrix of  $\mathbf{X}$  is no longer linear in the symbols  $x_k$ . Therefore, the maximum likelihood detection reads

$$\hat{d} = \text{tr}(2\Re(\mathbf{H}^H \tilde{\mathbf{X}}^H \mathbf{Y}) - \mathbf{H}^H \tilde{\mathbf{D}} \mathbf{H} + \mathbf{K}_{\mathbf{I}}(F_n(x_i, x_j))), \quad (2.38)$$

where  $F_n(x_i, x_j)$  indicates that considering all the entries of the matrix  $\tilde{\mathbf{X}}_{\mathbf{I}}$ , if symbols which combine non-linearly in  $k_{th}$  entry can be represented by  $k_{th}$  set, then there are  $n$  such disjoint sets and  $\mathbf{K}_{\mathbf{I}} = \mathbf{H}^H \tilde{\mathbf{X}}_{\mathbf{I}} \mathbf{H}$ . For example, consider two non-orthogonal designs, the PSK full rank scheme of [59]

$$\mathbf{X} = \begin{bmatrix} x_1 & x_2 & x_3 & x_4 \\ x_2 & x_3 & x_4 & x_1 + x_2 \\ x_3 & x_4 & x_1 + x_2 & x_2 + x_3 \\ x_4 & x_1 + x_2 & x_2 + x_3 & x_3 + x_4 \end{bmatrix}. \quad (2.39)$$

and the ‘‘ABBA’’ scheme of [49]

$$\mathbf{X} = \begin{bmatrix} x_1 & x_2 & x_3 & x_4 \\ -x_2^* & x_1^* & -x_4^* & x_3^* \\ x_3 & x_4 & x_1 & x_2 \\ -x_4^* & x_3^* & -x_2^* & x_1^* \end{bmatrix}. \quad (2.40)$$

In the PSK scheme, computing the Grammian matrix shows that all the symbols combine non-linearly with each other and therefore  $n = 0$ . In contrast, for the ABBA scheme the Grammian matrix of  $\mathbf{X}$  has symbols within sets  $\{x_1, x_3\}$  and  $\{x_2, x_4\}$  combining non-linearly. This makes  $n = 2$  for this scheme. Therefore, maximum likelihood detection of the PSK scheme, is typically joint detection of all the symbols  $\{x_1, x_2, x_3, x_4\}$ , while for ABBA scheme, joint detection of symbols  $\{x_1, x_3\}$  and  $\{x_2, x_4\}$  can be carried out separately which reduces the complexity of ML detection. This ‘‘pairwise detection’’ becomes possible because of the ‘‘Quasi-Orthogonal’’ [67] structure of the space-time transmission matrix in Eq(2.40) in which two pairs of symbols out of 4 symbols are mutually orthogonal.

To illustrate this further, consider the NO-STBC for  $N_T = 4$  in [54] given by the matrix

$$\mathbf{X} = \begin{bmatrix} x_1 & x_2 & x_3 & x_4 \\ x_2^* & -x_1^* & x_4^* & -x_3^* \\ x_3 & -x_4 & -x_1 & x_2 \\ x_4^* & x_3^* & -x_2^* & -x_1^* \end{bmatrix}. \quad (2.41)$$

We can easily calculate the Grammian matrix as,

$$\mathbf{X}^H \mathbf{X} = \begin{bmatrix} \sum_{i=1}^4 |x_i|^2 & 0 & -2j\Im(x_1x_3^*) - 2j\Im(x_2^*x_4) & 0 \\ 0 & \sum_{i=1}^4 |x_i|^2 & 0 & 2j\Im(x_1x_3^*) + 2j\Im(x_2^*x_4) \\ 2j\Im(x_1x_3^*) + 2j\Im(x_2^*x_4) & 0 & \sum_{i=1}^4 |x_i|^2 & 0 \\ 0 & 2j\Im(x_1x_3^*) + 2j\Im(x_2^*x_4) & 0 & \sum_{i=1}^4 |x_i|^2 \end{bmatrix} \quad (2.42)$$

It can be observed from Eq(2.42) that  $\mathbf{D} = \sum_{i=1}^4 |x_i|^2 \mathbf{I}_4$ . Therefore we can conclude that this scheme offers MSD. Also, only symbols within sets  $\{x_1, x_3\}$  and  $\{x_2, x_4\}$  combine non-linearly, i.e, interference is only between symbols in the same set. Therefore, similar to the decoding of ABBA scheme, the ML decoding for this NO-STBC system also decomposes into decoding of two pairs of symbols  $\{x_1, x_3\}$  and  $\{x_2, x_4\}$ .

The maximum likelihood distance metric for detection with  $N_R = 1$  is given by,

$$d = \|\mathbf{y} - \tilde{\mathbf{X}}\mathbf{h}\|^2 \quad (2.43)$$

Upon expanding Eq(2.43), the metric conveniently breaks down to a sum  $\hat{d}_1 + \hat{d}_2$  where

$$\hat{d}_1 = \left( \sum_{i=1}^4 |h_i|^2 (|x_1|^2 + |x_3|^2) \right) + 2\Re((-h_1y_1^* + h_2^*y_2 + h_3y_3^* + h_4^*y_4)\tilde{x}_1) \quad (2.44)$$

$$+((-h_3y_1^* + h_4^*y_2 - h_1y_3^* - h_2^*y_4)\tilde{x}_3) + ((h_1h_3^* - h_1^*h_3 + h_2^*h_4 - h_2h_4^*)(\tilde{x}_1 * \tilde{x}_3^*)); \quad (2.45)$$

and

$$\acute{d}_2 = \left( \sum_{i=1}^4 |h_i|^2 (|x_2|^2 + |x_4|^2) \right) + 2\Re((( -h_2y_1^* - h_1^*y_2 - h_4y_3^* + h_3^*y_4)\tilde{x}_2)) \quad (2.46)$$

$$+ ((-h_4y_1^* - h_3^*y_2 - h_1^*y_4 + h_2y_3^*)\tilde{x}_4) + ((-h_1h_3^* + h_1^*h_3 - h_2^*h_4 + h_2h_4^*)(\tilde{x}_2 * \tilde{x}_4^*)) \quad (2.47)$$

In the light of above example we can observe that, increase in symbol rate could be engineered using a “quasi-orthogonal” design which also significantly reduces the complexity of ML detection.

## 2.5 Constellation rotation

The concept of signal diversity or modulation diversity was first introduced to realize time diversity in the spirit of product distance criterion in [54],[55]. An example of this approach to realize time diversity for PSK signals by symbol interleaving is the constellation rotation technique in [57]. In this technique, QPSK symbols are rotated and their quadrature components are interleaved to achieve temporal diversity. The basic idea of this concept is to maximize the distance between coordinate dimensions in a  $D$ -dimensional signal space. This technique can be similarly applied in space-time coding [54],[58] for realizing spatial diversity based on the rank and determinant criterion. For this purpose, consider the quasi-orthogonal scheme given by Eq(2.41). It follows from the rank criteria, that diversity order of the NO-STBC is equal to minimum rank of code distance matrix. The asymptotic BER performance can therefore be maximized using the space-time code design principles of maximizing the rank first and then maximizing the minimum determinant. Due to linearity of the transmission matrix Eq(2.41), the code difference matrix can be easily expressed as  $\mathbf{A} = \mathbf{X}(\mathbf{\Delta})$ . The code difference vector  $\mathbf{\Delta}$  between transmitted and received symbols is  $\mathbf{\Delta} = \begin{bmatrix} \Delta_1 & \Delta_2 & \Delta_3 & \Delta_4 \end{bmatrix}$  where  $\Delta_i = x_i - \tilde{x}_i$ , such that

$$\mathbf{A} = \begin{bmatrix} \Delta_1 & \Delta_2 & \Delta_3 & \Delta_4 \\ \Delta_2^* & -\Delta_1^* & \Delta_4^* & -\Delta_3^* \\ \Delta_3 & -\Delta_4 & -\Delta_1 & \Delta_2 \\ \Delta_4^* & \Delta_3^* & -\Delta_2^* & -\Delta_1^* \end{bmatrix}. \quad (2.48)$$

According to the rank criterion, to achieve full diversity, the code distance matrix given by  $\mathbf{B} = \mathbf{A}^H \mathbf{A}$  should be full rank for all possible error events.

It is easy to show that the determinant of code distance matrix  $\mathbf{B} = \mathbf{A}^H \mathbf{A}$  is

$$D = [|\Delta_1^2 + \Delta_3^2|^2 + |\Delta_2^2 + \Delta_4^2|^2 + 2(|\Delta_1^2| + |\Delta_3^2|)(|\Delta_2^2| + |\Delta_4^2|) - 8\Im(\Delta_1\Delta_3^*)\Im(\Delta_4\Delta_2^*)]^2, \quad (2.49)$$

where  $\Im(x + jy) = y$ .

Denoting  $\xi_1 = |\Delta_1^2 + \Delta_3^2|^2$ ,  $\xi_2 = |\Delta_2^2 + \Delta_4^2|^2$ ,  $t_1 = \Im(\Delta_1\Delta_3^*)$  and  $t_2 = \Im(\Delta_4\Delta_2^*)$ ,  $D$  can be rewritten as

$$D = [\xi_1 + \xi_2 + 2\sqrt{\xi_1 + 4t_1^2}\sqrt{\xi_2 + 4t_2^2} - 8t_1t_2]^2. \quad (2.50)$$

It can be observed from Eq(2.50) that the matrix  $\mathbf{B}$  is singular when both  $\xi_1 = 0$  and  $\xi_2 = 0$ ,  $t_1, t_2 > 0$  or  $t_1, t_2 < 0$ . Since constellation  $\mathcal{Q}_i = \mathcal{Q}_{i+1}$ , where  $\mathcal{Q}_i$  denotes the constellation from which the symbol  $x_i$  is obtained, all combinations of  $(\Delta_1, \Delta_3)$  and  $(\Delta_2, \Delta_4)$  are symmetric. Therefore it suffices to make  $\xi_1 \neq 0$   $\xi_2 \neq 0$  to achieve a non singular  $\mathbf{B}$  over all possible error events. This can be achieved by rotating the symbols  $x_3, x_4$  optimally to  $x_3e^{j\phi}, x_4e^{j\phi}$  respectively. For those particular combinations of  $(\Delta_1, \Delta_3)$ ,  $(\Delta_2, \Delta_4)$  which result in the minima of  $\xi_1$ , maximizing the minima of  $\xi_1$  using rotations of the type  $e^{j\phi}$ , minimizes  $t_1$  as well. Therefore, it can be observed from Eq(2.50) that the minima of  $\xi_1$  (and simultaneously of  $\xi_2$ ), equivalently maximizes  $D$  over all possible error events.

It is notable that at  $\xi_1 = 0$ , we have  $\pm\Delta_1 = j\Delta_3$ , therefore  $x_1 \pm jx_3 = \tilde{x}_1 \pm j\tilde{x}_3$  leading to zero Euclidean distance between certain constellation points in the ‘‘super symbol’’ constellations  $\mathcal{Q}_1 \pm j\mathcal{Q}_3$ ,  $x_1 \in \mathcal{Q}_1, x_3 \in \mathcal{Q}_3$ , as in [14]. The plot of minima of  $\xi_1$  against angle of rotation  $\phi$  when  $\mathcal{Q}_1, \mathcal{Q}_3$  are  $\pi/4$  QPSK constellations is shown in Fig 2.2. It can also be seen that optimum angle of rotation is in the vicinity of 0.5 radian for QPSK constellation. The constellation rotation scheme

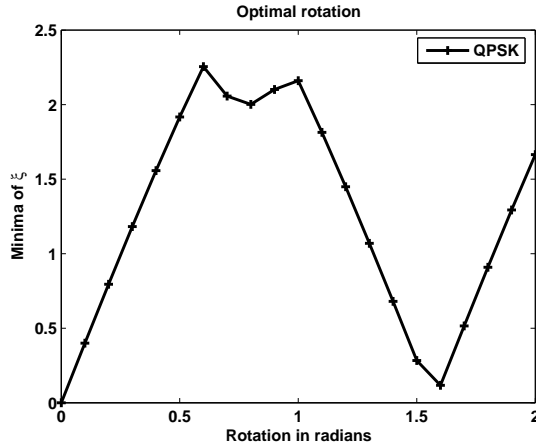


Figure 2.2: Minima of  $\xi$  against angle of rotation.

can be represented as

$$\begin{bmatrix} \hat{x}_3 \\ \hat{x}_4 \end{bmatrix} = \begin{bmatrix} \exp j\phi & 0 \\ 0 & \exp j\phi \end{bmatrix} \begin{bmatrix} x_3 \\ x_4 \end{bmatrix} \quad (2.51)$$

where  $\hat{x}_3, \hat{x}_4$  are the symbols after rotation. Rewriting the code matrix with rotated symbols, we have

$$\mathbf{X} = \begin{bmatrix} x_1 & x_2 & \hat{x}_3 & \hat{x}_4 \\ x_2^* & -x_1^* & \hat{x}_4^* & -\hat{x}_3^* \\ \hat{x}_3 & -\hat{x}_4 & -x_1 & x_2 \\ \hat{x}_4^* & \hat{x}_3^* & -x_2^* & -x_1^* \end{bmatrix}. \quad (2.52)$$

and from its Gramian matrix, it is straightforward that

$$\mathbf{D} = \sum_{i=1}^4 |x_i|^2 \mathbf{I}_4. \quad (2.53)$$

Therefore, a constellation rotation of the type given by Eq(2.51) retains the MSD property of quasi-orthogonal scheme in Eq(2.41). On the other hand, it follows from Eq(2.33) that the interference caused by non-orthogonality of signal sequences changes but does not vanish by these constellation rotations. This indicates that due to complete absence of interference in its ML detection, the

design which sets the rigorous lower limit on BER performance at all SNR's and the capacity optimal design for  $N_R = 1$  is a full rate orthogonal design, but if only such an object existed. However, the constellation rotation technique, employed in the light of rank and determinant criteria, achieves full diversity degree at asymptotic SNR's.

## 2.6 Multimodulation scheme

Increasing the symbol rate using non-orthogonal space-time transmission schemes was discussed in the previous section. It was also seen that the degradation of diversity degree in such non-orthogonal schemes can be overcome using constellation rotation technique. However, another very simple technique would be to choose symbols from different modulation alphabets to compensate for rate loss in orthogonal schemes. This concept has been analyzed and termed "multimodulation" in [60]. For example, consider a power balanced version [16] of  $R = \frac{3}{4}$  orthogonal scheme in Eq(2.20)

$$\mathbf{X} = \begin{bmatrix} x_1 & x_2 & x_3 & x_3 \\ -x_2^* & x_1^* & x_3 & x_3 \\ x_3^* & x_3^* & -\Re[x_1] + j\Im[x_2] & j\Im[x_1] - \Re[x_2] \\ x_3^* & -x_3^* & j\Im[x_1] + \Re[x_2] & -\Re[x_1] - j\Im[x_2] \end{bmatrix} \quad (2.54)$$

where  $x_1, x_2 \in Q_1$ ,  $x_3 \in Q_3$  such that  $Q_3$  is a bigger constellation to increase the bit rate. For example,  $Q_1$  can be taken as QPSK constellation and  $Q_3$  as 16-QAM constellation. For doing this, symbol  $x_3$  has been suitably scaled in Eq(2.54) so that symbols from alphabet  $Q_3$  are transmitted with higher power because they contain more bits. However, upon scaling, the code in Eq(2.54) does not satisfy the MSD criterion in Eq(2.13). This affects the performance of this scheme for low-medium SNR's while for asymptotic SNR'S a diversity degree of 4 is reflected in the slope of its BER curve.

The multimodulation concept above is employed to compensate for the rate loss in an orthogonal code. In the same manner, multimodulation can be employed to compensate for diversity degree loss in a non-orthogonal code at asymptotic SNR's. For this purpose, consider the code in

Eq(2.41)

$$\mathbf{X} = \begin{bmatrix} x_1 & x_2 & x_3 & x_4 \\ x_2^* & -x_1^* & x_4^* & -x_3^* \\ x_3 & -x_4 & -x_1 & x_2 \\ x_4^* & x_3^* & -x_2^* & -x_1^* \end{bmatrix}. \quad (2.55)$$

It was seen that the determinant of the code distance matrix of this code vanishes for certain code error vectors. It was also established that constellation rotation technique could be employed to make the code distance matrix non-singular for all code error vectors,  $\Delta$ . However, instead of constructing new symbol alphabets  $Q_3, Q_4$  for symbols  $x_3, x_4$  from existing symbol alphabets  $Q_1, Q_2$ , alphabets  $Q_3, Q_4$  can also be altogether different symbol alphabets but chosen such that they would guarantee non-vanishing determinant of code distance matrix. For example, if  $Q_1, Q_2$  are QPSK signal constellations then  $Q_3, Q_4$  can be altogether different constellations like 16-QAM and this will automatically make the determinant in Eq(2.49) non-zero for all code error vectors,  $\Delta$ . However, symbols from constellations of bigger size would need to be transmitted with higher power, sacrificing the MSD property of the code in Eq(2.53). This affects the performance of this scheme at low-medium SNR'S but for asymptotically high SNR'S a transmit diversity degree of 4 dominates the performance of this scheme.

## 2.7 Conclusion

In this chapter, space-time block coding designs were considered. First, orthogonal designs which provide the benchmark for BER performance of space-time block codes were briefed. Later, increasing the symbol rate using non-orthogonal designs and increasing the diversity order of such non-orthogonal designs using constellation rotation technique were explained in detail. It was also seen that multimodulation concept can be used to increase the rate of an orthogonal design as well as to maximize the diversity degree of a non-orthogonal design. In the next chapter, we analyse the performance of the linear space-time block coding techniques which have been discussed in this chapter in a spatially correlated environment.

## Chapter 3

# Space-Time block Coding in correlated channels

### 3.1 Introduction

It is well known that the MIMO theoretical link capacity grows linearly with  $\min(N_R, N_T)$ , making it a promising technique for high speed wireless communications. Alternatively, a diversity advantage of  $N_T \times N_R$  can be targeted using  $N_T$  transmit antennas and  $N_R$  receive antennas to increase the reliability in communication. However, the assumption that the transmit and receive antennas are statistically independent is fundamental to the linear capacity growth with  $\min(N_R, N_T)$  observed in [52],[64]. Similarly, the basic idea of antenna diversity is that a combination of independent and identically distributed (i.i.d) faded samples of the same signal collected using multiple antennas can be used to improve the decision statistics at the receiver for signal recovery with the same transmission power. In fact, the diversity advantage of a space-time code which can be achieved using the rank and determinant criteria is defined as the exponent of  $SNR$  at asymptotic  $SNR$ 's when the fading distributions are Rayleigh and independent [47]. Therefore large spectral efficiencies promised by MIMO spatial multiplexing and/or power efficiency of space-time coding can be realized if the fading between transmit and receive antennas follow independent distributions.

In reality however, closely spaced antennas, poor scattering environment or narrow angular spread

can cause the individual antennas to be correlated. In the downlink of a cellular network, the feasibility of having sufficiently spaced transmit antennas makes transmit diversity a very attractive approach. In peer-peer links of an ad hoc networking setup, however, it is not always possible for small mobile terminals to support sufficiently spaced antennas and therefore fading gains could be statistically correlated as a result of transmit-side or receive-side antenna correlation. The motivation of this chapter is to study the effect of transmit-side correlation on a rank achieving full rate space-time design. For this purpose, constellation rotated non-orthogonal space time block codes (NO-STBC), which achieve full diversity and full transmission rate are considered for analysis. These codes have been shown to outperform NO-STBC in link reliability over Rayleigh fading i.i.d channels. A full rank transmit correlation matrix is employed and the performance of these codes analyzed in correlated quasi-static Rayleigh fading channels. The effect of spatial correlation on pairwise error probability (PEP) is analyzed first and then the behavior of code structure over channel correlation is investigated. The results for BER performance of constellation rotated robust NO-STBC over highly correlated channels is also presented.

### 3.2 Channel correlation model

The channel correlation between the transmit antennas can be modelled using the well known AR(1) process:

$$h_{i+1} = \alpha h_i + \sqrt{1 - \alpha^2} w_{i+1}, \quad 1 \leq i \leq 3 \quad (3.1)$$

where  $\alpha = E[h_i h_{i+1}^*]$  is the correlation coefficient between two adjacent transmit antennas and  $w_{i+1}$  is an independent complex Gaussian variable with the variance of 1 (0.5 per dimension) and zero mean. The channel is assumed to be quasi-static within a STBC block and the temporal correlation is assumed to be zero. Therefore, the fading gains between the first transmit antenna and receive antenna is an independent complex Gaussian variable with the variance of 1 (0.5 per dimension) and zero mean. The fading gains of the other transmit antennas can be expressed in terms of  $h_1$  as

$$h_{i+1} = \alpha^i h_1 + \sum_{k=0}^{i-1} \alpha^k \sqrt{1 - \alpha^2} w_{i-k+1}. \quad (3.2)$$

From Eq(3.2) is is straight forward to show that

$$\text{var}(h_{i+1}) = 1 \quad \forall i \quad (3.3)$$

$$E(h_{i+1}) = 0 \quad \forall i. \quad (3.4)$$

The channel vector  $\mathbf{h}$  can be represented based on [66] as

$$\mathbf{h}^T = \mathbf{h}_w^T \mathbf{S}^{1/2}, \quad (3.5)$$

where  $\mathbf{h}_w^T = [w_1 \ w_2 \ w_3 \ w_4]$ .  $w_i$  is an independent complex Gaussian variable with the variance of 1 (0.5 per dimension) and zero mean. The vector  $\mathbf{h}_w^T$  thus relates to the independent and hence perfectly uncorrelated Rayleigh fading condition. From the correlation model in Eq(3.1), the matrix  $\mathbf{S}^{1/2}$  can be determined:

$$\mathbf{S}^{1/2} = \begin{bmatrix} 1 & \alpha & \alpha^2 & \alpha^3 \\ 0 & \sqrt{1-\alpha^2} & \alpha\sqrt{1-\alpha^2} & \alpha^2\sqrt{1-\alpha^2} \\ 0 & 0 & \sqrt{1-\alpha^2} & \alpha\sqrt{1-\alpha^2} \\ 0 & 0 & 0 & \sqrt{1-\alpha^2} \end{bmatrix}, \quad (3.6)$$

where  $0 \leq \alpha \leq 1$ . The channel correlation matrix is then  $\mathbf{\Theta} = E[\mathbf{h}\mathbf{h}^H]$ .

$$\mathbf{\Theta} = \begin{bmatrix} 1 & \alpha & \alpha^2 & \alpha^3 \\ \alpha & 1 & \alpha & \alpha^2 \\ \alpha^2 & \alpha & 1 & \alpha \\ \alpha^3 & \alpha^2 & \alpha & 1 \end{bmatrix}.$$

Finally, as in [66] the transmit correlation matrix  $\mathbf{S}$  is defined as  $\mathbf{S} = \mathbf{S}^{1/2}\mathbf{S}^{H/2}$ , which has full rank for  $0 \leq \alpha < 1$  and rank 1 when  $\alpha = 1$ .

### 3.3 Constellation rotation scheme over correlated channels

#### 3.3.1 Effect on the PEP

Consider the quasi-orthogonal scheme given by

$$\mathbf{X} = \begin{bmatrix} x_1 & x_2 & x_3 & x_4 \\ x_2^* & -x_1^* & x_4^* & -x_3^* \\ x_3 & -x_4 & -x_1 & x_2 \\ x_4^* & x_3^* & -x_2^* & -x_1^* \end{bmatrix}. \quad (3.7)$$

It was seen that the code difference matrix of this NO-STBC has a minimum rank 2 and by rotating symbols  $x_3$ ,  $x_4$  full rank of 4 can be realized. If  $\mathbf{Y} = \mathbf{A}\mathbf{h}$ , where  $\mathbf{A}$  is the code difference matrix and  $\mathbf{h}$  is the channel vector by denoting  $\mathbf{C}_\mathbf{Y} = E(\mathbf{Y}\mathbf{Y}^H)$  the pairwise error probability (PEP) can be expressed, for  $N_R = 1$ , as [66]

$$P(\mathbf{X}, \tilde{\mathbf{X}}) \leq \prod_{i=1}^{\nu} (\lambda_i(\mathbf{C}_\mathbf{Y}))^{-1} \left(\frac{E_s}{4N_o}\right)^{-\nu}, \quad (3.8)$$

where  $\nu$  is the minimum rank of matrix  $\mathbf{C}_\mathbf{Y}$  over all codeword pairs and throughout the paper  $\lambda_i(\mathbf{Z})$  denotes the  $i^{\text{th}}$  eigenvalue of a matrix  $\mathbf{Z}$ .

Using Eq(3.5), the covariance matrix of  $\mathbf{Y}$  can be written as

$$\mathbf{C}_\mathbf{Y} = \mathbf{A}\mathbf{S}^T\mathbf{A}^H. \quad (3.9)$$

Therefore the upper bound of PEP is given by

$$P(\mathbf{X} \rightarrow \tilde{\mathbf{X}}) \leq (E_s/4N_o)^{-\nu} \prod_{i=1}^{\nu} \lambda_i^{-1}(\mathbf{A}\mathbf{S}^T\mathbf{A}^H), \quad (3.10)$$

where  $\nu$  is the minimum rank of  $\mathbf{A}\mathbf{S}^T\mathbf{A}^H$ . The transmit correlation matrix  $\mathbf{S}$  exhibits full rank for  $0 \leq \alpha < 1$  and from the Sylvester's theorem it is straightforward that  $rank(\mathbf{C}_\mathbf{Y}) = rank(\mathbf{A}\mathbf{A}^H)$ . Denoting the minimum rank of the matrix  $\mathbf{A}\mathbf{A}^H$  as  $r$ , the upper bound on PEP can be rewritten

for  $0 \leq \alpha < 1$  as [66]

$$P(\mathbf{X} \rightarrow \tilde{\mathbf{X}}) \leq (E_s/4N_o)^{-r} \prod_{i=1}^r \lambda_i^{-1}(\mathbf{S}) \prod_{i=1}^r \lambda_i^{-1}(\mathbf{A}\mathbf{A}^H). \quad (3.11)$$

Noting that  $\text{rank}(\mathbf{A}\mathbf{A}^H) = \text{rank}(\mathbf{A}^H\mathbf{A})$  and nonzero eigenvalues of the matrix  $\mathbf{A}\mathbf{A}^H$  are equal to nonzero eigenvalues of the matrix  $\mathbf{A}^H\mathbf{A}$ , this can be further rewritten for  $N_R = 1$  as

$$P(\mathbf{X} \rightarrow \tilde{\mathbf{X}}) \leq (E_s/4N_o)^{-r} \prod_{i=1}^r \lambda_i^{-1}(\mathbf{S}) \prod_{i=1}^r \lambda_i^{-1}(\mathbf{A}^H\mathbf{A}). \quad (3.12)$$

The nonzero eigenvalues of  $\mathbf{S}$  and  $\mathbf{A}^H\mathbf{A}$  are arranged in increasing order for discussion.

Comparing Eq(3.12) with Eq(2.7), the loss in PEP due to transmit correlation for  $N_R = 1$  can be characterized by

$$\omega = \prod_{i=1}^r \lambda_i(\mathbf{S}). \quad (3.13)$$

For the NO-STBC in this paper when  $\xi_1 = 0$  and  $\xi_2 = 0$  in Eq(2.49), the rank of the matrix  $\mathbf{A}^H\mathbf{A}$  is equal to 2 which is its minimum rank  $r$ . An optimal rotation scheme should allow the minimum rank  $r$  to be 4 for all error events and maximize  $\det \mathbf{B} = \prod_{i=1}^r \lambda_i(\mathbf{A}^H\mathbf{A})$ .

Since  $|\Delta_i| = |\Delta_i e^{j\phi}|$ , we have  $\text{tr}(\mathbf{A}^H\mathbf{A})_{rot} = \text{tr}(\mathbf{A}^H\mathbf{A}) = \theta$ . We can therefore have the optimal rotation scheme maximize  $\prod_{i=1}^4 \lambda_i(\mathbf{A}^H\mathbf{A})$  with the following constraint,

$$\sum_{i=1}^4 \lambda_i(\mathbf{A}^H\mathbf{A}) = \theta, \text{ or equivalently, } 0 < \lambda_i(\mathbf{A}^H\mathbf{A}) \leq \theta. \quad (3.14)$$

Also, for the transmit correlation structure employed in this paper,

$$\text{tr}(\mathbf{S}) = \sum_{i=1}^4 \lambda_i(\mathbf{S}) = 4, \quad (3.15)$$

which is independent of  $\alpha$ . Therefore,  $\prod_{i=1}^r \lambda_i(\mathbf{S})$  follows the constraint,  $0 < \lambda_i(\mathbf{S}) < 4$  and consequently a change in distribution of the eigenvalues of  $\mathbf{S}$  excites a loss in the PEP. The plot of  $\omega$  for NO-STBC ( $r=2$ ) and constellation rotated NO-STBC ( $r=4$ ) schemes against correlation coefficient is shown in Fig. 3.1.

It can be observed that as correlation increases  $\omega$  for both schemes converges to zero. Then

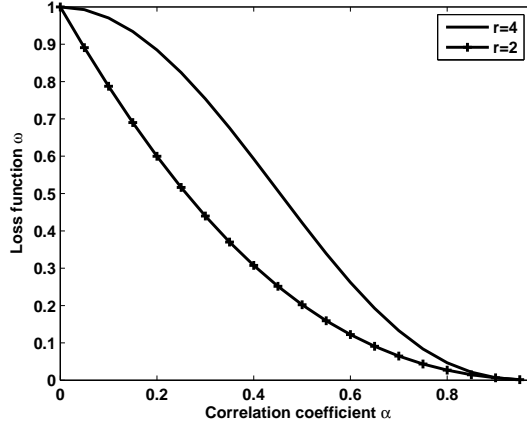


Figure 3.1: Loss function against correlation coefficient.

intuitively, maximizing  $\prod_{i=1}^r \lambda_i(\mathbf{A}^H \mathbf{A})$  using a full rank constellation rotation scheme with the constraint in Eq(3.14) does not absorb the loss in  $\omega$  at high correlations. This happens for high channel correlations. Consequently there is no significant performance improvement due to constellation rotations at high spatial correlations.

### 3.3.2 Analysis

In this section we investigate the behavior of the code structure as the correlation coefficient increases. The equivalent channel matrix for the NO-STBC in Eq(3.7) can be written in the form used in Eq(2.26) as

$$\hat{\mathbf{H}} = \begin{bmatrix} h_1 & h_2 & h_3 & h_4 \\ -h_2^* & h_1^* & -h_4^* & h_3^* \\ -h_3 & h_4 & h_1 & -h_2 \\ -h_4^* & -h_3^* & h_2^* & h_1^* \end{bmatrix}. \quad (3.16)$$

The properties of the code is reflected in the matrix  $\hat{\mathbf{H}}^H \hat{\mathbf{H}}$

$$\hat{\mathbf{H}}^H \hat{\mathbf{H}} = \begin{bmatrix} \Sigma & 0 & c & 0 \\ 0 & \Sigma & 0 & -c \\ -c & 0 & \Sigma & 0 \\ 0 & c & 0 & \Sigma \end{bmatrix}, \quad (3.17)$$

where  $\Sigma = \sum_{i=1}^{i=4} |h_i|^2$ , and  $c = 2j(\Im(h_1^* h_3) + \Im(h_2 h_4^*))$ .

For this NO-STBC,  $\det(\hat{\mathbf{H}}^H \hat{\mathbf{H}}) \neq 0$  for  $0 \leq \alpha \leq 1$  making the equivalent channel matrix full rank for all correlation coefficients. The interference term  $c$  is observed to have a low mean and decreasing variance at high channel correlations and becomes 0 when  $\alpha = 1$ . Due to this the above NO-STBC is robust [65] and its matched filter output properties tend to the O-STBC properties at high correlation coefficients.

From Eq(3.2), the term  $\Sigma$  can be rewritten as

$$\Sigma(\alpha) = \sum_{i=0}^{i=3} |\alpha^i \chi + \sqrt{1 - \alpha^{2i}} \mu_i|^2, \quad (3.18)$$

where  $\chi$  and  $\mu_i$  are zero mean, unit variance complex Gaussian variables denoting the correlating component and the spatial diversity component of  $i^{th}$  antenna respectively. It can be seen that as the correlation coefficient  $\alpha$  increases, occurrences of deep fade in  $\chi$  lead to a smaller signal power at the decoder, thereby deteriorating the performance at medium to high SNR. Moreover, power preserving constellation rotations do not increase the Euclidean distance between signal points and hence the performance of constellation rotated NO-STBC scheme becomes identical to the performance of NO-STBC without rotation as  $\alpha$  approaches 1. The NO-STBC has diversity degree of 2 and the constellation rotated NO-STBC diversity degree of 4. However, in the absence of diversity at high spatial correlations, the performance of both the schemes become similar to each other.

### 3.4 Numerical examples

In this section numerical examples are used to illustrate the performance of the schemes under transmit side correlation. The system is  $\pi/4$  QPSK modulation. The symbol power has been normalized to 1. 560000 QPSK symbols are transmitted per SNR point using 4 Tx antennas and 1 Rx antenna. The NO-STBC scheme in Eq (3.7) [54] with and without optimal rotation is investigated.

#### *Example 1: Uncorrelated channels*

In this example, the channels are mutually independent:  $\alpha = 0$ . Fig.3.2 shows the uncoded BER performance as a function of SNR for the NO-STBC in Eq(3.7) with and without optimal rotations. We observe that constellation rotation of 0.5 radians significantly improves the BER performance of the space-time code. At low SNR'S, because both the schemes offer maximal symbolwise diversity there is not a significant difference in the performance. However, at asymptotically high SNR's, performance is determined by the codeword difference matrix. The codeword difference matrix has a minimum rank 2 in the event of multiple symbol error events making  $\xi_1 = 0$  or  $\xi_2 = 0$  in Eq(2.49). This determines the slope of the BER curve at high SNR'S. Constellation rotation scheme provides better diversity protection against rank deteriorating error events and maximizes the minimum rank of code difference matrix. Therefore, the slope of BER curve upon employing such rotations improves significantly and makes the constellation rotated scheme more power efficient.

#### *Example 2: Correlated channels*

The BER performance of the NO-STBC in Eq(3.7) when the transmitter antenna gains are correlated is illustrated in this example. Two cases of channel correlations with  $\alpha = 0.9$  and  $\alpha = 1$  are considered. The results are plotted in Fig.3.3 and Fig.3.4 respectively. The performance degradation due to the effect of loss function in Eq(3.13) is significant at these correlation coefficients. The property of full rank code distance matrix in the PEP is masked by the loss function due to channel correlation. It can be observed from the matched filter output that the BER performance of constellation rotated NO-STBC scheme tends to the BER of NO-STBC without rotation and eventually becomes exactly the same when the antennas are perfectly correlated. If the MSD property of the code is disturbed by using arbitrary weights  $w_1$  to  $x_1, x_2$  and  $w_2$  to  $x_3, x_4$  such that

$w_1^2 + w_2^2 = 2$ , then the performance would only get worse. It can also be verified using Eq (3.17) that when  $\alpha = 1$ , this code resembles the matched filter bound or the MRC bound which rigorously sets the lower limit on BER performance. An interesting observation is that the performance gap between this NO-STBC and the matched filter bound reduces as the correlation increases. The lack of spatial diversity in channel realization at the receiver eventually degrades the BER performance.

## Results

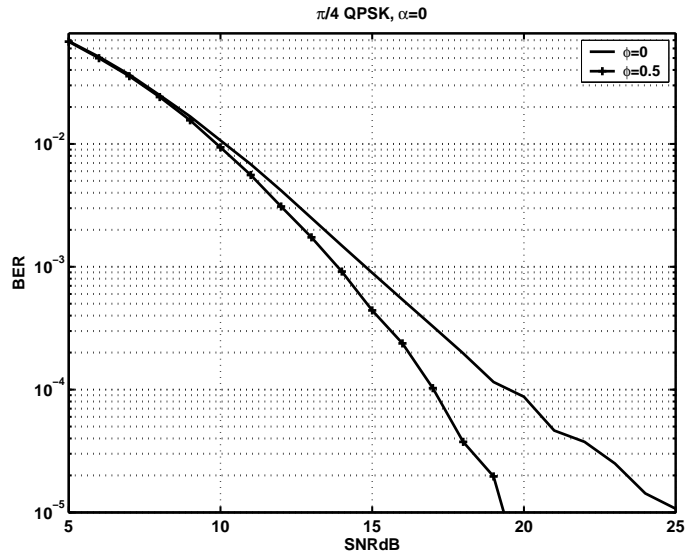


Figure 3.2: Uncoded bit error rate for QPSK modulation for uncorrelated antennas ( $\alpha = 0$ ).

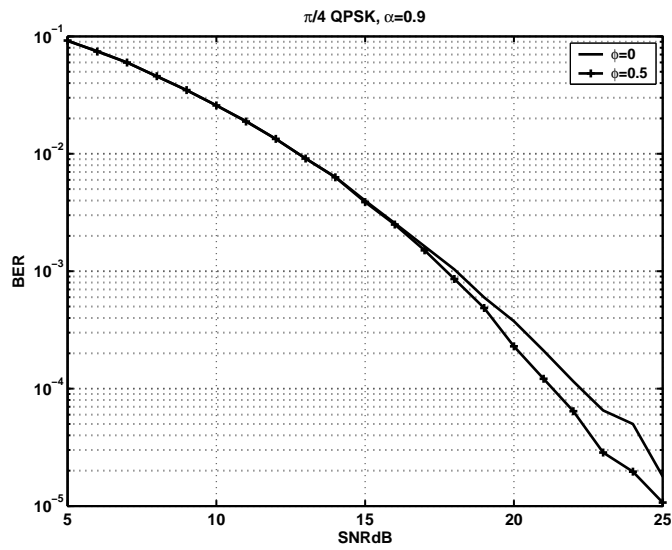


Figure 3.3: Uncoded bit error rate for QPSK modulation for uncorrelated antennas ( $\alpha = 0.9$ ).

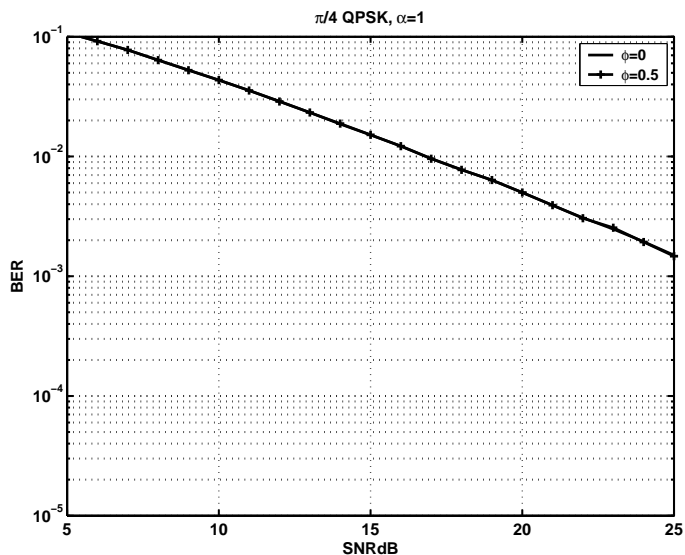


Figure 3.4: Uncoded bit error rate for QPSK modulation for uncorrelated antennas ( $\alpha = 1$ ).

### 3.5 Conclusion

The performances of NO-STBC and constellation rotated NO-STBC schemes were compared and analyzed using a correlation model between four transmit antennas represented by a full rank transmit correlation matrix. The loss function on the PEP which causes degradation in BER performance has been characterized. It has been shown that power preserving scalar constellation rotation schemes do not provide any significant performance benefit at high correlation coefficients in spite of providing better diversity protection at rank deteriorating error events. Simulations establishing these results have also been presented in this chapter. Overall, it has been seen that open loop transmit diversity schemes do not yield significant performance benefits when the channels between multiple antennas are highly correlated. In the next chapter, we introduce relay diversity systems formed by users who share their resources and imitate a multiple antenna system. These relay systems are useful in scenarios where channels between multiple transmit antennas are highly correlated or when many users are equipped with only one antenna in the network. However, as we would see in the rest of the thesis, although they promise rich spatial diversity, relaying systems are fundamentally limited by noise propagation or error propagation along the relay route.

## Chapter 4

# User Cooperation

### 4.1 Introduction

Relaying between radio nodes has been observed to reduce the aggregate path loss and improve performance in wireless channels. This concept exploits the inherent broadcast [19] nature of a wireless channel and is popularly referred to as multi-hopping. Relays can also be used to assist communication between two hops in a multiple hop wireless route. This concept exploits the parallel topology available when peer-peer links are allowed in cellular networks and in wireless ad hoc networks. The relay channel formulation and protocols [3], [20] have been studied in various works recently in which the gains achievable with cooperation are observed to be promising.

In addition to relaying, if users have their own information to transmit, then they form a “user cooperation” channel [4]. In fact, a classical relay channel is a special case of “user cooperation channel” when only one terminal has information to transmit to one receiver with others assisting it. The diversity realized when different nodes transmit each other’s information has been termed “cooperative diversity” [40],[3]. The relay channel first studied by van der Meulen [45] in his pioneering work is central to user cooperation in multiple-access, broadcast and interference channels. Since then, user cooperation has found more interest among researchers due to the following motivations.

1) They are a very attractive means of reliable communication in the upcoming ad hoc network scenarios. Radio nodes are more likely to be found distributed as clusters [23] in large wireless networks which makes user cooperation even more feasible and beneficial in large networks. The power gains due to shorter wireless links formed by relaying is a main incentive to investigate such systems. Cooperative communications combines the usual power advantages of multiple hop networking with the cooperative diversity achievable via multiple route relaying and therefore holds promise to improve the throughput in such networks. Moreover, cooperative diversity is vital to the framework of cooperative communications to try and reduce the number of hops and thereby reduce end-end latency in a multiple hop network. This can be achieved by complementing multi hopping transmit power savings with the cooperative diversity gain .

2) If the channel between two communicating terminals is deeply faded, occurrence of outages can be reduced by routing the information via a relay [13]. Multi hop packet radio networks (MPRN) is an attractive architecture on these lines that could accommodate such scenarios by organizing cooperation between mobile radio nodes. This benefit is also relevant to the uplink of cellular network [13] where there are strict transmit power constraints. Information can then be routed from the mobile terminal around the obstacles to the base station.

3) The recent developments in MIMO technology has also fueled interests for cooperative communications. The idea of using radio nodes to resemble an antenna array at a single user based on cooperation was proposed in [16] and termed “Virtual Antenna Array” (VAA). User terminals equipped with only one antenna can enjoy the benefits of multiple antenna communications when other terminals “share” their antennas. MIMO channels formed by VAA’s also promise good spatial multiplexing gains as the channels are potentially rich in rank [33] due to large spatial separation between collaborating users. Therefore, with user collaboration and antenna sharing, multiple antenna techniques which improve spectral efficiency and power efficiency can be used for single antenna users, albeit, there is additional delay in communication due to the need for information transfer between cooperating terminals.

At this point, it is vital to point out that the process of neighbor discovery [32], establishing a dynamic route or implementing a “network code” [30] are typically network layer issues. However, the broadcast nature of wireless channels, issues of radio interference and wireless channel impairments make link layer solutions relevant at the network and MAC layers. Similarly, rate adaptation, power control and coding at link layer would largely depend on the network conditions and the MAC layer protocols. These layer interdependencies makes cross-layer design imperative to meet the application requirements of these networks.

In this chapter, link layer relay channel model widely used in literature is first presented. Then few forwarding strategies and user cooperation techniques are briefed and the schematic of cooperative diversity is explained in detail. Finally, conditional SNRs of the cooperative diversity schemes are compared.

## 4.2 Multihop network

An example of a wireless multiple hop model with 3 hops is shown in Fig.4.1.

In this model, every radio receiver decodes the signal it receives from the previous hop and

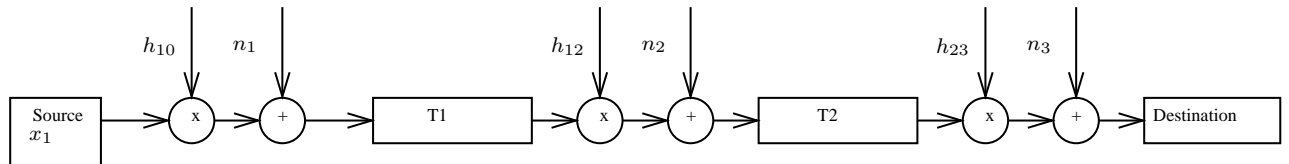


Figure 4.1: Multihop network with 3 hops.

forwards it to the next hop.  $h_{ij}$  is the zero-mean fading gain between hops  $i$  and  $j$  with variance  $\sigma_{ij}^2$  and  $n_i$  is AWGN noise at  $i^{th}$  radio receiver with variance  $N_0$ . The shorter wireless links because of hopping reduces the effective path loss between a source-destination pair and therefore reduces the total transmission power in a wireless network containing many such source-destination pairs. To explain this further, consider the setting with  $n$  hops as shown in Fig 4.2.

Here  $d_i$  is the Euclidean distance between two adjacent hops and the wireless link between a source and destination consists of  $n$  hops formed by  $n - 1$  collinear radio nodes willing to cooperate. The

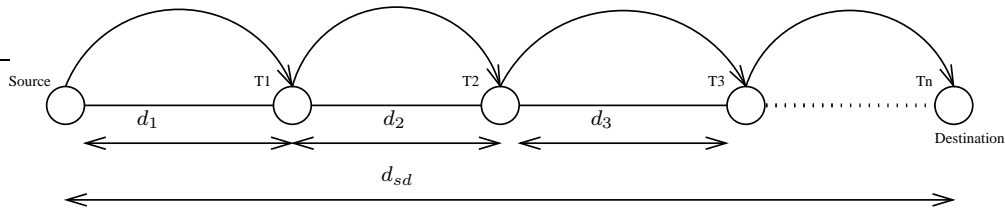


Figure 4.2: Multihop model with  $n$  hops.

distance between source and destination can then be written as

$$d_{sd} = \sum_{i=1}^n d_i. \quad (4.1)$$

The path loss between two wireless nodes separated by a Euclidean distance  $d_{ij}$  is simplistically given by

$$\sigma_{ij}^2 = \frac{1}{d_{ij}^r}, \quad (4.2)$$

where  $r$  is the path loss exponent of the wireless channel model. If  $P_{ti}$  is the average transmitted power from  $i^{th}$  node to its neighbor, then the average received power at the  $i + 1^{th}$  node is  $P_{ri} = P_{ti}\sigma_{ii+1}^2$ . In addition, if all radio nodes employ a minimum threshold average received power of  $P_{ri} = P'$  before codeword detection, then the above setting would allow us to characterize the transmit power savings available using multi hopping. From Eq(4.1) the gain  $g$  can be shown to be,

$$g = \frac{P}{\sum_{i=1}^n P_{ti}} = \frac{d_{sd}^r}{\sum_{i=1}^n d_i^r} = \frac{[\sum_{i=1}^n d_i]^r}{\sum_{i=1}^n d_i^r}. \quad (4.3)$$

Eq(4.3) shows that increasing the number of hops increases the transmit power savings in the network.

### 4.3 Three terminal model

In a wireless multi-hop link, each receiver in the route can decode information using transmissions from all or some preceding hops to increase the achievable rates in the network. Based on the above idea, the classical three terminal relay channel model was originally introduced and examined by Van der Meulen in [45]. Cover and El Gamal [20] made further progress by theoretically developing

the lower and upper bounds of capacity for AWGN channels via random coding. The cooperation strategy between the source and relay nodes for coding in [20] is shown in Fig.4.3.

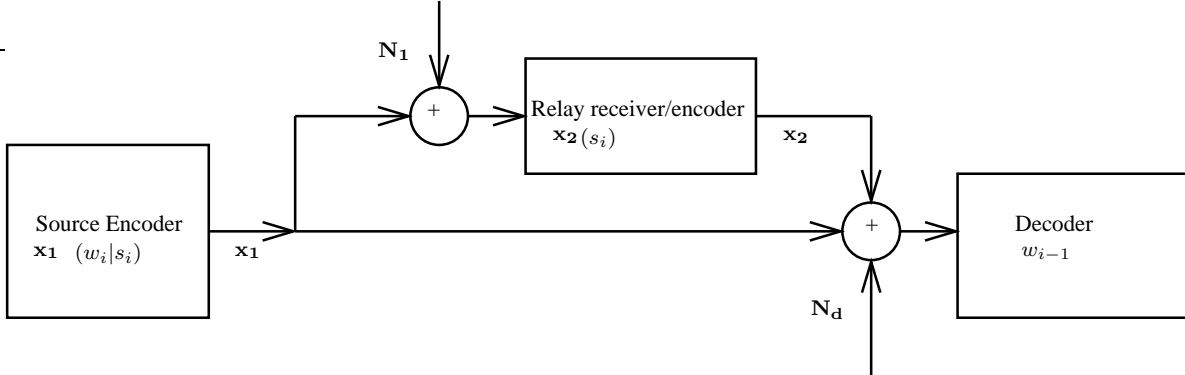


Figure 4.3: Three terminal model.

The scheme in [20] operates as follows. At time index  $i$ , current message  $w_i$  arrives at the source encoder for transmission.  $w_{i-1}$  denotes the previous message and  $s_i$  is the index of the partition  $\mathcal{S}$  in which the message  $w_{i-1}$  is contained. Then the source superimposes  $w_i$  and  $s_i$  at its encoder and transmits  $\mathbf{x}_1(w_i|s_i)$ , thereby maintaining a steady flow of information. The relay obtains  $s_i$  by correctly decoding message  $w_{i-1}$  and transmits signal  $\mathbf{x}_2(s_i)$  to the destination. The destination uses multiple receptions of  $s_i$  to identify the cell  $\mathcal{S}$  and successfully decode  $w_{i-1}$ . In this scheme, the source and the destination use superposition block Markov encoding and backward decoding respectively. If repetition coding is used at the relays to achieve the aforementioned relay assisted decoding, then a diversity channel is formed by relaying.

### 4.3.1 Relay diversity

Relaying can be used to realize diversity using multiple receptions of the same signal from different cooperating users. This form of diversity has been termed “multi-user spatial diversity” [13] and has superficial similarities to antenna diversity concepts. The three terminal model for relay diversity is shown in Fig 4.4.

The wireless relay system consists of a source node, a destination node and a relay node. Two

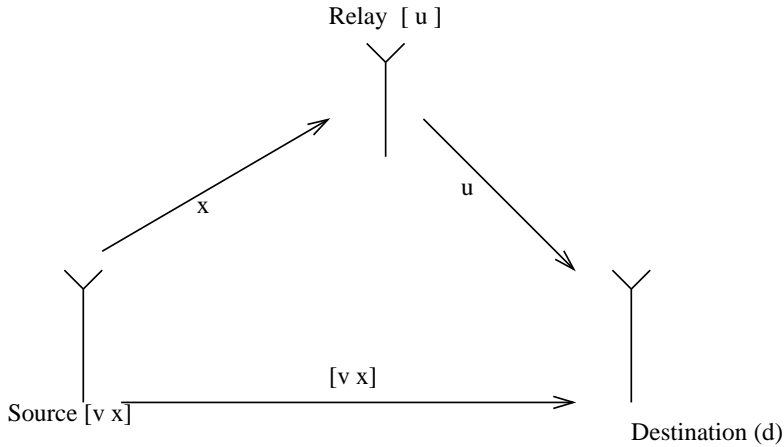


Figure 4.4: Three terminal relay diversity.

orthogonal subspaces are assumed for the received and transmitted data from a radio node to preclude the terminals from receiving and transmitting at the same time in the same frequency band [1],[3]. The orthogonal subspaces for transmission and reception can be formed for example, by a two time frame transmission scheme explained below.

**Frame  $i$**

In the first frame, digitally encoded symbols  $x \in C_1$  of unit modulus is transmitted by the source, where  $C_1$  is a modulation alphabet. Let  $\mathbf{x}$  be the transmission vector at the source. The received signal at the destination in the first subchannel is

$$\mathbf{r}_d^{(1)}(i) = \sqrt{P_1}h_{sd1}^{(1)}\mathbf{x} + \sqrt{N_0}\mathbf{n}_d^{(1)}(i), \quad (4.4)$$

and the received signal at the relay is

$$\mathbf{r}_r^{(1)}(i) = \sqrt{P_1}h_{sr}^{(1)}\mathbf{x} + \sqrt{N_0}\mathbf{n}_r^{(1)}(i), \quad (4.5)$$

where  $h_{sd1}^{(1)}$ ,  $h_{sr}^{(1)}$  are the channel gains from the source to destination and relay respectively in the first orthogonal subchannel and  $\mathbf{n}_d^{(1)}(i)$ ,  $\mathbf{n}_r^{(1)}(i)$  are noise vectors whose entries are complex Gaussian with zero mean and unit variance (0.5 per dimension).

**Frame  $i + 1$**

In the second frame, the source optionally transmits  $\mathbf{x}$  again while the relay transmits vector  $\mathbf{u}$  based on the reception  $\mathbf{r}_r^{(1)}(i)$ . For medium access control, the source-destination channel and the relay-destination channel are orthogonal to each other to avoid interference between the transmitting terminals. The destination receives the signal

$$\mathbf{r}_{rd}^{(2)}(i+1) = \sqrt{P_r} \mathbf{u} h_{rd}^{(2)} + \sqrt{N_0} \mathbf{n}_d^{(2)}(i+1) \quad (4.6)$$

from the relay in the second subchannel, where  $h_{rd}^{(2)}$  is the channel gain between the relay and destination in the second orthogonal subchannel. It also receives the signal

$$\mathbf{r}_{sd}^{(1)}(i+1) = \sqrt{P_2} \mathbf{x} h_{sd2}^{(1)} + \sqrt{N_0} \mathbf{n}_d^{(1)}(i+1) \quad (4.7)$$

from the source, where  $h_{sd2}^{(1)}$  is the channel gain between source and destination in the frame  $i + 1$  over the first orthogonal sub channel. The channel gains are assumed to be zero mean complex Gaussian variables with variances  $\sigma_{sr}^2$ ,  $\sigma_{rd}^2$  and  $\sigma_{sd}^2$  respectively and are assumed to be quasi-static over a frame length.  $\mathbf{n}_d^{(1)}(i+1)$  is the noise column vector and entries of  $\mathbf{n}_d^{(1)}(i+1)$  are additive white Gaussian with zero mean and a variance of 1.

The destination receiver then carries out symbol detection as shown in Fig 4.5.

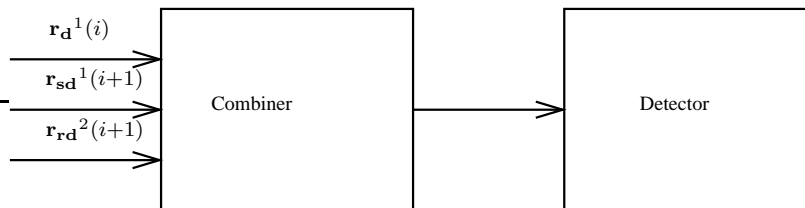


Figure 4.5: Destination receiver.

At the combiner, the destination combines the signals  $\mathbf{r}_{rd}^{(2)}(i+1)$ ,  $\mathbf{r}_d^{(1)}(i)$ ,  $\mathbf{r}_{sd}^{(1)}(i+1)$  before symbol detection. It can be intuitively seen from Eqs (4.4) - (4.7) that if the signals are maximal ratio combined then the performance benefit will be totally dependent on source-relay channel quality.

On this basis, a weighted combining scheme has been proposed in [1],[5]. An expression for the post-combining conditional SNR for weighted combining scheme is presented in Section 4.7.2.1.

In the three terminal relay diversity model which has been discussed in this section, the relay nodes do not hear each other's transmission. For completeness, in the next section we outline the schematic of a generalized multiple-relay mechanism in which relays can also 'hear' each others transmissions.

### 4.3.2 Multiple relay network

In the landmark paper by Gupta and Kumar[22], the upper bound of aggregate capacity of wireless networks consisting of  $n$  nodes per unit area with point to point coding has been shown to follow a bit-distance product of  $O(\sqrt{n})$  bit-meters per second behavior, or equivalently a maximum transmission rate of  $O(\frac{1}{\sqrt{n}})$  bits per second per node. Gastpar [30] considers a traffic pattern in which all other nodes in the network act simply as relays for a source-destination communication. It is shown that a transmission rate behavior of  $O(\log n)$  bits per second per node can be achieved if the relay network allows cooperation such as multiple access cooperation or broadcast cooperation and also allows coding for networking between the nodes. This concept of coding in the network, is well known as "network coding"[30] and a significant body of research work from the networking community is focussed on this concept.

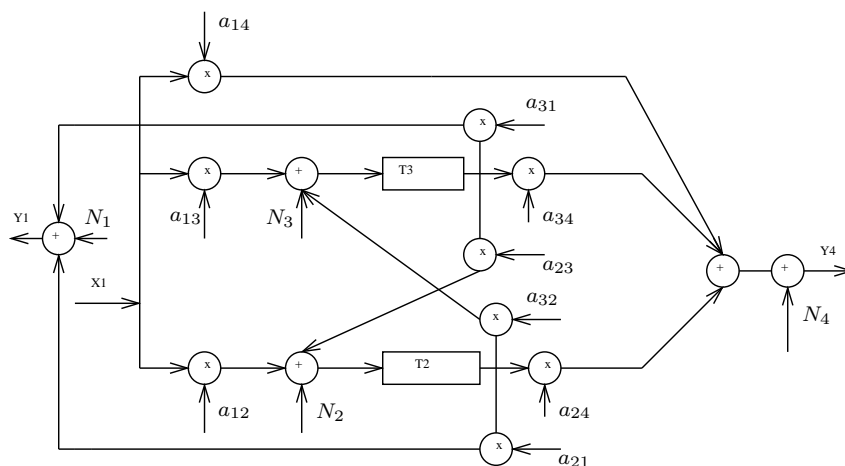


Figure 4.6: Multiple relay model.

Fig 4.6 shows a multiple relay model of a wireless network with 2 relays where each node can “hear” transmissions from all other nodes.  $a_{ij}$  is the path loss between two radio nodes and  $N_i$  is AWGN noise at  $i^{th}$  receiver node. The received signal in node  $k$  in the network is linear superposition of faded transmission signals from all other nodes and AWGN noise. The network model depicts a scenario in which a source-destination communication takes place with all other nodes at their service but without any kind of feedback from the final destination to the other nodes. The source repeats the signal  $X1$  unrestricted and the approach is to consider set of all feedforward graphs to the destination. However, in a restricted system as discussed in section 4.3.1, the source node transmits a signal  $X1$  only for half of the time. This signal is also received by relay nodes  $T2$  and  $T3$  and they re-transmit the signal to the final destination in the next half of the time without hearing each other. This network called the parallel relay network for multiple relay case is discussed in the next section.

### 4.3.2.1 Parallel relay network

A multiple relay network simplifies to the “parallel relay” architecture [17],[32],[39] when the relays do not hear each other and when the source is oblivious to relay transmissions. Such an architecture consisting of  $n + 1$  transmitting nodes is shown in Fig 4.7.

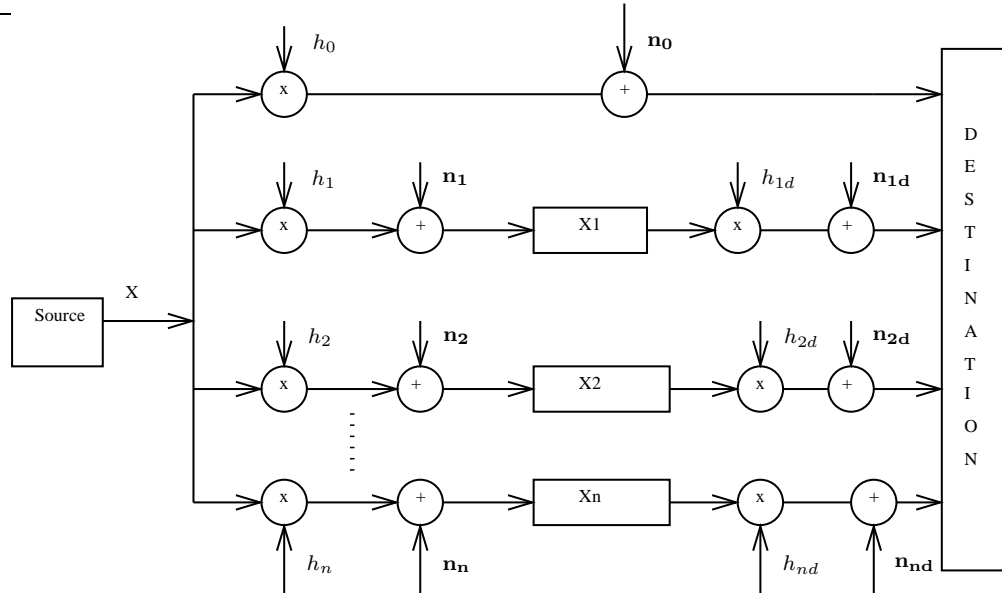


Figure 4.7: Parallel relay model.

The source terminal has information to transmit and  $n$  other user nodes act as relays for the source terminal. For medium access control,  $n + 1$  orthogonal channels are allocated for the  $n + 1$  transmitting terminals. In addition, due to the half duplex constraint, each channel is further divided into two orthogonal subspaces for signal transmission and reception.

As in the three terminal relay diversity model, at time index  $i$  the source transmits a vector  $\mathbf{x}$  of digitally modulated symbols  $x \in C$  to the destination and all the relays in the first subchannel, where  $C$  is the modulation alphabet. The received signal at the destination is

$$\mathbf{r}_d^{(1)}(i) = \sqrt{P_1} h_{sd1}^{(1)} \mathbf{x} + \sqrt{N_0} \mathbf{n}_0^{(1)}(i), \quad (4.8)$$

where  $h_{sd1}^{(1)}$  is the complex fading coefficient between the source and destination in the first sub-channel and  $\mathbf{n}_0^{(1)}$  is AWGN noise vector with zero mean and unit variance entries.

The received signal at the  $k^{th}$  relay receiver is then

$$\mathbf{r}_k^{(1)}(i) = \sqrt{P_1}h_k^{(1)}\mathbf{x} + \sqrt{N_k}\mathbf{n}_k^{(1)}(i), \quad (4.9)$$

where  $h_k^{(1)}$  is the complex fading coefficient between the source and  $k^{th}$  relay in the first subchannel and  $\mathbf{n}_k^{(1)}$  is the AWGN noise at the relay with zero mean and unit variance entries. If  $\mathbf{v}^k$  is the information transmitted by the  $k^{th}$  relay based on its received signal from the source, then the received signal at the destination over the  $k^{th}$  orthogonal channel from the relay is

$$\mathbf{r}_{rd}^{(k)}(i+1) = \sqrt{P_{rk}}\mathbf{v}^k h_{kd}^{(k)} + \sqrt{N_0}\mathbf{n}_{kd}^{(k)}(i+1). \quad (4.10)$$

The source optionally re transmits the information over the first subchannel again which is received by the destination as

$$\mathbf{r}_{sd}^{(1)}(i+1) = \sqrt{P_2}\mathbf{x}h_{sd2}^{(1)} + \sqrt{N_0}\mathbf{n}_2^{(1)}(i+1). \quad (4.11)$$

The signal receptions over the  $n+1$  orthogonal channels are then combined before symbol detection similarly to Fig 4.5. Intuitively, relay diversity can be understood as a form of receiver diversity with  $n$  relays imitating  $n$  receiver antennas for signal detection. Also, it can also be noted that the first phase of communication resembles a broadcast channel (BC) while the second phase of communication resembles a multiple access channel (MAC). This BC-MAC combination is an interesting feature of the parallel relay architecture.

## 4.4 Relay node functionality

In user cooperation, each assisting node has a certain functionality associated with it for extending cooperation. The functionality of the relay node would indeed depend on the coding strategy, cooperation architecture and the decoding technique at both the relay receiver and the destination receiver [24]. However, all forwarding functionalities of the relay node can be argued to be one of either facilitation, cooperation or transmitting “alternate information” [20].

The facilitation scheme is simple. The relay does not interfere in source transmissions and therefore relay assisted communication degenerates to a single hop communication between the source and destination.

The cooperation scheme in [20] is also popularly known as “decode and forward” (DF) [1],[36] or “regenerative relaying” and is a variant of multi hopping in wireless networks. Here, in addition to information routing via selected hops, decoding at every radio receiver along the route is carried out in a assisted manner based on all or some cooperative transmissions. The relays usually wait for the source to transmit the entire codeword for error checking [36] and error correction. If the information is successfully decoded, relays either apply repetition coding or use more powerful codes to assist the decoder at successive receivers.

A variant of the decode and forward technique which is often considered in relay case is the “symbol decode and forward” technique as in [1], [4], [5],[13, [15]. In this approach, rather than waiting for correct reception of the entire codeword from the source, relays cooperate by making an hard estimate of the received signal, encoding it again digitally and forward it to the destination. The vector  $\mathbf{u}$  in Eq(4.6) for symbol decode and forward strategy is then simply

$$\mathbf{u} = \hat{\mathbf{x}}, \tag{4.12}$$

where  $\hat{\mathbf{x}}$  is the hard estimate of  $\mathbf{x}$ .

Also, if along a multi-hop route as in Fig 4.2, signal transmissions  $\mathbf{u}_i$   $i = 1..m$  from  $m$  preceding hops are used for realizing diversity at each successive receiver then a “decode and forward multi hop diversity channel”[15] is formed.

In the “alternate information” class of forwarding, the relays convey a representation of their received signal to the destination so that the destination can effectively fuse its own received signal

with the signal from relay to decode the message. The alternate information is useful when it is a high quality representation of the signal. This strategy is also termed as “estimate and forward” [20], “compress and forward” [31] or “observe and forward” [2] by different authors. For example, a relay could “amplify and forward” (AF) [1],[26] the information when the channel between it and the source is not noisy and deeply faded. The vector  $\mathbf{u}$  in Eq(4.6) for amplify and forward strategy will be

$$\mathbf{u} = \beta \mathbf{r}_r(i), \tag{4.13}$$

where  $\beta$  is the amplification factor at the relay.

## 4.5 Cooperation schemes

### 4.5.1 Virtual antenna array

Cooperative communications by adopting techniques from multiple antenna systems is the fundamental idea of VAA architecture. By exchanging messages and then sharing their antennas with the other users, cooperating users can form a VAA. The recent advances made in MIMO, multi-user MIMO and space-time coding for local antenna arrays can then be suitably extended for the VAA case [25],[29]. A brief overview of the cooperative techniques under the VAA concept is given below.

#### 4.5.1.1 Transmitter cooperation

If the transmitters were allowed to jointly encode their messages then the channel becomes a multiple antenna broadcast channel [41]. For such a channel, the sum capacity has been shown to be achieved by dirty paper coding technique [27],[28]. Users employing transmitter cooperation can also jointly encode the data using techniques like zero forcing beam forming.

Figure 4.8 shows two transmitting terminals T1 and T2 collaborating to form a multiple antenna broadcast channel. The receivers do not collaborate for joint detection. T1 and T2 exchange information in codewords for reliable information transfer. The messages are precoded and then transmitted by the terminals.

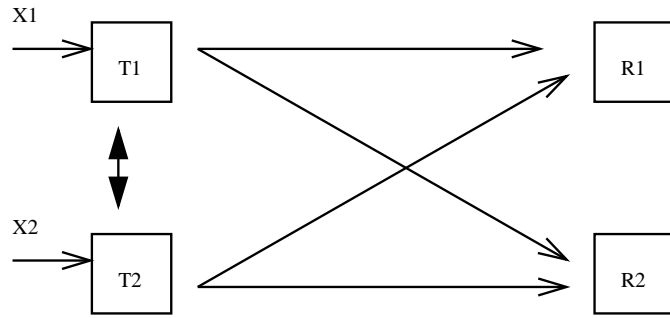


Figure 4.8: Transmitter cooperation: Broadcast channel.

#### 4.5.1.2 Receiver cooperation

If receivers cooperate to decode independent messages transmitted by user terminals as in Fig 4.9, the channel then resembles a multiple antenna multiple access channel (MAC) [41]. Joint detection based on cooperation would achieve a diversity order of number of receiver nodes for this case. Alternatively, for interference cancellation, iterative detection like in V-BLAST [76] can be carried out. Also, it can be observed that if the channels between the nodes are all symmetric, then the information decodable at the relay node from the source is same as at the destination. For this reason, receiver cooperation usually involves the “alternate information” [20],[31] class of forwarding. For instance, cooperating users can amplify and forward the message or can use a “compress and forward” scheme [31].

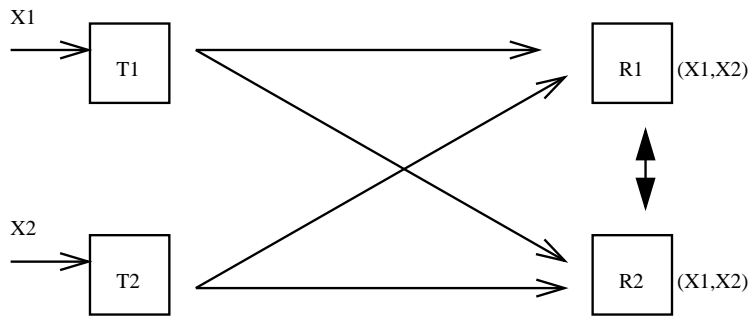


Figure 4.9: Receiver cooperation: MAC.

### 4.5.1.3 Cooperative MIMO

If both the transmitting terminals and the receiving terminals cooperate then the topology resembles a point-point MIMO link as show in Fig 4.10.

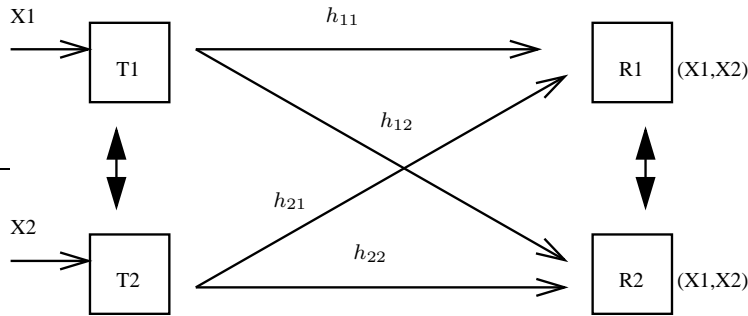


Figure 4.10: Cooperative MIMO.

This scenario can be realized in communication between clusters with node collaboration within a cluster. A topology of cluster communication is shown in Fig 4.11 where nodes  $A_i, B_i, C_i, D_i$  in cluster  $i$  communicate to nodes  $A_j, B_j, C_j, D_j$  in cluster  $j$ , mimicking a point-to-point MIMO communication link between clusters  $i$  and  $j$ .

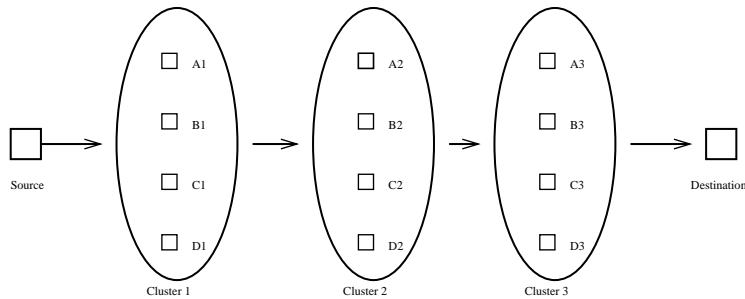


Figure 4.11: Cluster cooperation.

## 4.5.2 User cooperation in MAC

### 4.5.2.1 Repetition coding

User cooperation in multiple access channels via generalized feedback from the final receiver has been considered by Carleial in [21]. More generally, multiple access channels with cooperative di-

versity are special cases of multiple access channels with generalized feedback. The feedback signals in “user cooperation” case are the channel outputs of user transmissions at the partners’ encoders and not a “feedback” about other user’s transmission from the final receiver based on channel outputs at its decoder. Sendonaris et.al [4],[5] consider cooperative diversity for a faded multiple access channel using relaying and show that significant power savings and robustness to channel variations could be achieved upon using user cooperation diversity. This translates to increase in data rate and/or extra cell coverage. In Fig 4.12,  $X_1$ ,  $X_2$  are the user encoder outputs based on

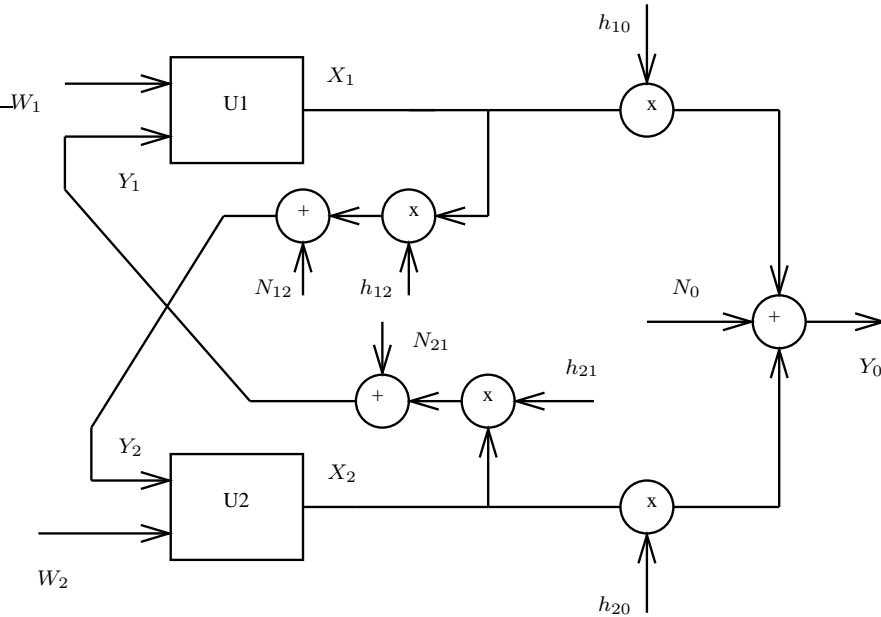


Figure 4.12: User cooperation in MAC.

user information signals  $W_1$ ,  $W_2$  and cooperative signals  $Y_1$  and  $Y_2$  respectively. The transmitters thus exchange messages and relay the messages and under the condition of high SNR between cooperating terminals, cooperative diversity of this form has been shown to enlarge achievable rate region for ergodic channels and improve outage performance for non-ergodic channels.

From Fig 4.12 [4], we have the following equations for cooperation in multiple access channel

$$Y_0(t) = h_{10}X_1(t) + h_{20}X_2(t) + N_0(t) \quad (4.14)$$

$$Y_1(t) = h_{21}X_2(t) + N_{21}(t) \quad (4.15)$$

$$Y_2(t) = h_{12}X_1(t) + N_{12}(t) \quad (4.16)$$

A CDMA implementation of this scheme has been presented [4]

$$X_1(t) = a_{11}b_1^{(1)}c_1(t), \quad a_{12}b_1^{(2)}c_1(t), \quad a_{13}b_1^{(2)}c_1(t) + a_{14}\hat{b}_2^{(2)}c_2(t) \quad (4.17)$$

$$X_2(t) = a_{21}b_2^{(1)}c_2(t), \quad a_{22}b_2^{(2)}c_2(t), \quad a_{24}b_2^{(2)}c_2(t) + a_{23}\hat{b}_1^{(2)}c_1(t), \quad (4.18)$$

where the parameter  $a_{ij}$  controls power allocation,  $b_j^i$  denotes user  $j$ 's  $i^{th}$  bit,  $c_j(t)$  is user  $j$ 's spreading code.

The cooperation strategy employed above is a two-user generalization of the cooperation scheme in [20] where the transmitters and receivers employ block Markov encoding and backward decoding. The CDMA scheme makes use of orthogonal spreading codes to maintain orthogonality while allowing superpositioning of signals at transmitter. This in turn lets the scheme implement a simple symbol-wise decode and forward relaying as relay node functionality. Further, phase knowledge at the transmitting terminals [6] is used to coherently combine the signals at the destination receiver.

#### 4.5.2.2 Coded cooperation

Cooperation via channel coding methods instead of direct relay or repetition coding is known as “coded cooperation” [11],[12],[14]. In this approach, cooperation occurs through partitioning of a user’s codeword such that a part of codeword is transmitted by user itself while the remainder is transmitted by the partner through partial or complete decoding. The relay upon successful decoding of the channel output, re-encodes the information to get additional parity bits that was not transmitted by the source node. This method shows better use of bandwidth as compared to repetition coding at the relay.

Fig 4.13 shows two users cooperating by time sharing [11],[12],[14]. Each user transmits the parity bits of the other user to the destination and the two users transmit in a TDMA manner.  $x_2$  and  $x_1$  are the partitions of the codeword. User 2 obtains  $x_2$  based on correct reception of  $x_1$  and transmits it to the base station. The above scheme is very efficient when the coherence time of the source-destination channel is greater than block length of the codeword.

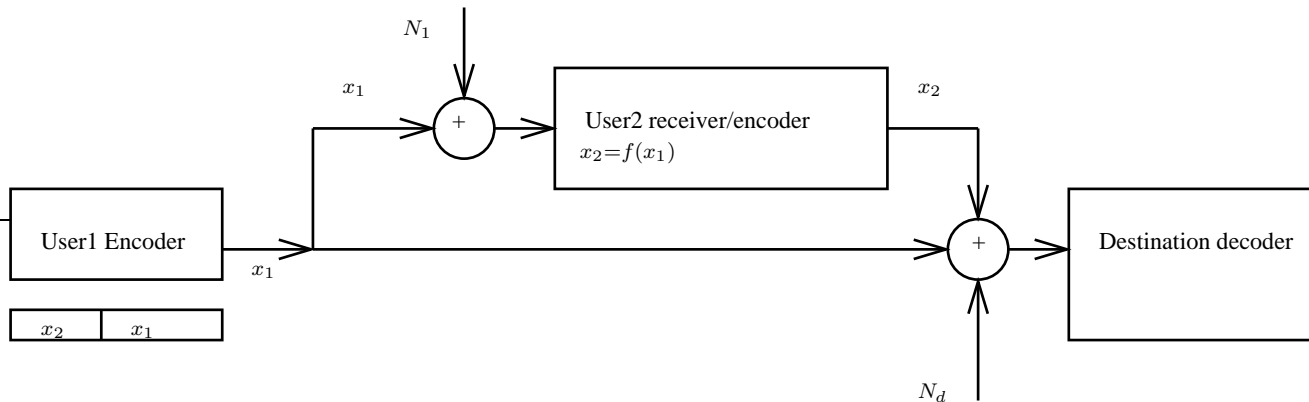


Figure 4.13: Coded cooperation.

The above discussions show that user cooperation can be implemented with a view of either forming a multiple antenna BC/MAC channel or for assisting an already existing BC/MAC channel.

## 4.6 Distributed space-time coding

Relay diversity topology shown in Fig 4.7 uses repetition coding at the relays with the relays transmitting at mutually orthogonal channels. The advantage of orthogonalizing signal transmissions is that the received signal at the receiver antenna(s) is not a phasor addition of signals transmitted from the relays. This avoids the inter-relay interference which would arise if there is time delay between the relay transmissions. However, orthogonal channel allocation makes inefficient use of bandwidth. The bandwidth efficiency of a time switched parallel relay scheme in Eq(4.8)-(4.9) which has  $n$  relays assisting a source is given by

$$\eta = \frac{m}{n+1} \text{ bits/s/Hz}, \quad (4.19)$$

where  $2^m$  is the size of signal constellation. A way of removing this inefficiency is to allow superpositioning of signals at the destination by letting the relays transmit in the same subchannel. The parallel relay case with superpositioning at the receiver is shown in Fig 4.14.

However, superpositioning of repetition coded signals does not achieve diversity gain at the destination receiver and transmit-side phase information is required to transmit beamform the repetition

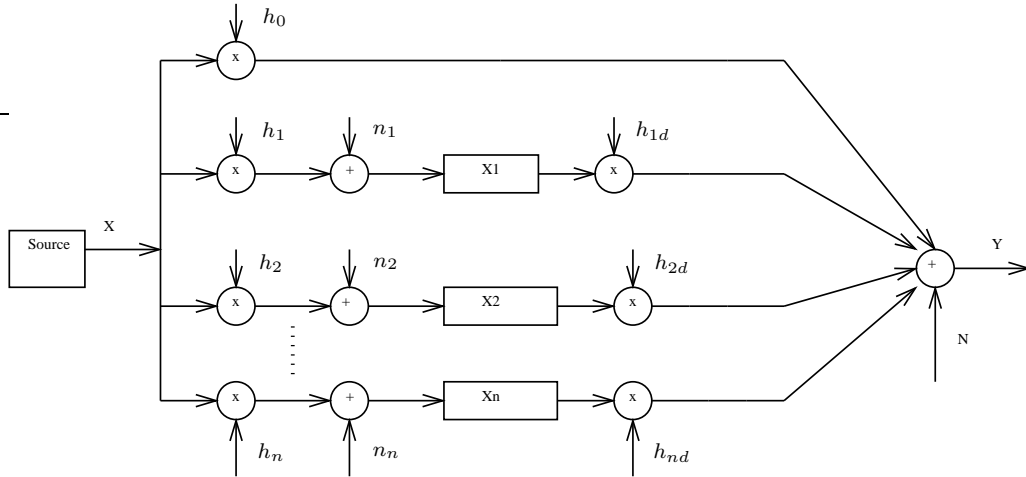


Figure 4.14: Parallel relay case with superpositioning.

coded signals to the destination receiver [4],[18].

If reliable transmit-side phase information cannot be acquired by the transmitting terminals then a way for achieving diversity gain is to use space-time coding instead of repetition coding at the relays. This approach of space-time coding by making use of VAAs has been termed distributed space-time coding [2].

Fig 4.15 shows a distributed space-time coding architecture [7]-[10] with  $n$  relays where a space time code defined by  $n + 1$  transmission vectors is used to achieve diversity at the destination using  $n$  relays.

Therefore, we see that a space-time code defined as

$$\mathbf{X} = \begin{bmatrix} \mathbf{v}_0 & \mathbf{v}_1 & \cdot & \cdot & \mathbf{v}_n \end{bmatrix} \quad (4.20)$$

can be utilized even by a single antenna user if vectors  $\mathbf{v}_i$  can be transmitted by the relays on behalf of the source to the destination in a symbol level synchronized manner. Space-Time coding based on algebraic code constructions [42]-[44] make efficient use of both temporal and spatial diversity available in the relay architecture.

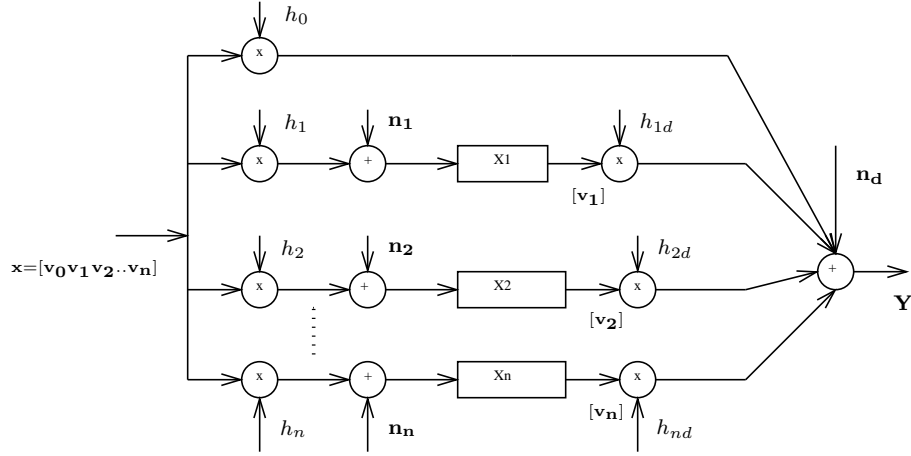


Figure 4.15: Distributed space-time coding.

### 4.6.1 Distributed Alamouti coding

A simple space-time code that can be used for the three terminal relay model in Fig 4.4 is the Alamouti space-time block code given by

$$\mathbf{X} = \begin{bmatrix} x_1 & x_2 \\ x_2^* & -x_1^* \end{bmatrix}. \quad (4.21)$$

For this purpose, consider a wireless relay system which consists of a source node, a destination node and a relay node. The system as in [2] operates under the following two-frame mechanism. It can be noted that all transmissions occur over the same subchannel in this scheme.

#### Frame $i$

Two unit modulus symbols  $x_1$  and  $x_2$ , or  $\mathbf{x} = [x_1 \ x_2]^T$  are transmitted to the destination and relay by the source. The received signal at the destination is

$$\mathbf{r}_d(i) = \sqrt{P_1} h_{sd1} \mathbf{x} + \sqrt{N_0} \mathbf{n}_d(i), \quad (4.22)$$

and the received signal at the relay is

$$\mathbf{r}_r(i) = \sqrt{P_1} h_{sr} \mathbf{x} + \sqrt{N_0} \mathbf{n}_r(i), \quad (4.23)$$

where  $h_{sd1}$ ,  $h_{sr}$  are the channel gains from the source to destination and relay respectively.  $\mathbf{n}_d(i)$ ,  $\mathbf{n}_r(i)$  are noise vectors whose entries are complex Gaussian with zero mean and unit variance. The relay then detects  $\mathbf{x}$  from  $\mathbf{r}_r(i)$  and maps it to vector  $\mathbf{u} = \begin{bmatrix} x_2 & -x_1^* \end{bmatrix}$  while the source maps it to vector  $\mathbf{v} = \begin{bmatrix} x_1 & x_2^* \end{bmatrix}^T$  such that  $\mathbf{X} = \begin{bmatrix} \mathbf{v} & \mathbf{u} \end{bmatrix}$  is an Alamouti matrix.

### Frame $i + 1$

The source transmits  $\mathbf{v}$  while the relay transmits  $\mathbf{u}$  (imitating the two antennas in the conventional Alamouti scheme). Assuming perfect symbol synchronization at the destination, we have

$$\mathbf{r}_d(i + 1) = \mathbf{XPh} + \sqrt{N_0} \mathbf{n}_d(i + 1), \quad (4.24)$$

where  $\mathbf{h} = \begin{bmatrix} h_{sd2} & h_{rd} \end{bmatrix}^T$ ,  $h_{sd2}$ ,  $h_{rd}$  are the channel gains from the source to destination and relay destination during frame  $i + 1$  and  $\mathbf{P} = \text{diag}(\sqrt{P_2}, \sqrt{P_r})$ . The channel gains are assumed to be zero mean complex Gaussian variables with variances  $\sigma_{sr}^2, \sigma_{rd}^2$  and  $\sigma_{sd}^2$  respectively and are assumed to be quasi-static over a frame length.  $\mathbf{n}_d(i + 1)$  is the noise column vector and entries of  $\mathbf{n}_d(i + 1)$  are additive white Gaussian with zero mean and a variance of 1 (0.5 per dimension). The schematic at the destination receiver for the aforementioned scheme is shown in Fig 4.16.

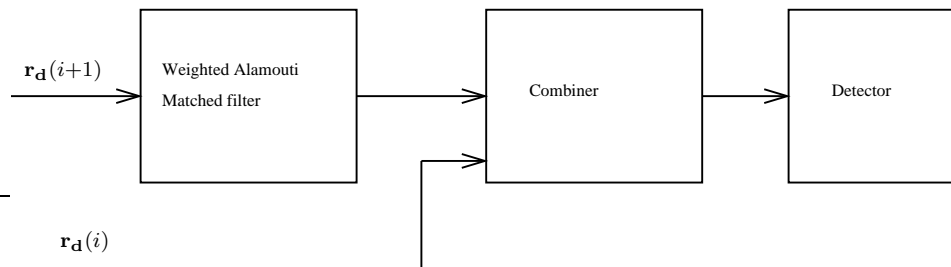


Figure 4.16: Receiver schematic.

## 4.7 Detection techniques

The destination receiver can employ various block decoding strategies based on the cooperation architecture and the coding strategy between the transmitting terminals. For example, in [20]

the terminals employ block superposition Markov encoding and backward decoding. Cooperating nodes can also engage in joint decoding in a broadcast channel scenario [37],[38] or can coordinate for joint detection in cooperative MIMO architecture. The above detection techniques are however useful only if the terminals exchange information in block lengths employing error checking and error correction.

In the case of symbol-wise decode and forward strategy, due to finite transmission power at the source it is possible that the relaying terminals might detect few symbols incorrectly. The relaying terminals as well as the destination would not be aware of the error which then results in error propagation along the route.

#### 4.7.1 Maximum likelihood detection

If the input symbols are equally likely, then it is straightforward that minimum probability of error detection is achieved by ML decoding at the destination receiver. However, ML decoding at the destination by taking into account the likelihood of decision errors at the terminals could be high in complexity. Moreover, even if such a detection technique is used at the destination, closed form expressions for the error bounds at the receiver are hard to obtain.

For example, consider the simplest of all relay networks, the three terminal relay network with the system model in 4.3.1 simplified as given below. The source transmits a unit modulus symbol  $x \in C$  to the relay, where  $C$  represents the BPSK constellation. The source transmitted signal is white and is equally likely to take values  $x_0$  and  $x_1$ . The received signal at the relay is then

$$r_1(i) = \sqrt{P_1}h_1x + \sqrt{N_0}n_1(i), \quad (4.25)$$

where  $h_1$  represents complex fading coefficient,  $n_1(i)$  represents complex AWGN noise of unit variance and  $N_0$  is the average noise power at the receiver. Relay then does an hard estimate  $\hat{x}$  using  $r_1(i)$  and forwards  $\hat{x}$  to the destination in the next orthogonal time slot. For simplicity, we assume that source-destination communication takes place only via the relay and the source does

not communicate directly to the destination. The received signal at destination in the next time slot is then given by

$$r_2(i+1) = \sqrt{P_r}h_2\hat{x} + \sqrt{N_0}n_2(i+1), \quad (4.26)$$

The relay decision process can be characterized by a random variable  $a_i$  defined as

$$a_i = \begin{cases} 1 & : \hat{x} = x \\ 0 & : \hat{x} \neq x \end{cases}$$

with  $E[a_i] = 1 - \epsilon$ . It can be observed that the above model is akin to a binary symmetric channel with average error probability  $\epsilon$ . Therefore by extending the total probability theorem to probability densities and using Eqs(4.24)-Eq(4.25), we have that

$$f(r_2|h_2, x_1) = P(a_i = 1)f(r_2|h_2, \hat{x} = x_1) + P(a_i = 0)f(r_2|h_2, \hat{x} = x_0). \quad (4.27)$$

Therefore the conditional PDFs at the destination for  $x = x_1$  and  $x = x_0$  can be written as

$$f(r_2|h_2, x = x_1) = (1 - \epsilon)\frac{1}{\pi N_0} \exp[-|r_2 - \sqrt{P_r}h_2x_1|^2] + \epsilon\frac{1}{\pi N_0} \exp[-|r_2 - \sqrt{P_r}h_2x_0|^2] \quad , \quad (4.28)$$

and

$$f(r_2|h_2, x = x_0) = (1 - \epsilon)\frac{1}{\pi N_0} \exp[-|r_2 - \sqrt{P_r}h_2x_0|^2] + \epsilon\frac{1}{\pi N_0} \exp[-|r_2 - \sqrt{P_r}h_2x_1|^2] \quad . \quad (4.29)$$

Maximum likelihood decoding based on Eq(4.27)- Eq(4.29) can be simplistically written as

$$\max_{\forall x_i} \ln \left[ (1 - \epsilon)\frac{1}{\pi N_0} \exp[-|r_2 - \sqrt{P_r}h_2x_i|^2] + \epsilon\frac{1}{\pi N_0} \exp[-|r_2 - \sqrt{P_r}h_2x'_i|^2] \right] \quad i = 0, 1, \quad (4.30)$$

where  $x'_i = x_0$  for  $x_i = x_1$  and  $x'_i = x_1$  for  $x_i = x_0$ . It can be observed from Eq(4.30) that the ML detection at the destination for the relay case is high in complexity.

## 4.7.2 Weighted combiner

As an alternative to the high complexity ML detection a low complexity weighted combiner scheme has been proposed in [1] and [5].

### 4.7.2.1 Orthogonal relaying

For this purpose, consider Eq(4.4)-Eq(4.7) for decode and forward case such that  $\mathbf{u} = \hat{\mathbf{x}}$ , where  $\hat{\mathbf{x}}$  is a hard estimate of  $\mathbf{x}$ .

If the combiner in Fig 4.5 uses weights  $w_i$  to combine the received signal sample from node  $i$ , then the output of the combiner can be given as

$$\mathbf{y}_c = w_0 h_{sd1}^{(1)*} \frac{\sqrt{P_1}}{N_0} \mathbf{r}_d^{(1)}(i) + w_0 h_{sd2}^{(1)*} \frac{\sqrt{P_2}}{N_0} \mathbf{r}_{sd}^{(1)}(i+1) + w_1 h_{rd}^{(2)*} \frac{\sqrt{P_r}}{N_0} \mathbf{r}_{rd}^{(2)}(i+1). \quad (4.31)$$

Eq(4.31) can also be equivalently written as

$$\mathbf{y}_c = h_{sd1}^{(1)*} \frac{\sqrt{P_1}}{N_0} \mathbf{r}_d^{(1)}(i) + h_{sd2}^{(1)*} \frac{\sqrt{P_2}}{N_0} \mathbf{r}_{sd}^{(1)}(i+1) + w'_1 h_{rd}^{(2)*} \frac{\sqrt{P_r}}{N_0} \mathbf{r}_{rd}^{(1)}(i+1). \quad (4.32)$$

From Eq(4.32) it is easy to deduce that the conditional SNR at the detector assuming correct symbol detection at the relay is

$$SNR_i = \frac{1}{N_0} \frac{[|h_{sd1}^{(1)}|^2 P_1 + |h_{sd2}^{(1)}|^2 P_2 + w'_1 |h_{rd}^{(2)}|^2 P_r]^2}{|h_{sd1}^{(1)}|^2 P_1 + |h_{sd2}^{(1)}|^2 P_2 + w_1'^2 |h_{rd}^{(2)}|^2 P_r}. \quad (4.33)$$

Extending this for the case of  $n$  parallel relays with orthogonal channel allocation we have the conditional SNR as

$$SNR_i = \frac{1}{N_0} \frac{[|h_{sd1}^{(1)}|^2 P_1 + |h_{sd2}^{(1)}|^2 P_2 + \sum_{i=1}^n w'_i |h_{id}^{(i+1)}|^2 P_{ri}]^2}{|h_{sd1}^{(1)}|^2 P_1 + |h_{sd2}^{(1)}|^2 P_2 + \sum_{i=1}^n w_i'^2 |h_{id}^{(i+1)}|^2 P_{ri}}. \quad (4.34)$$

By observing the term  $w'_i |h_{id}^{(2)}|^2$  in the conditional SNR in Eq(4.34), the transmitted power of the  $i$ th relay transmitter can be weighted by a factor  $\sqrt{w_i}$ . This, apart from achieving a weighted

combing naturally, also reduces the average transmit power from the relays. Upon doing this, the conditional SNR is

$$SNR_i = \frac{1}{N_0} [|h_{sd1}^{(1)}|^2 P_1 + |h_{sd2}^{(1)}|^2 P_2 + \sum_{i=1}^n w'_i |h_{id}^{(i+1)}|^2 P_{ri}] \quad (4.35)$$

#### 4.7.2.2 Distributed Alamouti coding

For distributed Alamouti scheme, weighting at the receiver would decrease the conditional SNR at the destination receiver because of the inter symbol interference caused by imperfect matching when a weighting factor  $w_i$  is used at the destination. To explain this further, consider a distributed Alamouti scheme in Eqs(4.21)-(4.23) with BPSK transmissions such that the source transmitted symbols take values 1 and  $-1$  with equal probability. Then the output of the combiner in Fig 4.16 is

$$\mathbf{y}_c = \frac{\sqrt{P_1}}{N_0} [h_{sd1}^* \mathbf{r}_d(i) + \mathbf{H}_w^H \mathbf{r}_d(i+1)], \quad (4.36)$$

where

$$\mathbf{H}_w = \begin{bmatrix} \sqrt{P_2} h_{sd2} & w'_1 \sqrt{P_r} h_{rd} \\ -w'_1 \sqrt{P_r} h_{rd}^* & \sqrt{P_2} h_{sd2}^* \end{bmatrix}. \quad (4.37)$$

From Eq(4.36)-Eq(4.37), the conditional SNR for symbol  $x_1$  at the output of the combiner assuming correct detection at the relay can be written as

$$SNR_i \approx \frac{1}{N_0} \frac{|P_1 |h_{sd1}|^2 + P_2 |h_{sd2}|^2 + w'_1 P_r |h_{rd}|^2}{|(w_1 - 1) \sqrt{P_2 P_r} h_{sd2}^* h_{rd}|^2 + |^2 P_1 |h_{sd1}|^2 + P_2 |h_{sd2}|^2 + w_1^2 P_r |h_{rd}|^2}. \quad (4.38)$$

Therefore we see that the detection technique in Eq(4.36) reduces the conditional SNR at the receiver for distributed Alamouti case resulting in poor BER at the receiver. This problem can be overcome by pre-multiplying the transmission vector  $\mathbf{u}$  at the relay by  $\sqrt{w_1}$  and modifying Eq(4.37)

as

$$\mathbf{H}_w = \begin{bmatrix} \sqrt{P_2}h_{sd2} & \sqrt{P_r w'_1}h_{rd} \\ -\sqrt{P_r w'_1}h_{rd}^* & \sqrt{P_2}h_{sd2}^* \end{bmatrix}. \quad (4.39)$$

Upon doing this, the conditional SNR then increases to

$$SNR_i = |h_{sd1}|^2 \frac{P_1}{N_0} + |h_{sd2}|^2 \frac{P_2}{N_0} + \sum_{i=1}^n w'_i |h_{rdi}|^2 \frac{P_{ri}}{N_0}, \quad (4.40)$$

which is similar to that of orthogonal relaying. However, it could be observed that the conditional SNR in Eq(4.40) assumes the case of perfect symbol detection at the relay. It is straightforward that averaging the conditional SNR over both correct and incorrect symbol detections will further reduce the conditional SNR. The interference caused by incorrect symbol detection by the relay is larger in a distributed space-time block coding scheme (DSTBC) than in a orthogonal relaying scheme. Therefore, it is natural that the conditional SNR of DSTBC is less than that of orthogonal relaying scheme when averaged over both correct and incorrect symbol detections by the relay. However, for realizing good BER at the receiver it is imperative that  $w'_1 = f(\epsilon) = g(|h_{sr}|)$ , i.e, the value of  $0 \leq w'_1 \leq 1$  should show the confidence the destination receiver has on the relay. For example, the optimal weight for simple BPSK transmissions in a three terminal network by combining the expectation of symbols is given as [1]

$$w'_1 = \frac{(1 - 2\epsilon)}{\epsilon(1 - \epsilon)|x_1 - x_0|^2 \gamma_r + 1}, \quad (4.41)$$

where  $\gamma_r = |h_{rd}|^2 \frac{\sqrt{P_r}}{N_0}$ .

#### 4.7.2.3 Coherent combining

For the case of coherent combining, we assume that all transmitting terminals acquire transmit side phase information. Then Eqs(4.8)-(4.9) modify as follows. The received signal at the destination is

$$\mathbf{r}_d(i) = \sqrt{P_1}h_0\mathbf{x} + \sqrt{N_0}\mathbf{n}_0(i), \quad (4.42)$$

where  $h_0$  is the real fading coefficient between the source and destination and  $\mathbf{n}_o$  is AWGN noise vector with zero mean, unit variance entries.

The received signal at the  $k^{th}$  relay receiver is

$$\mathbf{r}^k(i) = \sqrt{P_1}h_k\mathbf{x} + \sqrt{N_k}\mathbf{n}_k(i), \quad (4.43)$$

where  $h_k$  is the real fading coefficient between the source and  $k^{th}$  relay and  $\mathbf{n}_k$  is the AWGN noise vector at the relay with zero mean and unit variance entries. Then every  $i^{th}$  relay makes a hard estimate  $\hat{x}_i$  based on its received signal from the source  $\mathbf{r}^k(i)$ . The relay transmitters use their transmit-side phase information to phase-offset the transmitted symbol. All relay transmissions take place in the same subchannel such that the signals are superimposed at the destination receiver. The received signal at the destination is then

$$\mathbf{r}_{\mathbf{rd}}(i+1) = \sqrt{P_2}h_{sd2}\mathbf{x} + \sum_{i=1}^n \sqrt{P_{ri}}h_{id}\hat{\mathbf{x}}_i + \sqrt{N_0}\mathbf{n}_d(i+1), \quad (4.44)$$

where  $h_{sd2}$  and  $h_{id}$  is modeled as a real fading coefficient between the  $i^{th}$  relay and the destination and  $\mathbf{n}_d(i+1)$  is the AWGN noise vector at the destination with zero mean and unit variance entries.

The output of the combiner is then given by

$$\mathbf{y}_c = h_0 \frac{\sqrt{P_1}}{N_0} \mathbf{r}_d(i) + w(\sqrt{P_2}h_{sd2} + \sum_{i=1}^n \sqrt{P_{ri}}h_{id})\mathbf{r}_{\mathbf{rd}}(i+1). \quad (4.45)$$

From Eq(4.42), the conditional SNR at the output of the combiner assuming correct detection at the relay is given as

$$SNR_i = \frac{[h_0^2 P_1 + w(\sqrt{P_2}h_{sd2} + \sum_{i=1}^n \sqrt{P_{ri}}h_{id})]^2}{N_0[P_1 h_0^2 + w^2(\sqrt{P_2}h_{sd2} + \sum_{i=1}^n \sqrt{P_{ri}}h_{id})^2]}. \quad (4.46)$$

## 4.8 Simulation example

We compare the performance of various strategies mentioned in section as a part of our literature survey for BPSK modulation. The performance of the schemes is then logically verified with the conditional SNRs presented above. In the example, we assume equally balanced channels in a

three terminal network. In the simulation example it can be observed that the performance of orthogonal relaying with weighting at receiver and orthogonal relaying with weighting at transmitter perform almost identically. This is in line with the conditional SNR derivations in Eq(4.34) and Eq(4.35). The conditional SNRs are approximately equal for both the techniques even though the transmitter weighting technique uses less transmit power in average.

The performance of transmitter weighted- DSTBC technique is slightly worse than transmitter-weighted orthogonal relaying technique. As was pointed out earlier in section 4.7.2.2, this can be attributed to the stronger interference caused in DSTBC technique if the relay detects the symbol incorrectly. The performance of receiver-weighted DSTBC technique is worse than all other schemes. This is due to the lower conditional SNR realised at the receiver as in Eq(4.38). Finally, the performance of an ideal multiple antenna second order diversity technique is depicted. A performance gap is observed to exist between relay diversity schemes and the multiple antenna diversity. This is clearly due to the error propagation caused by incorrect symbol detections by the relay.

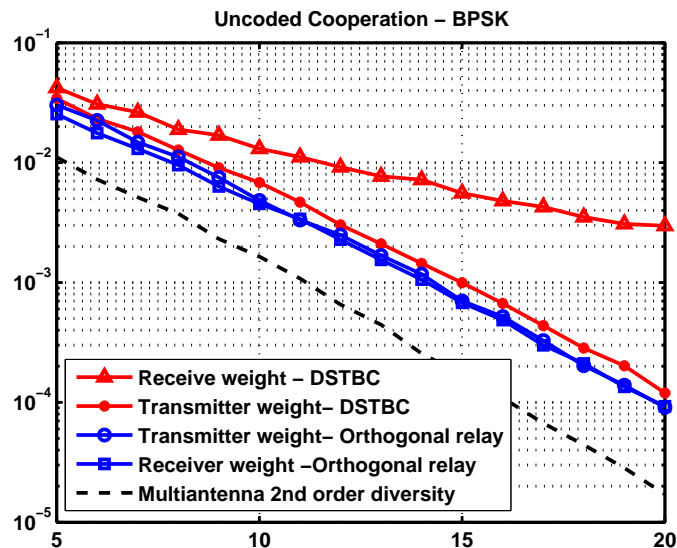


Figure 4.17: Distributed Alamouti scheme with channel estimation errors at the relay.

## 4.9 Conclusion

The schematics of a three terminal relay model, parallel relay architecture and an overview of various cooperative architectures based on VAA concept and user cooperation in MAC channels have been presented in this chapter. Cooperative diversity using orthogonal channel allocation and distributed space-time coding were also explained. Finally, conditional SNRs achieved by a weighted combiner for different cooperative diversity schemes were analytically compared and logically verified using simulation results. The performance gap between relay diversity scheme and multiple antenna transmit diversity scheme has also been shown. In the next chapter, we consider a simple transmitter weighting scheme with weights of just 0 or 1 at the transmitter. As we would see later, this simple “on-off” relaying technique provides good performance gains over blind relaying.

# Chapter 5

## Selection Relaying

### 5.1 Introduction

Relaying between radio nodes can be used to assist decoding at every successive radio receiver in a multiple terminal communication link. This form of diversity, called multi-user spatial diversity can be used along with or instead of hopping in a wireless network. The relay diversity formulation, however, has a fundamental limitation. The source-relay channel is normally noisy and fading and therefore relay communication to the destination is not always a high quality representation of the source transmitted information. This means that regenerative relays could communicate erroneous sequences to the destination receiver and non regenerative relays could amplify noise along the route.

Indeed, for regenerative relays, error propagation along the route can be controlled by employing error checking, error correction and ARQ protocols for the source-relay communication but this could increase end-end latency in the network and is not always desirable. To reduce complexity, regenerative relays can employ a simple symbol decode and forward technique and let the error checking, correction and ARQ messaging be accomplished at the destination. But maximum likelihood decoding at the destination incorporating the likelihood of decision errors at the relays involves logarithmic computations and again incurs high complexity. On the other hand, if the destination were to assume perfect detection at the relay to implement ML decoding, decoding is simple but performance benefits of cooperation turns out to be completely dependent on the

source-relay channel conditions.

In view of the above problem, in this chapter, we consider a simple thresholding method that can be adopted by the relay to try and communicate “high quality signals” to the final receiver. In this approach known as “selection relaying” [3], the relay “facilitates” [20] source transmissions by not communicating to the destination whenever the source-relay channel is deeply faded. We consider thresholding at the relay for the simple three terminal network using the knowledge of channel variances in the network to maximize performance at the destination and observe that this can provide good performance benefits with low complexity detection.

Here, we also note a subtle difference between user diversity and transmit diversity systems. In transmit diversity, it is direct and straightforward that employing additional resources such as transmit power would increase reliability in communication. However in user diversity systems, it is not so. The challenge in the relay diversity setup here is therefore to use the additional resources such as user battery power for good benefit. Accordingly, we refrain from imposing a transmit power constraint for transporting a bit over the network but instead impose user power constraints and concentrate on maximizing the benefit given these additional resources. Nevertheless, the basic belief behind these relay systems is that if a user acted as a relay for the benefit of some other user at one time, he would in turn be benefited some other time. Therefore, we perceive that unless network power is a performance criteria, transmit power constraint is not entirely necessary for investigating single source systems.

## 5.2 Optimal threshold for orthogonal relaying

We consider the simple three terminal relay network with orthogonal channel allocations to investigate optimal thresholding for the relay case. A half-duplex constraint is imposed at all radio nodes to avoid simultaneous transmission and reception. The channel is assumed to be quasi-static over a frame length. Also, transmitting terminals do not possess any transmit side channel information but the fading process is known to the receiver. A prior global knowledge of long-term fading or the channel variances between the radio nodes is assumed to determine the threshold. For clarity,

we repeat the system model for orthogonal relaying which was explained earlier in Chapter 4.

The source transmits a symbol  $x \in C$  to the relay and destination in frame  $i$ . The received signals in time index  $i$  are

$$r_d^{(1)}(i) = \sqrt{P_1} h_{sd1}^{(1)} x + \sqrt{N_0} n_d^{(1)}(i). \quad (5.1)$$

$$r_r^{(1)}(i) = \sqrt{P_1} h_{sr}^{(1)} x + \sqrt{N_0} n_r^{(1)}(i). \quad (5.2)$$

The relay makes an estimate  $\hat{x}$  based on its reception from the source which can be written as

$$\hat{x} = a_1 x + (1 - a_1) x', \quad (5.3)$$

where

$$a_1 = \begin{cases} 1 & : \text{ relay decodes symbol } x \text{ correctly} \\ 0 & : \text{ relay decodes symbol } x \text{ incorrectly} \end{cases}$$

and  $x' \neq x$  with  $x' \in C$ . The relay forwards its estimate  $\hat{x}$  to the destination in the next frame  $i + 1$  in an orthogonal channel while the source optionally re-transmits  $x$  to the destination.

The destination receives the signal

$$r_{rd}^{(2)}(i + 1) = \sqrt{P_r} \hat{x} h_{rd}^{(2)} + \sqrt{N_0} n_d^{(2)}(i + 1) \quad (5.4)$$

from the relay in the second subchannel, where  $h_{rd}^{(2)}$  is the channel gain between the relay and destination in the second orthogonal subchannel. The channel gains are assumed to be zero mean complex Gaussian variables with variances  $\sigma_{sr}^2$ ,  $\sigma_{rd}^2$  and  $\sigma_{sd}^2$  respectively and are assumed to quasi-static over a frame length.  $n_d^{(1)}(i)$ ,  $n_d^{(1)}(i + 1)$  and  $n_d^{(2)}(i + 1)$  represent additive white Gaussian noise with zero mean and unit variance and  $N_0$  is the noise power at all receivers. The output of the combiner is then,

$$y_c = h_{sd1}^{(1)*} \frac{\sqrt{P_1}}{N_0} r_d^{(1)}(i) + h_{rd}^{(2)*} \frac{\sqrt{P_r}}{N_0} r_{rd}^{(2)}(i + 1). \quad (5.5)$$

Using Eq(5.1)-(5.3) in Eq(5.5) the decision statistics can be written as

$$\tilde{x} = (a_1 \frac{P_r}{N_0} |h_{rd}|^2 + \frac{P_1}{N_0} |h_{sd2}|^2)x + (1 - a_1) \frac{P_r}{N_0} |h_{rd}|^2 x' + h_{sd1}^{(1)*} \frac{\sqrt{P_1}}{N_0} n_d^{(1)} + h_{rd}^{(2)*} \frac{\sqrt{P_r}}{N_0} n_d^{(2)}(i + 1). \quad (5.6)$$

If the conditional probability  $P(a = 0|h_{sr}) = \epsilon$ , then we have

$$E[\tilde{x}|h_{sr}, h_{rd}, h_{sd2}] = ((1 - \epsilon) \frac{P_r}{N_0} |h_{rd}|^2 + \frac{P_1}{N_0} |h_{sd2}|^2)x + \epsilon \frac{P_r}{N_0} |h_{rd}|^2 x'. \quad (5.7)$$

The destination then makes an hard estimate  $x_d$  of the symbol  $x$  based on its received signals over the two time frames. The probability of bit error  $P(x_d \neq x)$  at the destination denoted as  $P(e_d)$  throughout this chapter is given by

$$P(e_d) = P(a_1 = 1)P(e_d|a_1 = 1) + P(a_1 = 0)P(e_d|a_1 = 0). \quad (5.8)$$

### 5.2.1 Thresholding

It was seen that maximum likelihood detection incorporating the possibility of detection errors at the relay is high in complexity even for a simple three terminal network with BPSK transmissions. In view of this complexity, a thresholding scheme is used at the relay followed by a traditional combiner at the destination. Upon threshold testing, the relay decodes a symbol only if the estimated quasi-static channel gain is greater than a certain threshold. If the channel gain is below a certain threshold, the relay does not decode the symbol for transmitting to the destination and the destination assumes that the relay-destination channel gain is zero for its decoder. The thresholding decision process at the relay can be represented by a random variable  $b$  such that

$$b = \begin{cases} 1 & : |h_{sr}|^2 \geq T \\ 0 & : |h_{sr}|^2 < T, \end{cases}$$

where  $T$  is the threshold for channel gain. The idea of thresholding at relays is in essence to minimize the effect of deep fades in the source-relay channel.

A threshold  $T_o$  based on outage probability has been provided in [3]:  $T_o = (2^{2R} - 1)/\bar{\gamma}$ , where  $R = \frac{r_s}{W} b/s/Hz$ , is the spectral efficiency,  $r_s$  is the transmission rate of source node,  $W$  is the continuous-time bandwidth available for transmission and  $\bar{\gamma}$  is the signal to noise ratio (SNR) at the source. However, this threshold does not incorporate the wireless path loss between the radio nodes represented by the channel gain variances (i.e., the network geometry) and therefore is not designed to minimize the BER at the destination.

In view of the above limitation, we now derive a new threshold.

The probability of bit error at the destination upon using a threshold at the relay is given by

$$\begin{aligned} P(e_d) = & P(b = 0)P(e_d|b = 0) + P(b = 1)P(a_1 = 0|b = 1)P(e_d|b = 1, a_1 = 0) \\ & + P(b = 1)P(a_1 = 1|b = 1)P(x_d \neq x|b = 1, a_1 = 1). \end{aligned} \quad (5.9)$$

Investigating Eq(5.9) termwise, we have from [75],

$$P(b = 1)P(a_1 = 0|b = 1) = \frac{1}{\sigma_{sr}^2} \int_T^\infty e^{-\beta/\sigma_{sr}^2} [P_s(\beta.\bar{\gamma})] d\beta, \quad (5.10)$$

and

$$P(b = 1)P(a_1 = 1|b = 1) = \frac{1}{\sigma_{sr}^2} \int_T^\infty e^{-\beta/\sigma_{sr}^2} [1 - P_s(\beta.\bar{\gamma})] d\beta, \quad (5.11)$$

where  $\bar{\gamma} = \frac{P_t}{N_0}$  is the transmit SNR at source in frame index  $i$ ,  $T$  is the threshold (no units),  $P_s(\beta.\bar{\gamma})$  is the symbol error probability at the relay and  $\beta = |h_{sr}|^2(\beta \geq T)$ .

By denoting  $P(b = 0) = \lambda_1(T, \bar{\gamma})$ ,  $P(e_d|b = 0) = \Omega(\bar{\gamma})$ ,  $P(b = 1)P(a_1 = 0|b = 1) = \lambda_2(T, \bar{\gamma})$ ,  $P(e_d|b = 1, a_1 = 0) = C(\bar{\gamma}, \bar{\gamma}_r)$ ,  $P(b = 1)P(a_1 = 1|b = 1) = \lambda_4(T, \bar{\gamma})$ ,  $P(e_d|b = 1, a_1 = 1) = \Psi(\bar{\gamma}_1, \bar{\gamma}_r)$  where  $\bar{\gamma}_r = \frac{P_r}{N_0} \sigma_{rd}^2$  is the average received power at the destination from the source in frame  $i+1$ ,  $\bar{\gamma}_1 = \bar{\gamma} \sigma_{sd}^2$  is the average received power at the destination from the source in frame index  $i$ . we can rewrite

Eq(5.9) as

$$P(e_d) = \lambda_1(T, \bar{\gamma})\Omega(\bar{\gamma}_1) + \lambda_2(T, \bar{\gamma})C(\bar{\gamma}_1, \bar{\gamma}_r) + \lambda_4(T, \bar{\gamma}, \bar{\gamma}_r)\Psi(\bar{\gamma}_1, \bar{\gamma}_r). \quad (5.12)$$

We now treat this as a constrained optimization problem, i.e, we obtain the threshold  $T$  which minimizes the BER by treating the other variables as constants. This can be achieved by

$$\frac{\partial P(e_d)}{\partial T} = 0. \quad (5.13)$$

Using  $\frac{\partial(\lambda_1(T, \bar{\gamma}))}{\partial T} = (\frac{1}{\sigma_{sr}^2})e^{\frac{-T}{\sigma_{sr}^2}}$ ,  $\frac{\partial(\lambda_2(T, \bar{\gamma}))}{\partial T} = (\frac{-1}{\sigma_{sr}^2})e^{\frac{-T}{\sigma_{sr}^2}}P_s(T, \bar{\gamma})$ , from Eq(5.10) and Eq(5.11), and  $\lambda_1(T, \bar{\gamma}) + \lambda_2(T, \bar{\gamma}) + \lambda_4(T, \bar{\gamma}) = 1$ , and then solving for  $P_s(T, \bar{\gamma})$  we obtain

$$P_s(T, \bar{\gamma}) = \frac{\Omega(\bar{\gamma}_1) - \Psi(\bar{\gamma}_1, \bar{\gamma}_r)}{C(\bar{\gamma}_1, \bar{\gamma}_r) - \Psi(\bar{\gamma}_1, \bar{\gamma}_r)}. \quad (5.14)$$

$P_s(T, \bar{\gamma})$  is now the threshold for instantaneous symbol error probability at the relay for the source's transmission.

## 5.2.2 Additional diversity

The source can optionally re-transmit  $x$  in frame index  $i + 1$  using the first orthogonal subchannel to the destination. The destination receiver can make use of temporal diversity, if available in the channel, to achieve a higher diversity in its signal detection. The distributed Alamouti scheme targets a diversity degree 2 with one receiver antenna and with temporal diversity the target diversity becomes 3. The received signal at the destination is then

$$r_{sd}^{(1)}(i + 1) = \sqrt{P_2}xh_{sd2}^{(1)} + \sqrt{N_0}n_d^{(1)}(i + 1) \quad (5.15)$$

from the source, where  $h_{sd2}^{(1)}$  is the channel gain between source and destination in the frame  $i + 1$  over the first orthogonal sub channel.

The output of the combiner is then,

$$y_c = h_{sd2}^{(1)*} \frac{\sqrt{(P_2)}}{N_0} r_d^{(1)}(i+1) + h_{sd1}^{(1)*} \frac{\sqrt{(P_1)}}{N_0} r_d^{(1)}(i) + h_{rd}^{(2)*} \frac{\sqrt{(P_r)}}{N_0} r_{rd}^{(2)}(i+1). \quad (5.16)$$

Accordingly, the solution of instantaneous symbol error probability threshold  $P_s(T, \bar{\gamma})$  modifies to

$$P_s(T, \bar{\gamma}) = \frac{\Omega'(\bar{\gamma}_1, \bar{\gamma}_2) - \Psi'(\bar{\gamma}_1, \bar{\gamma}_2, \bar{\gamma}_r)}{C'(\bar{\gamma}_1, \bar{\gamma}_2, \bar{\gamma}_r) - \Psi'(\bar{\gamma}, \bar{\gamma}_2, \bar{\gamma}_r)} \quad (5.17)$$

where  $\bar{\gamma}_2 = \frac{P_2}{N_0} \sigma_{sr}^2$  and  $\Omega'(\bar{\gamma}_1, \bar{\gamma}_2), \Psi'(\bar{\gamma}_1, \bar{\gamma}_2, \bar{\gamma}_r), C'(\bar{\gamma}_1, \bar{\gamma}_2, \bar{\gamma}_r)$  are the new error bounds suitably modified for this case.

### 5.3 Optimal threshold for Alamouti relaying

The threshold scheme explained in 5.2.1 can also be used for distributed Alamouti relay diversity. For clarity, we first describe the Alamouti relay scheme before proceeding to present the thresholds for this case. For this purpose, consider a wireless relay system which consists of a source node, a destination node and a relay node cooperating using the Alamouti space-time block code given by

$$\mathbf{X} = \begin{bmatrix} x_1 & x_2 \\ x_2^* & -x_1^* \end{bmatrix}. \quad (5.18)$$

The system as in [2] operates under the following two-frame mechanism. For clear exposition, we repeat the system model that was explained in Chapter 4 . It can be noted that all transmissions occur over the same subchannel in this scheme.

#### Frame $i$

Two unit modulus symbols  $x_1$  and  $x_2$ , or  $\mathbf{x} = \begin{bmatrix} x_1 & x_2 \end{bmatrix}^T$  are transmitted to the destination and relay by the source. The received signal at the destination is

$$\mathbf{r}_d(i) = \sqrt{P_1} h_{sd1} \mathbf{x} + \sqrt{N_0} \mathbf{n}_d(i), \quad (5.19)$$

and the received signal at the relay is

$$\mathbf{r}_r(i) = \sqrt{P_1} h_{sr} \mathbf{x} + \sqrt{N_0} \mathbf{n}_r(i), \quad (5.20)$$

where  $h_{sd1}$ ,  $h_{sr}$  are the channel gains from the source to destination and relay respectively.  $\mathbf{n}_d(i)$ ,  $\mathbf{n}_r(i)$  are noise vectors whose entries are complex Gaussian with zero mean and unit variance. The relay then detects  $\mathbf{x}$  from  $\mathbf{r}_r(i)$  and maps it to vector  $\mathbf{u} = \begin{bmatrix} x_2 & -x_1^* \end{bmatrix}$  while the source maps it to vector  $\mathbf{v} = \begin{bmatrix} x_1 & x_2^* \end{bmatrix}^T$  such that  $\mathbf{X} = \begin{bmatrix} \mathbf{v} & \mathbf{u} \end{bmatrix}$  is an Alamouti matrix.

### Frame $i + 1$

The source transmits  $\mathbf{v}$  while the relay transmits  $\mathbf{u}$  (imitating the two antennas in the conventional Alamouti scheme). Assuming perfect symbol synchronization at the destination, we have

$$\mathbf{r}_d(i+1) = \mathbf{XPh} + \sqrt{N_0} \mathbf{n}_d(i+1), \quad (5.21)$$

where  $\mathbf{h} = \begin{bmatrix} h_{sd2} & h_{rd} \end{bmatrix}^T$ ,  $h_{sd2}$ ,  $h_{rd}$  are the channel gains from the source to destination and relay destination during frame  $i + 1$  and  $\mathbf{P} = \text{diag}(\sqrt{P_2}, \sqrt{P_r})$ . The channel gains are assumed to be zero mean complex Gaussian variables with variances  $\sigma_{sr}^2$ ,  $\sigma_{rd}^2$  and  $\sigma_{sd}^2$  respectively and are assumed to quasi-static over a frame length.  $\mathbf{n}_d(i+1)$  is the noise column vector with entries  $n_{d1}(i+1)$ ,  $n_{d2}(i+1)$  which are additive white Gaussian with zero mean and a variance of 1 ( 0.5 per dimension).

#### 5.3.1 Detection at the destination node

The above distributed Alamouti scheme setup leads to the following structure for  $\mathbf{X}$

$$\mathbf{X} = \begin{bmatrix} x_1 & a_2 x_2 + (1 - a_2) x_4 \\ x_2^* & -a_1 x_1^* - (1 - a_1) x_3^* \end{bmatrix} \quad (5.22)$$

where,

$$a_i = \begin{cases} 1 & : \text{ relay decodes symbol } x_i \text{ correctly} \\ 0 & : \text{ relay decodes symbol } x_i \text{ incorrectly} \end{cases}$$

and  $x_3$  and  $x_4$  are the incorrectly decoded symbols corresponding  $x_1$  and  $x_2$  respectively. In a view that  $\Pr(a_i = 0)$  could be minimized by thresholding or by other means such as channel coding, a low complexity detection similar to [1] normally carried out at the destination.

The output of the combiner is

$$\mathbf{y}_c = \mathcal{H}^H \mathbf{r}_d(i+1) \quad (5.23)$$

where

$$\mathcal{H} = \begin{bmatrix} \frac{\sqrt{P_2}}{N_0} h_{sd2} & \frac{\sqrt{P_r}}{N_0} h_{rd} \\ -\frac{\sqrt{P_r}}{N_0} h_{rd}^* & \frac{\sqrt{P_2}}{N_0} h_{sd2}^* \end{bmatrix}. \quad (5.24)$$

From Eq(5.24), the decision statistics are

$$\begin{aligned} \tilde{x}_1 &= (a_1 \frac{P_r}{N_0} |h_{rd}|^2 + \frac{P_2}{N_0} |h_{sd2}|^2) x_1 + \frac{\sqrt{P_2 P_r}}{N_0^2} h_{sd2}^* h_{rd} (1 - a_2) (x_4 - x_2) + \\ &\quad (1 - a_1) \frac{P_r}{N_0} |h_{rd}|^2 x_3 + \frac{\sqrt{P_2}}{\sqrt{N_0}} h_{sd2}^* n_{d1}(i+1) - \frac{\sqrt{P_r}}{\sqrt{N_0}} h_{rd} n_{d2}(i+1). \\ \tilde{x}_2 &= (a_2 \frac{P_r}{N_0} |h_{rd}|^2 + \frac{P_2}{N_0} |h_{sd2}|^2) x_2 + \frac{\sqrt{P_2 P_r}}{N_0^2} h_{sd2} h_{rd}^* (1 - a_1) (x_1 - x_3) + \\ &\quad (1 - a_2) \frac{P_r}{N_0} |h_{rd}|^2 x_4 + \frac{\sqrt{P_r}}{\sqrt{N_0}} h_{rd}^* n_{d1}(i+1) + \frac{\sqrt{P_2}}{\sqrt{N_0}} h_{sd2} n_{d2}(i+1). \end{aligned} \quad (5.25)$$

As can be observed from the above equation, the system is interference limited when the relay decodes incorrectly ( $a_i = 0$ ). The probability of bit error at the destination for this system is given by

$$\begin{aligned} P(e_d) &= P(a_1 = 0, a_2 = 1)P(e_d|a_1 = 0, a_2 = 1) + P(a_2 = 0, a_1 = 1)P(e_d|a_2 = 0, a_1 = 1) + \\ &\quad P(a_1 = 0, a_2 = 0)P(e_d|a_1 = 0, a_2 = 0) + P(a_1 = 1, a_2 = 1)P(e_d|a_1 = 1, a_2 = 1). \end{aligned} \quad (5.26)$$

### 5.3.2 Thresholding

The Space-Time Alamouti code when distributed and thresholded becomes

$$\mathbf{X} = \begin{bmatrix} x_1 & a_2 b x_2 + b(1 - a_2) x_4 \\ x_2^* & -a_1 b x_1^* - b(1 - a_1) x_3^* \end{bmatrix} \quad (5.27)$$

where,

$$b = \begin{cases} 1 & : |h_{sr}|^2 \geq T \\ 0 & : |h_{sr}|^2 < T. \end{cases}$$

and  $T$  is the threshold for channel gain.

The decision statistics at the destination when a threshold is used at the relay is given by,

$$\begin{aligned} \tilde{x}_1 &= (a_1 b^2 \frac{P_r}{N_0} |h_{rd}|^2 + \frac{P_2}{N_0} |h_{sd2}|^2) x_1 + \frac{\sqrt{P_2 P_r}}{N_0^2} h_{sd2}^* h_{rd} b (1 - a_2) (x_4 - x_2) + \\ & \quad b^2 (1 - a_1) \frac{P_r}{N_0} |h_{rd}|^2 x_3 + \frac{\sqrt{P_2}}{\sqrt{N_0}} h_{sd2}^* n_{d1} (i + 1) - b \frac{\sqrt{P_r}}{\sqrt{N_0}} h_{rd} n_{d2} (i + 1). \\ \tilde{x}_2 &= (a_2 \frac{P_r}{N_0} b^2 |h_{rd}|^2 + \frac{P_2}{N_0} |h_{sd2}|^2) x_2 + \frac{\sqrt{P_2 P_r}}{N_0^2} b h_{sd2} h_{rd}^* (1 - a_1) (x_1 - x_3) + \\ & \quad (1 - a_2) \frac{P_r}{N_0} b^2 |h_{rd}|^2 x_4 + \frac{\sqrt{P_r}}{\sqrt{N_0}} b h_{rd}^* n_{d1} (i + 1) + \frac{\sqrt{P_2}}{\sqrt{N_0}} h_{sd2} n_{d2} (i + 1). \end{aligned} \quad (5.28)$$

The bit error probability at the destination upon using a threshold at the relay is then simply

$$\begin{aligned} P(e_d) &= P(b = 0)P(e_d|b = 0) + P(b = 1)P(a_1 = 0, a_2 = 1|b = 1)P(e_d|b = 1, a_1 = 0, a_2 = 1) \\ &+ P(b = 1)P(a_2 = 0, a_1 = 1|b = 1)P(e_d|b = 1, a_2 = 0, a_1 = 1) + P(b = 1)P(a_2 = 0, a_1 = 0|b = 1) \\ & \quad P(e_d|b = 1, a_2 = 0, a_1 = 0) + P(b = 1)P(a_1 = 1, a_2 = 1|b = 1)P(e_d|b = 1, a_1 = 1, a_2 = 1). \end{aligned} \quad (5.29)$$

Investigating Eq(5.29) termwise, we have from [75] for Rayleigh fading channels,

$$P(b = 1)P(a_1 = 0, a_2 = 1|b = 1) = P(b = 1)P(a_2 = 0, a_1 = 1|b = 1) = \frac{1}{\sigma_{sr}^2} \int_T^\infty e^{-\beta/\sigma_{sr}^2} [P_s(\beta, \bar{\gamma})(1 - P_s(\beta, \bar{\gamma}))] d\beta, \quad (5.30)$$

and

$$P(b = 1)P(a_1 = 0, a_2 = 0|b = 1) = \frac{1}{\sigma_{sr}^2} \int_T^\infty e^{-\beta/\sigma_{sr}^2} [P_s(\beta, \bar{\gamma})]^2 d\beta, \quad (5.31)$$

where  $\bar{\gamma} = \frac{P_t}{N_0}$  is the transmit SNR at source,  $T$  is the threshold (no units),  $P_s(\beta, \bar{\gamma})$  is the symbol error probability at the relay and  $\beta = |h_{sr}|^2(\beta \geq T)$ .

By denoting  $P(b = 0) = \lambda_1(T, \bar{\gamma})$ ,  $P(b = 1)P(a_1 = 0, a_2 = 1|b = 1) = \lambda_2(T, \bar{\gamma})$ ,  $P(b = 1)P(a_1 = 0, a_2 = 0|b = 1) = \lambda_3(T, \bar{\gamma})$ ,  $P(e_d|b = 0) = \Omega(\bar{\gamma}_2)$ ,  $P(e_d|b = 1, a_1 = 0, a_2 = 1) = P(e_d|b = 1, a_2 = 0, a_1 = 1) = C_1(\bar{\gamma}_r, \bar{\gamma}_2)$ ,  $P(e_d|b = 1, a_2 = 0, a_1 = 0) = C_3(\bar{\gamma}_r, \bar{\gamma}_2)$ ,  $P(b = 1)P(a_1 = 1, a_2 = 1|b = 1) = \lambda_4(T, \bar{\gamma})$ ,  $P(e_d|b = 1, a_1 = 1, a_2 = 1) = \Psi(\bar{\gamma}_r, \bar{\gamma}_r)$ , where  $\bar{\gamma}_r = \frac{P_r}{N_0} \sigma_{rd}^2$  and  $\bar{\gamma}_2 = \frac{P_2}{N_0} \sigma_{sd}^2$  in frame index  $i + 1$ , we can rewrite Eq(5.29) as

$$P(e_d) = \lambda_1(T, \bar{\gamma})\Omega(\bar{\gamma}_2) + 2\lambda_2(T, \bar{\gamma})C_1(\bar{\gamma}_r, \bar{\gamma}_2) + \lambda_3(T, \bar{\gamma})C_3(\bar{\gamma}_r, \bar{\gamma}_2) + \lambda_4(T, \bar{\gamma})\Psi(\bar{\gamma}_r, \bar{\gamma}_2). \quad (5.32)$$

Following the same approach as before, we have

$$\frac{\partial P(e_d)}{\partial T} = 0. \quad (5.33)$$

Using  $\frac{\partial(\lambda_1(T, \bar{\gamma}))}{\partial T} = \left(\frac{1}{\sigma_{sr}^2}\right) e^{\left(\frac{-T}{\sigma_{sr}^2}\right)}$ ,  $\frac{\partial(\lambda_2(T, \bar{\gamma}))}{\partial T} = \left(\frac{-1}{\sigma_{sr}^2}\right) e^{\left(\frac{-T}{\sigma_{sr}^2}\right)} P_s(T, \bar{\gamma})(1 - P_s(T, \bar{\gamma}))$ ,  $\frac{\partial(\lambda_3(T, \bar{\gamma}))}{\partial T} = \left(\frac{-1}{\sigma_{sr}^2}\right) e^{\left(\frac{-T}{\sigma_{sr}^2}\right)} [P_s(T, \bar{\gamma})]^2$  from Eq(5.30) and Eq(5.31),  $\lambda_1(T, \bar{\gamma}) + 2\lambda_2(T, \bar{\gamma}) + \lambda_3(T, \bar{\gamma}) + \lambda_4(T, \bar{\gamma}) = 1$ , solving the resulting

quadratic equation in  $P_s(T.\bar{\gamma})$  and dropping those variables in the brackets for clarity, we have

$$P_s(T.\bar{\gamma}) = \begin{cases} \frac{(C_1 - \Psi) - \sqrt{(C_1 - \Psi)^2 - (2C_1 - C_3 - \Psi)(\Omega - \Psi)}}{2C_1 - C_3 - \Psi}, & C_3 \geq C_1 \geq \Psi, \Omega \geq \Psi. \\ \frac{(\Omega - \Psi)}{(2C_1 - \Psi)} & C_3 = 2C_1 - \Psi \end{cases} \quad (5.34)$$

such that the real valued solution of  $\frac{\partial P(e_d)}{\partial T} = 0$ , if it exists will be within  $(0, 1]$ . We now denote  $P_s(T.\bar{\gamma}) = k \in (0, 1]$ . The solution  $k$  is then the threshold for instantaneous symbol error probability at the relay.

We now show that  $k$  does minimize the bit error probability at the destination. For this purpose, we have  $\frac{\partial^2 P(e_d)}{\partial T^2} = \left(\frac{1}{\sigma_{sr}^2}\right) e^{\left(\frac{-T}{\sigma_{sr}^2}\right)} \left[-2 \frac{\partial P_s(T.\bar{\gamma})}{\partial T} (C_1(\bar{\gamma}_r, \bar{\gamma}_2) - \Psi(\bar{\gamma}_r, \bar{\gamma}_2)) - 2P_s(T.\bar{\gamma}) \frac{\partial P_s(T.\bar{\gamma})}{\partial T} (C_3(\bar{\gamma}_r, \bar{\gamma}_2) - 2C_1(\bar{\gamma}_r, \bar{\gamma}_2) + \Psi(\bar{\gamma}_r, \bar{\gamma}_2))\right]$  when  $\frac{\partial P(e_d)}{\partial T} = 0$ .

Since  $\frac{\partial P_s(T.\bar{\gamma})}{\partial T} < 0$  (i.e., when  $\gamma_t = T.\bar{\gamma}$  increases, error probability decreases in an AWGN channel), we have that  $\frac{\partial^2 P(e_d)}{\partial T^2} > 0$  if  $|P_s(T.\bar{\gamma})| < \left|\frac{C_1(\bar{\gamma}_r, \bar{\gamma}_2) - \Psi(\bar{\gamma}_r, \bar{\gamma}_2)}{2C_1(\bar{\gamma}_r, \bar{\gamma}_2) - C_3(\bar{\gamma}_r, \bar{\gamma}_2) - \Psi(\bar{\gamma}_r, \bar{\gamma}_2)}\right|$ . We can see from Eq(5.34), that the solution  $P_s(T.\bar{\gamma}) = k \in (0, 1]$  does satisfy the above condition. Therefore,

$\frac{\partial^2 P(e_d)}{\partial T^2} |_{P_s(T.\bar{\gamma})=k} > 0$  and hence the solution  $k$  of  $\frac{\partial P(e_d)}{\partial T} = 0$  minimizes  $P(e_d)$ .

### 5.3.3 Additional diversity

The information sent by the source in frame index  $i$  could be MRC combined at the destination to provide a greater diversity degree. This leads to,

$$\bar{\mathbf{r}} = \frac{\sqrt{P_1}}{N_0} h_{sd1}^* \mathbf{r}_d(i) + \mathcal{H}^H \mathbf{r}_d(i+1) \quad (5.35)$$

where  $\mathcal{H} = \begin{bmatrix} h_{sd2} & bh_{rd} \\ -bh_{rd}^* & h_1^* \end{bmatrix}$ .

To obtain a threshold for this case, we follow the same method as before and after suitably replacing  $\Psi(\bar{\gamma}_r, \bar{\gamma}_2)$  with  $\Psi'(\bar{\gamma}_r, \bar{\gamma}_2, \bar{\gamma}_1)$ ,  $\Omega(\bar{\gamma}_2)$  with  $\Omega'(\bar{\gamma}_1, \bar{\gamma}_2)$ ,  $C_1(\bar{\gamma}_r, \bar{\gamma}_2)$  with  $C_1'(\bar{\gamma}_r, \bar{\gamma}_2, \bar{\gamma}_1)$ ,  $C_3(\bar{\gamma}_r, \bar{\gamma}_2)$  with

$C'_3(\bar{\gamma}_r, \bar{\gamma}_2, \bar{\gamma}_1)$ , where  $\bar{\gamma}_1 = \bar{\gamma}\sigma_{sd}^2$  and dropping those variables in the brackets for clarity, we have,

$$P_s(T, \bar{\gamma}) = \begin{cases} \frac{(C'_1 - \Psi') - \sqrt{(C'_1 - \Psi')^2 - (2C'_1 - C'_3 - \Psi')(\Omega' - \Psi')}}{2C'_1 - C'_3 - \Psi'}, & C_3 \geq C'_1 \geq \Psi', \Omega' \geq \Psi'. \\ \frac{(\Omega' - \Psi')}{(2C'_1 - \Psi')} & C'_3 = 2C'_1 - \Psi' \end{cases} \quad (5.36)$$

such that a real solution,  $\in (0, 1]$ , if it exists. We denote this solution as  $P_s(T, \bar{\gamma}) = k'$ .

It could be noted from Eq(5.36) that upon MRC combining, the instantaneous symbol error probability threshold  $P_s(T, \bar{\gamma})$  now changes.

In all the above discussions,  $\Omega(\bar{\gamma}_1, \bar{\gamma}_2)$  represents the BER at the destination for non-cooperative single hop communication and  $\Psi(\bar{\gamma}_1, \bar{\gamma}_r, \bar{\gamma}_2)$  represents BER at the destination when the cooperation is ideal which then resembles an  $m$ -branch MRC combiner with different channel fading powers[75].  $C_1(\bar{\gamma}_1, \bar{\gamma}_r, \bar{\gamma}_2)$ ,  $C_3(\bar{\gamma}_1, \bar{\gamma}_r, \bar{\gamma}_2)$  are the BER at the destination in the interference limited case when the relay decodes one or both the symbols incorrectly. For network topologies with  $P_1\sigma_{sd}^2 \leq P_2\sigma_{rd}^2$ , i.e, at the destination receiver the average received power from the relay is equal to or more than the average received power from source, it can be seen from Eq(5.6), Eq(5.25) that the system becomes highly interference limited and therefore  $C_1(\bar{\gamma}_r, \bar{\gamma}_2) \approx C_3(\bar{\gamma}_1, \bar{\gamma}_r, \bar{\gamma}_2) \approx 0.5$ . Also, convenient bounds for  $\Omega(\bar{\gamma}_1, \bar{\gamma}_2)$  and  $\Psi(\bar{\gamma}_1, \bar{\gamma}_r, \bar{\gamma}_2)$  as discussed in [2] would give the threshold region which contains the optimal threshold.

To determine channel gain threshold  $T$  from the solution of  $P_s(T, \bar{\gamma})$ , we need closed form expression for  $P_s(T, \bar{\gamma})$  which depends on the modulation/detection combination and can be found in [75].

For coherent BPSK [75],  $P_s(T, \bar{\gamma}) = Q(\sqrt{2T, \bar{\gamma}})$ , where  $Q(x) = \frac{1}{\sqrt{2\pi}} \int_x^\infty e^{-\frac{t^2}{2}} dt$ , and therefore

$$T = \frac{1}{2\bar{\gamma}} [Q^{-1}(k)]^2. \quad (5.37)$$

For coherent  $M$ -QAM [75],  $P_s(T, \bar{\gamma}) = \frac{4(\sqrt{M}-1)}{\sqrt{M}}Q(\sqrt{\frac{3T\bar{\gamma}}{M-1}}) - 4(\frac{\sqrt{M}-1}{\sqrt{M}})^2Q(\sqrt{\frac{3T\bar{\gamma}}{M-1}})^2$ , and therefore we can obtain

$$T = \frac{M-1}{3\bar{\gamma}} [Q^{-1}[\frac{\sqrt{M}}{2(\sqrt{M}-1)}[1 - \sqrt{1-k}]]]^2. \quad (5.38)$$

For coherent  $M$ -PSK [75], we have from the well-known union bound,  $P_s(T, \bar{\gamma}) \approx 2Q(\sqrt{2T\bar{\gamma}} \sin(\frac{\pi}{M}))$ , which gives

$$T \approx \frac{1}{2\bar{\gamma}} [\csc(\frac{\pi}{M})Q^{-1}(k/2)]^2. \quad (5.39)$$

The thresholds provided above minimize the BER at the destination when the channels between the radio nodes are Rayleigh fading, the channel variances are globally known and when the relay transmit power  $P_2$  is fixed.

## 5.4 Channel estimation errors

Relaying based on thresholding scheme discussed in this paper rely on the channel estimation of the source-relay channel. Also, for regenerative relaying, imperfect channel estimation at the relays would increase the symbol decoding errors at the relays. It is therefore important to account for channel estimation errors at the relays and its impact on relaying protocols.

Channel estimation at the relay can be modeled as

$$\tilde{h} = h + \sqrt{m-1} \sqrt{\frac{N_0}{P_1}} h_e, \quad (5.40)$$

where  $h_e$  is a zero mean, unit variance complex Gaussian variable. The relay receiver uses the above channel estimate for its combiner before detection. If the received signal at the relay is

$$r_r(i) = \sqrt{P_1} h_{sr} x + \sqrt{N_0} n_r(i), \quad (5.41)$$

then the output of the combiner becomes

$$y_c = \frac{\sqrt{P_1}}{N_0} \tilde{h}_{sr} r_r(i). \quad (5.42)$$

Using Eq (5.40) and Eq (5.41) in Eq (5.42), we obtain

$$y_c = \frac{P_1}{N_0} |h_{sr}|^2 x + \sqrt{\frac{(m-1)P_1}{N_0}} h_{sr}^* h_e x + \sqrt{\frac{P_1}{N_0}} h_{sr} n_r(i) + \sqrt{m-1} h_e n_r(i). \quad (5.43)$$

It can be observed from Eq(5.43) that imperfect channel estimation increases the average noise power at the output of combiner but does not change the average signal power. The average noise power is now

$$N_{av} = E[N_0(m|h_{sr}|^2 + (m-1)\frac{N_0}{P_1})] = N_0\sigma_{sr}^2[m + (m-1)\gamma_r^{-1}]. \quad (5.44)$$

where  $\gamma_r = \frac{P_1}{N_0}\sigma_{sr}^2$ . For  $(m-1)\gamma_r^{-1} \ll 1$ , Eq(5.44) approximates to

$$N_{eff} \approx m\sigma_{sr}^2 N_0. \quad (5.45)$$

Note that, under perfect channel estimation the average noise power at the output of combiner is  $\sigma_{sr}^2 N_0$ . From Eq (5.45) we see that the ratio of average signal power to average noise power has a loss factor  $\frac{1}{m}$ .

The conditional SNR is given by

$$SNR_i = |h_{sr}|^2 \frac{P_1}{N_0} \left[ \frac{1}{m + (m-1)\gamma_r^{-1}} \right]. \quad (5.46)$$

For  $(m-1)\gamma_r^{-1} \ll 1$ , the conditional SNR can be somewhat simplistically written as

$$SNR_i = |h_{sr}|^2 \frac{P_1}{N_0} \left[ \frac{1}{m} \right]. \quad (5.47)$$

Note that the conditional  $SNR$  with perfect channel estimation is  $|h_{sr}|^2 \frac{P_1}{N_0}$ . Therefore we see that an approximate loss factor  $\frac{1}{m}$  is introduced for the conditional SNR due to increase in the noise power. Expressing  $SNR_i = |h_{sr}|^2 \bar{\gamma}_{eff}$ , we have  $\gamma_{eff} = \frac{1}{m}\bar{\gamma}$  implying that  $\frac{1}{m}$  is the SNR penalty in

the source-relay channel due to imperfect channel estimation. Then by replacing  $\bar{\gamma}$  with  $\frac{\bar{\gamma}}{m}$  in the source-relay channel for Eq(5.37)-Eq(5.39) it can be easily seen that the thresholds become,

$$T_e = mT. \quad (5.48)$$

where  $T_e$  is the new threshold when there are channel estimation errors at the relay.

## 5.5 Numerical examples

We now construct several thresholds based on the theoretical derivation of an optimal threshold. We consider the case of distributed Alamouti relaying for this purpose. The system was simulated with  $\pi/4$  QPSK modulation. The symbol power has been normalized to 1. The total transmit energy by source is twice the energy per frame i.e,  $P_1 = P_2$ . Relay transmit power  $P_r$  is equal to the source transmit power  $P_2$  in frame  $i + 1$ . Quasi-static, Rayleigh fading channels have been assumed. We consider a network topology with  $\sigma_{sd}^2 = \sigma_{rd}^2 = 1$  i.e, the source-destination and relay-destination channels are equally balanced and  $\sigma_{sr}^2 = 2$  i.e, the relay is closer to the source than destination. In the simulations, ‘blind DF’ represent a symbol decode and forward (DF) scheme without any thresholding, error checking or weighting and  $T_o = \frac{(2^{2R}-1)}{\bar{\gamma}}$  is the threshold based on the outage probability as discussed in [3] where  $R = 1$  for QPSK modulation. It is recalled here that  $\bar{\gamma} = \frac{P_1}{N_0}$  is the transmit SNR at the source in frame  $i$ ,  $\bar{\gamma}_1 = \frac{P_1}{N_0}\sigma_{sd}^2$  is the received SNR at destination from source in frame  $i$ ,  $\bar{\gamma}_2 = \frac{P_2}{N_0}\sigma_{sd}^2$  is the received SNR at destination from source in frame  $i + 1$ ,  $\bar{\gamma}_r = \frac{P_r}{N_0}\sigma_{rd}^2$  is the received SNR at destination from relay in frame  $i + 1$ . For the examples below we have  $\bar{\gamma}_1 = \bar{\gamma}_2 = \bar{\gamma}_r = \bar{\gamma}_x$  and BER results are plotted against  $\bar{\gamma}_x$ .

### *Example 1: Distributed Alamouti without MRC*

Fig. 5.1 shows the BER performance comparison of distributed Alamouti scheme for three cases. The instantaneous symbol error probability threshold  $k$  is obtained using Eq(5.34) and  $T_2$  is the channel gain threshold obtained by substituting  $k$  and  $M = 4$  in Eq(5.38). For doing this we use the well known closed form expression for BER of a single hop single antenna rayleigh fading channel

as  $\Omega(\bar{\gamma}_x) = 0.5(1 - \sqrt{\frac{\bar{\gamma}_x}{(\bar{\gamma}_x+2)}})$  and the BER expression of a 2-branch MRC combiner with equal channel fading powers as  $\Psi(\bar{\gamma}_x) = (0.5(1 - \sqrt{\frac{\bar{\gamma}_x}{(\bar{\gamma}_x+2)}}))^2[2 + \sqrt{\frac{\bar{\gamma}_x}{(\bar{\gamma}_x+2)}}]$  [75]. We also approximate  $C_1(\bar{\gamma}_x) = C_3(\bar{\gamma}_x) \approx 0.5$  noting that if the relay decodes even one symbol incorrectly in a frame, the decision statistics of both the symbols in the frame at the destination become highly interference limited and is therefore deleterious for communication. It can be noted that this approximation is close numerically and therefore eventhough it might not yield an exact optimal numerical value of threshold, it would still yield a close to optimal numerical value. It can be observed in the plots that a ‘blind DF’ scheme does not achieve any significant benefit and therefore makes inefficient use of system resources. For low-medium SNR’s  $T_o$  lies in the close vicinity of  $T_2$  and it can be seen from the figure that their performance is therefore similar over this SNR region. However at high SNR’s  $T_2$  collects diversity better than  $T_o$  and outperforms it. The curve “multiple antenna 2nd order diversity” depicts the performance when multiple transmit antennas are used or equivalently, when there are no symbol detection errors made by relay (the transmit power has not been halved on each transmit antenna for fair comparison). This performance gap between multiple antenna systems and relay systems can be further reduced using ML detection as in example Eq(4.30), by sacrificing linear complexity in detection which is a very attractive feature of space-time block coding.

***Example 2: Distributed Alamouti without MRC - with channel estimation errors at the relay***

Channel estimation at the relay is modeled as  $\tilde{h} = h + \sqrt{\frac{1}{\gamma}}h_e$ , where  $h_e$  is a zero mean, unit variance complex Gaussian variable. Therefore for this model we have  $m \approx 2$  from Eq(5.40) and  $\gamma_r^{-1} = 0.5\gamma_x^{-1} \ll 1$ . In the plot  $T_2$  is the threshold obtained as in Example 1, and  $T_3 = T_e$  obtained from Eq(5.48), is the new threshold after accounting for the estimation errors. We retain the same modeling for other parameters as in Example 1 to obtain  $T_3$ . The results are plotted in Fig. 5.2 showing the effect of channel estimation errors on the schemes. The ‘blind DF’ scheme has a small performance loss as a result of imperfect channel estimation at the relay. The impact is significant on the performance of threshold  $T_o$  demonstrating the sensitivity of system performance of the threshold value. Due to near-optimality of threshold  $T_2$ , its performance does not deteriorate very

much, and the performance is further improved by threshold  $T_3$  which accounts for estimation errors and shows almost the same performance as when there are no channel estimation errors at the relay.

***Example 3: Distributed Alamouti with MRC***

Fig.5.3 shows the BER performance of distributed Alamouti scheme after MRC combining with information in frame index  $i$ .  $k'$  is obtained using Eq(5.36) and  $T_2 = T$  is the threshold obtained by substituting  $k'$  and  $M = 4$  in Eq(5.38) in this paper. To obtain  $T_2$ , we use the closed form expressions for 2-branch MRC combiner and 3-branch MRC combiner respectively as  $\Omega'(\bar{\gamma}_x) = (0.5(1 - \sqrt{\frac{\bar{\gamma}_x}{(\bar{\gamma}_x+2)}}))^2 [2 + \sqrt{\frac{\bar{\gamma}_x}{(\bar{\gamma}_x+2)}}]$ ,  $\Psi'(\bar{\gamma}_x) = (0.5(1 - \sqrt{\frac{\bar{\gamma}_x}{(\bar{\gamma}_x+2)}}))^3 [2 + \sqrt{\frac{\bar{\gamma}_x}{(\bar{\gamma}_x+2)}}] + 3(0.5(1 + \sqrt{\frac{\bar{\gamma}_x}{(\bar{\gamma}_x+2)}}))^2$  [75] and  $C_1(\bar{\gamma}_x) = C_3(\bar{\gamma}_x) \approx 0.5$ . From the results we see that a ‘blind DF’ scheme again makes inefficient use of resources and is far away from a target diversity 3 performance. Threshold  $T_o$  does not improve the performance significantly either. The threshold  $T_2$  achieves a better performance because it collects the additional diversity available at the destination. The curve “multiple antenna 3rd order diversity” depicts the matched filter bound performance when multiple transmit antennas are used or, equivalently, when there are no symbol detection errors made by the relay (the transmit power has not been halved on each transmit antenna for fair comparison),.

***Example 4: Distributed Alamouti with MRC - with channel estimation errors at the relay***

The results in this case are shown in Fig. 5.4 Channel estimation at the relays are modeled as in Example 2 ( $m = 2$ ) and we retain the same modeling of parameters as in Example 3. In the plot,  $T_2$  is the threshold as obtained in previous Example 3 and  $T_3$  is the threshold which accounts for channel estimation errors at the relay. We see that when ‘blind DF’ scheme has a further performance loss and  $T_o$  suffers from a significant performance loss due to estimation errors at relay,  $T_2$  does not show a significant performance loss. The performance is further improved by  $T_3$ , which has the lowest performance loss.

## Results

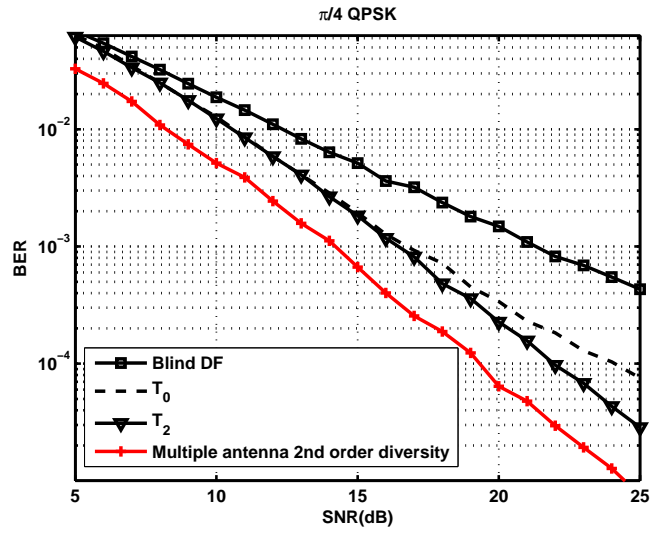


Figure 5.1: Distributed Alamouti scheme.

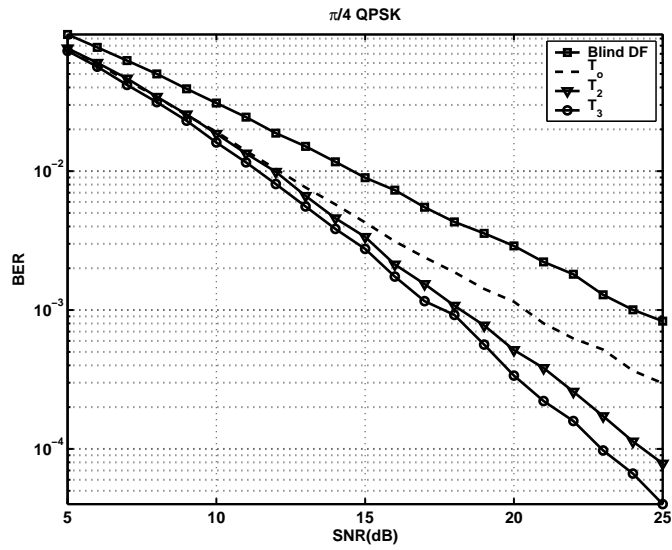


Figure 5.2: Distributed Alamouti scheme with channel estimation errors at the relay.

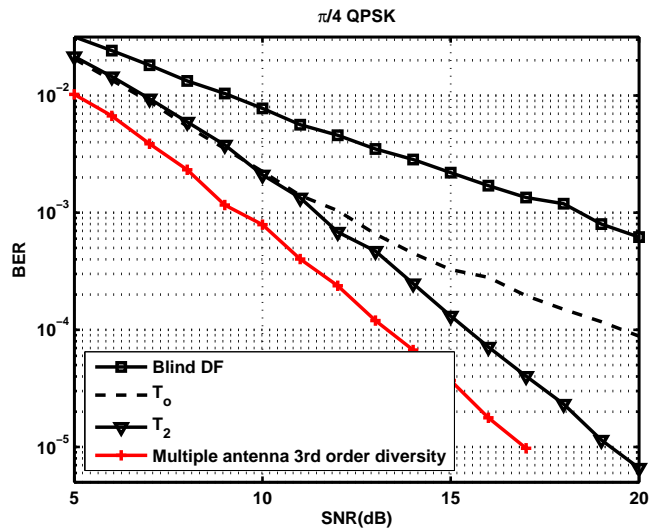


Figure 5.3: Distributed Alamouti scheme after MRC combining with information in frame index  $i$ .

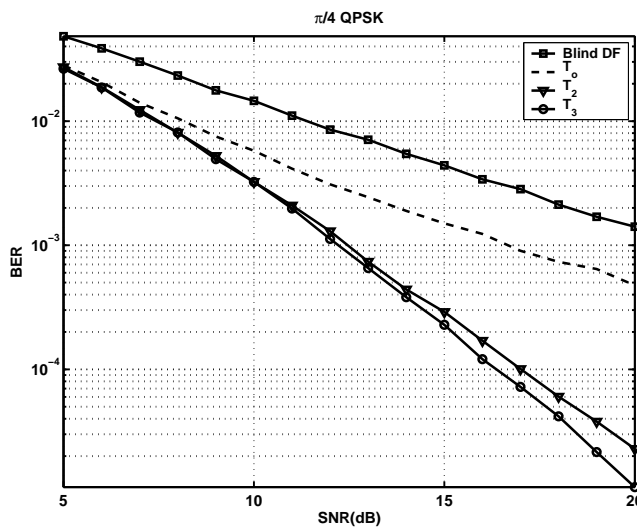


Figure 5.4: Distributed Alamouti scheme when MRC combined but with channel estimation errors at the relay.

## 5.6 Conclusion

Selection relaying for realizing relay diversity in a three terminal relay network was considered in this chapter. Optimal thresholding which would minimize the BER at the destination was analyzed and expressions for the optimal threshold have been derived. Thresholds constructed

based on the derivation is observed to provide better BER performance at the destination. Selection relaying when the relay receiver channel estimation is not perfect has also been considered in this chapter. The sensitivity of system BER performance on threshold selection is thereby demonstrated. Further, it is seen that certain degree of imperfect channel estimation at the relay does not affect the performance of the system significantly when the threshold is close to optimal. We conclude by noting that the approach adopted in this chapter is only a small step towards the larger problem of achieving the *relay complexity-reliability tradeoff* for practical wireless relay systems.

## Chapter 6

# Conclusions and Perspectives

### 6.1 Conclusions

The rising demand for speed in wireless communications has received widespread attention worldwide in recent years and much of research focus and energy has been dedicated to meeting this requirement. Wireless ad hoc peer-peer networking is a new dimension to wireless communications which would require high speed communication links in its mechanism to be able to cater for consumer performance demands. The end-end performance of these networks will also depend largely on the “reliability” of the component wireless links which form the network. This is because the true measure of achieved rate or throughput in various networks is the received symbols/second rather than transmitted symbols/second.

This thesis mainly dealt with two systems for improving reliability:- multiple antenna diversity systems and multi-user diversity systems.

In Chapter 2, we discussed transmit diversity using space-time block coding and focussed exclusively on orthogonal and non-orthogonal codes. It was shown that constellation rotations on a full rate non-orthogonal code achieves full diversity in the light of rank and determinant criteria (which are the design criteria for space-time codes at asymptotic SNR's). We then critically examined the impact of spatial correlation on the performance of this scheme in Chapter 3. Specifically,

the impact of transmit-side correlation was analyzed and characterized and not surprisingly it was observed that correlation deteriorates the performance due to lack of diversity in the channel. However, the interesting result there was that the performance gap between the non-orthogonal code in discussion and the matched filter bound closes down as the correlation increases.

In contrast to antenna diversity, a scenario where diversity is available in abundance is multi-user diversity. In Chapter 4, a concise description of user cooperation architecture was presented. User cooperation in general and relay diversity in particular were briefly explained followed by an analysis of few detection techniques for these systems.

Chapter 5 focussed on *low complexity high reliability* relaying. We showed that selection relaying partly solves this problem for a simple three terminal network although there is still some performance gap between antenna diversity and multi-user diversity systems as illustrated in section 5.5. We developed closed form expressions of optimal thresholds for this network and demonstrated their utility in various scenarios. These observations also suggest that the utility of user diversity systems will vary largely with the channel model and system characteristics. Based on the simulation results, we conclude that relay diversity systems are a promising means to make use of additional resources and increase reliability in communications.

## 6.2 Perspectives

- The thesis considered only a simple three terminal network for selection relaying. Selection relaying for an arbitrary  $n$  – *terminal* relay network with independent path loss coefficients therefore remains an open problem. We however at this stage conjecture that the gains available by selection relaying would decrease with the number of relaying terminals.
- Adaptive rate and power allocation for cooperating nodes in fading channels is a promising and practical problem that could be considered in future work.
- In current work, space-time coding for cooperative networks assumes symbol level synchronization. However, imperfect synchronization is a practical issue which has been neglected in

these protocols throughout the literature. This problem should be addressed while designing diversity achieving protocols.

- Current relaying protocols neglect user mobility and migration between strategies based on this mobility. Cooperative protocols which could adapt to such dynamic network topologies is an interesting scenario which could be further investigated.
- This thesis considered only the physical layer perspective of relaying. However, in the big picture, ad hoc network designs are very much incomplete without a cross layer solution. Potential benefits and challenges in cooperative networking by using a cross-layer approach should be studied in future work.

# References

- [1] N. Laneman and G. W. Wornell, “Energy-efficient antenna sharing and relaying for wireless networks,” *Proc. IEEE Wireless Communications and Networkings Conf. (WCNC)*, Chicago, IL, Sept. 2000.
- [2] N. Laneman, D. N. C Tse and G. W. Wornell, “Distributed space-time coded protocols for exploiting cooperative diversity in wireless network,” *IEEE Trans. Inform. Theory*, vol. 49, pp. 2415-2425, Oct. 2003.
- [3] N. Laneman, D. N. C Tse and G. W. Wornell, “Cooperative Diversity in Wireless Networks: Efficient Protocols and Outage Behaviour,” *IEEE Trans. Inform. Theory*, vol. 50, pp. 3062-3080, December 2004.
- [4] A. Sendonaris, E. Erkip and B. Aazhang, “User cooperation diversity, Part I: System description,” *IEEE Trans. Inform. Theory*, vol. 51, pp. 1927-1938, Nov. 2003.
- [5] A. Sendonaris, E. Erkip and B. Aazhang, “User cooperation diversity, Part II: Implementational aspects and performance analysis,” *IEEE Trans. Inform. Theory*, vol. 51, pp. 1939-1948, Nov. 2003.
- [6] A. Narula, M. Lopez, M. Trott and G. Wornell “Efficient use of side information in multiple-antenna data transmission over fading channels,” *IEEE J. Selec. Areas Commun*, vol. 16, pp. 1423-1436, Oct. 1998.
- [7] P. A Anghel, G. Leus, M. Kaveh, “Multi-user space time coding in cooperative networks,” *Proc. IEEE ICASSP 2003*, vol. 4, pp. IV-73-IV-76, April 6-10, 2003.

- [8] S. Barbarossa, G. Scutari, “Distributed space-time coding strategies for wideband multihop networks: Regenerative vs non-regenerative relays,” *Proc. IEEE ICASSP 2004*, Montreal , Canada , May 2004.
- [9] S. Barbarossa, G. Scutari, “Distributed space-time coding strategies for multi hop networks,” *Proc. IEEE ICC 2004*, Paris, France, June 2004.
- [10] P. A. Anghel, M. Kaveh, “On the diversity of cooperative systems,” *Proc. of IEEE ICASSP 2004*, vol. 4 , pp. 577-580, May 17-22, 2004.
- [11] T. E. Hunter and A. Nostrania “Diversity through coded cooperation,” *IEEE Trans Wireless Commun*, submitted for publication.
- [12] M. Janani, A. Hedayat, T. E. Hunter, A. Nostrania “Coded Cooperation in Wireless Communications: Space-Time Transmission and Iterative Decoding,” *IEEE Trans Signal processing*, vol. 52, pp. 362-371, Feb. 2004
- [13] V. Emamian, P. A. Anghel, M. Kaveh “Multi-user spatial diversity system in a shadow-fading environment,” *Proc. IEEE VTC 2002*, vol. 1, pp. 573-576, Sept. 24-28 2002.
- [14] A. Stefanov and Elza Erkip “Cooperative Coding for Wireless Networks,” *IEEE Trans. on Commun*, vol. 52, pp. 1470-1476, Sept. 2004.
- [15] J. Boyer , D. D. Falconer and H. Yanikomeroglu “Multihop Diversity in Wireless Relaying Channels,” *IEEE Trans. on Commun*, vol. 52, pp. 1820-1830, Oct. 2004.
- [16] Mischa Dohler , E. Lefranc, H. Aghvami “Virtual Antenna Arrays for Future Wireless Mobile Communication Systems,” *IEEE ICT 2002*, Beijing, China, 2002.
- [17] B. Schein and R. Gallager, “The Gaussian parallel relay network,” *Proc. ISIT 2000*, 25-30 June. 2000, Sorreno , Italy.
- [18] P. Larsson, “Methods and Architectures for Wireless Communication Networks using Cooperative Relaying,” *United States Patent Application Publication*, US 2004/0266339 A1, Dec 30 2004.

- [19] Thomas M.Cover, "Broadcast channels," *IEEE Trans.Inform.Theory*, 18(1):2-14, January 1972.
- [20] Thomas M.Cover and Abbas A.El Gamal, "Capacity theorems for relay channel," *IEEE Trans.Inform.Theory*, 25(5):572-584, September 1979.
- [21] A.B. Carleial, "Multiple-access channels with different generalized feedback signals," *IEEE Trans.Inform.Theory*, vol.iT-28: 841-850, November 1982.
- [22] P.Gupta and P.R. Kumar, "The capacity of wireless networks," *IEEE Trans.Inform.Theory*, 46(2):388-404, March 2000.
- [23] V.Kawadia and P.R. Kumar, "Power Control and Clustering in Ad Hoc Networks," *IEEE INFOCOM*, vol.1: 459-469, March 2003.
- [24] G.Kramer, M.Gastpar and P.Gupta, "Cooperative Strategies and Capacity Theorems for Relay Networks," *IEEE Trans.Inform.Theory*, 51(9):3037-3062, September 2005.
- [25] K.Azarian, H.El Gamal and P.Schniter "On the Achievable Diversity Multiplexing Tradeoff in Half-Duplex Cooperative Channels," *IEEE Trans.Inform.Theory*, 51(12): 4152-4172, December 2005.
- [26] A.S Avestimehr and D.N.C Tse "Outage-Optimal Relaying in the Low SNR Regime," *Proc. IEEE ISIT 2005*, 941-945, Adelaide, Sept. 2005.
- [27] M.Costa, "Writing on dirty paper," *IEEE Trans.Inform.Theory*, vol. 29: 439-441, May 1983.
- [28] C.T.K Ng and A.J. Goldsmith, "Transmitter Cooperation in Ad-Hoc Wireless Networks: Does Dirty-Paper Coding Beat Relaying," *IEEE Inform.Theory Workshop*, San Antonio, Texas, Oct 2004.
- [29] R.U. Nabar, H.Bolcskei and F.W. Kneubuhler "Fading Relay Channels: Performance Limits and Space-Time Signal Design," *IEEE J. Select. Areas Commun*, vol.22, no.6, pp. 1099-1108, Aug. 2004.

- [30] M.Gatstpar and M.Vetterli, "On the Capacity of wireless networks: The Relay case," *Proc. IEEE INFOCOM 2002*, 1577-1586, New York, NY, June 2002.
- [31] M.Gatstpar and M.Vetterli, "The multiple-relay channel: coding and antenna clustering capacity," *Proc. IEEE ISIT 2002*, page 195, Lausanne, Switzerland, July 1-5 2002.
- [32] M.Gatstpar and M.Vetterli, "On the asymptotic capacity of Gaussian relay networks," *Proc. IEEE ISIT 2002*, page 136, Lausanne, Switzerland, July 1-5 2002.
- [33] A.Blestas, A.Lippman and D.P. Reed, "A Simple Distributed Method for Relay Selection in Cooperative Diversity Wireless Networks, based on Reciprocity and Channel Measurements," *Proc. IEEE VTC 2005-Spring*, 1484-1488, Stockholm, Sweden, May 2005.
- [34] A.Witnebben and B.Rankov, "Impact of Cooperative Relays on the Capacity of Rank-Deficient MIMO Channels," *Proc. IST Summit on Mobile and Wireless Communications*, pp.421-425, Aviero, Portugal, June 2003.
- [35] E.Zimmerman, P.Herhold and G.Fettweis, "The Impact of Cooperation on Diversity-Exploiting Protocols," *Proc. IEEE VTC 2004-S*, pp.410-414, Milan, Italy, May 2004.
- [36] E.Zimmerman, P.Herhold and G.Fettweis, "On the Performance of Cooperative Relaying Protocols in Wireless Networks," *European Trans. Commun*, vol 16, Issue 1, pp. 17-35, Jan 2005.
- [37] Y.Liang, V.V.Veeravalli, "The impact of relaying on the capacity of broadcast channels," *Proc. IEEE ISIT 2004*, page 403, Chicago, USA, June 2004.
- [38] Y.Liang, V.V.Veeravalli, "Cooperative Relay Broadcast Channels," *Proc. IEEE WIRELESS-COM 2005*, page 1449-1454, Hawaii, USA, June 2005.
- [39] I.Maric, R.D.Yates, "Forwarding strategies for Gaussian parallel relay networks," *Proc. IEEE ISIT 2004*, page 270, Chicago, USA, June 2004.
- [40] A. Sendonaris, E.Erkip, and B.Aazhang, "Increasing uplink capacity via user cooperation diversity," *Proc. IEEE ISIT 1998*, page 156, Cambridge, MA, Aug. 1998.

- [41] N. Jindal, S.Vishwanath, and A.Goldsmith, "On the Duality of Gaussian Multiple-Access and Broadcast channels," *IEEE Trans.Inform.Theory*, 50(5), pp. 768-783, May 2004.
- [42] J.-C.Belfiore, G.Rekaya and E.Viterbo "The Golden Code: a  $2 \times 2$  full-rate space-time code with nonvanishing determinant," *IEEE Trans.Inform.Theory*, 51(4), pp. 1432-1436, April 2005.
- [43] J.-C.Belfiore and G.Rekaya "Quaternionic lattices for space-time coding," *Proc. IEEE Inform.Theory Workshop*, Paris, April 2003.
- [44] P.Mitran, H.Ochiai and V.Tarokh "Space-Time diversity enhancements using collaborative communications," *IEEE Trans. Inform. Theory*, vol.51, pp. 2041-2057, June 2005.
- [45] E.C. van der Meulen "Three-terminal communication channels," *Adv. Appl. Probab*, vol.3, pp. 120-154, 1971.
- [46] S. Alamouti, "A simple transmit diversity technique for wireless communications," *IEEE JSAC*, vol. 16, no. 8, pp. 1451-1458, 1998.
- [47] V. Tarokh, N. Seshadri and A.R Calderbank, "Space time codes for high data rate wireless communications:performance criterion and code construction," *IEEE Trans. Inform. Theory*, vol. 44, pp. 744-765, Mar. 1998.
- [48] V. Tarokh, H. Jafarkhani and A.R Calderbank, "Space time block codes from orthogonal designs," *IEEE Trans. Inform. Theory*, vol. 45, pp. 1456-1467, July 1999.
- [49] O. Tirkkonen, A. Boariu and A. Hottinen, "Minimal non-orthogonality rate 1 space time block code for 3+ Tx antennas," *Proc. IEEE ISSSTA 2000*, vol. 2, pp. 429-432, September 2000.
- [50] B. Hassibi and B. Hochwald "High rate codes that are linear in space and time," *IEEE Trans.Inform.Theory*, 48(7), pp. 1804-1824, July 2002.
- [51] O. Tirkkonen and A.Hottinen, "Complex modulation for four tx antennas," *Proc. IEEE GLOBECOM*, pp. 1005-1009, vol. 2, Nov. 2000
- [52] E. Telatar, "Capacity of multi-antenna gaussian channels," *Eur. Trans. Telecomm*, 10(6), pp. 585-595, Nov 1999.

- [53] L. Zheng and D.N.C Tse “Diversity and Multiplexing: A fundamental trade off in multiple-antenna channels,” *IEEE. Trans. Inform. Theory*, 49(5), pp.1073-1095, May 2003.
- [54] N. Sharma and C. Papadias, “Improved quasi-orthogonal codes through Constellation Rotations,” *IEEE Wireless Comm. and Network Conf , Orlando, FL, USA* , pp. 169-171 , March 2002.
- [55] J. Boutros and E. Viterbo, “Signal space diversity: a power and bandwidth efficient diversity technique for Rayleigh fading channels,” *IEEE Trans. Inform. Theory* , vol. 44, pp. 1453-1467, July 1998.
- [56] J. Boutros, E. Viterbo, C. Rastello, J.-C. Belfiore “Good Lattice Constellations for both Rayleigh fading and Gaussian channels,” *IEEE Trans. Inform. Theory* , 42(2), pp. 502-518, July 1996.
- [57] S.B. Slimane “An improved PSK scheme for fading channels,” *IEEE GLOBECOM* , vol.2, pp. 1276-1280, London, Nov 1996.
- [58] O. Tirkkonen, “Optimizing space time block codes by constellation rotations,” *Proc.Finnish Wireless communications Workshop, FWCW’01, Finland*, pp. 59-60, Oct 2001.
- [59] A. Hammons, H. El Gamal “On theory of space-time codes for PSK modulation,” *IEEE. Trans. Inform Theory*, 46(2), pp.524-542, 2000.
- [60] O. Tirkkonen and A. Hottinen, “Trade-offs between rate, puncturing and orthogonality in space-time codes” *Proc. IEEE ICC 2001*, vol. 4, pp. 1117-1121, June 2001.
- [61] O. Tirkkonen , “Maximal Symbolwise diversity in Non-Orthogonal Space-Time Block codes” *Proc. IEEE ISIT 2001*, page 197, Washington, June 24-29, 2001
- [62] O. Tirkkonen , “Square matrix embeddable space-time block codes for complex signal constellations” *IEEE. Trans. Inform. Theory*, 48(2), pp. 384-395, Feb 2002.
- [63] B. Hassibi and B. Hochwald “High rate codes that are linear in space and time,” *IEEE. Trans. Inform Theory*, 48(7), pp. 1804-1824, July 2002.

- [64] G. Foschini and M. Gans “On limits of wireless communications in a fading environment when using multiple antennas,” *Wireless. Pers. Comm*, 6(3), pp. 311-335, Mr 1998.
- [65] F.C Zheng and A.G. Burr, “A Robust Non-Orthogonal Space time Block code for four transmit antennas,” *Proc.IEEE VTC 2003-S*, vol.1, pp.301-305, April 2003.
- [66] H. Bolcskei and A.J. Paulraj, “Performance of Space-Time Codes in the Presence of Spatial Fading Correlation,” *Asilomar Conference On Signals, Systems and Computers, Pacific Grove (CA)* , vol.1 , pp.687 - 693, Oct./ Nov 2000.
- [67] H. Jafarkhani, “A quasi-orthogonal space time block code,” *Proc. IEEE WCNC'00*, vol.1, pp.42-45, Sept.2000.
- [68] M. Frodigh, P.Johansson and P. Larsson “Wireless ad hoc networking - The art of networking without a network,” *Ericsson Review*, no.4, pp. 248-263, 2000.
- [69] B.G. Evans and K. Baughan “Visions of 4G,” *Electronics and Commn Engg Journal*, 12(6), pp. 293-303, Dec 2000.
- [70] J. Sun, J. Sauvola and D. Howie “Features in Future: 4G Visions From a Technical Perspective,” *Proc. IEEE GLOBECOM*, 12(6), pp. 3533-3537, San Antonio, Texas, Dec. 2001.
- [71] U. Jonsson, F. Alriksson, T. Larsson, P. Johansson, G. Q. Maguire Jr., “MIPMANET- Mobile IP for Mobile Ad hoc networks,” *Mobihoc'00*, pages 75-85, Aug 2000.
- [72] M. Grossgaluser and D.N.C Tse “Mobility increases the capacity of ad hoc networks,” *IEEE/ACM Trans. Networking*, vol. 10, no.4, pp. 477-486, Aug. 2002.
- [73] J. Jubin and J.D. Tornow “The DARPA packet radio network protocol,” *Proc. of the IEEE*, vol. 75, no.1, pp. 21-32, Jan. 1987.
- [74] S. Toumpis, A. Goldsmith “New Media Access Protocols for Wireless Ad hoc Networks Based on Cross-Layer Principles,” *To appear in IEEE Trans. Wireless Commns.*
- [75] M. Simon and M. Alouini, *Digital Communications over Fading Channels:A Unified Approach to Performance Analysis* , New York:Wiley, 2002.

- [76] G. Foschini, "Layered space-time architecture for wireless communications in a fading environment when using multi-element antennas," *Bell labs Tech J.*, , pp. 41-59, 1996.